EFFECTIVE DIFFUSION COEFFICIENTS FOR TOLUENE IN CALCIUM CARBONATE FILLED POLY(VINYL ACETATE) FROM QUARTZ CRYSTAL MICROBALANCE SORPTION EXPERIMENTS

By

STEVEN LEE WILLOUGHBY

Bachelor of Science
Cameron University
Lawton, Oklahoma
1992

Master of Science
Oklahoma State University
Stillwater, Oklahoma
1994

Submitted to the Faculty of the
Graduate College of the
Oklahoma State University
in partial fulfillment of
the requirements for
the Degree of
MASTER OF SCIENCE
May, 1998

EFFECTIVE DIFFUSION COEFFICIENTS
FOR TOLUENE IN CALCIUM CARBONATE
FILLED POLY(VINYL ACETATE) FROM
QUARTZ CRYSTAL MICROBALANCE
SORPTION EXPERIMENTS

Thesis Approved:

Mark S. Hoy
Thesis Adviser

Allan Lee

Robert Robinson Jr.

Wayne B. Powell
Dean of the Graduate College

PREFACE

A quartz crystal microbalance (QCM) was used to obtain effective diffusion coefficients of toluene diffusing into $CaCO_3$ filled poly(vinyl acetate). Experimental diffusion data were obtained at 60°C and 80°C for weight percents of 0, 3.3, 4.9, and 10% $CaCO_3$ at concentrations of toluene below 0.15 weight fraction at 60°C and at toluene weight fraction below 0.10 at 80°C.

Effective diffusion coefficients were also calculated from a free-volume equation modified to account for the filler by fitting experimental effective diffusion coefficients to this equation. Several other models were also examined for their ability to accurately represent the experimental effective diffusion coefficient data.

I would like to express sincere appreciation to my advisor, Dr. Martin S. High, and committee members, Dr. Robert L. Robinson, Jr., and Dr. D. Alan Tree, for their advice, support, and interest in this work.

I want to thank Mr. Mark C. Drake and Rexam Graphics for financial support and for suggesting this study.

I also want to thank the students I've met at OSU for their help and friendship.

Finally, I want to express appreciation to my wife, Sheena, for her support and encouragement, and for her help and company in many classes.

TABLE OF CONTENTS

LIST OF TABLES

LIST OF FIGURES

CHAPTER I

INTRODUCTION

Heterogeneous materials such as filled polymers are used extensively in industrial processes and commercial applications. Fillers are important constituents of many elastomers, plastics and coatings. They come in the form of small particles of different shapes. Fillers may be crystalline or amorphous. They have a significant influence upon the properties of materials and can be used to increase the mechanical durability, improve elastic properties, or give certain color or optical properties to the polymeric materials. Fillers also modify the sorption and permeability to diffusants. Diffusion and transport of matter in filled polymers are important in processes such as the drying of coatings and adhesives; air or moisture permeability of paint films; and the use of membranes in separations processes.

Of particular interest is the process that led to this study, viz., drying of polymer based coatings on paper in which a filled polymer solution is coated on a continually moving web of paper. The web passes through a dryer where the solvents are removed from the surface of the coating with the help of nozzles blowing air at a controlled velocity and temperature. Solvents move to the surface of the coating by molecular diffusion, which is often the rate controlling step of solvent removal. Controlling the drying process is important in order to obtain a coating free of defects.

Appropriate modeling of the drying process facilitates the selection of optimum operating conditions to produce a dry coating without defects. Drying models are benificial in finding drying conditions for new products, in productivity improvements in which line speed increases, and in the design of new drying equipment. Models [Vrentas et al., 1994] have been developed to describe the drying

process of coatings on continuous webs. An important parameter in drying models is the diffusion coefficient for solvent diffusing through the coated film. The diffusion coefficient is a function of the solvent concentration in the film, the amount of filler in the film, and the temperature of the film and surrounding air.

Mass transfer in filled polymers is a complicated process which involves not only diffusion in the continuous polymer phase. Other factors such as adsorption of penetrant on the surface of fillers and small gaps in the structure, which are filled by diffusing gases, affect the overall transfer of penetrant in a filled polymer. An application of the classical solution of Fick's diffusion equation to sorption data for filled polymers leads to an "effective" diffusion coefficient which in most cases is smaller than the true diffusivity in the polymer phase due to immobilization of gases from the presence of fillers. This subject is discussed in the next chapter.

The objective of this work was to measure sorption data on a filled polymer using a piezoelectric quartz crystal microbalance and to evaluate effective diffusion coefficients from the data. The diffusion coefficient was evaluated for various solvent concentrations, filler contents and temperatures.

Acrylic polymers are used for most paper coating applications, and typical solvents are toluene or water. The polymer chosen for this study was poly(vinyl acetate) (PVAC) and the solvent was toluene. This choice showed similarities in properties with a typical coating for paper, and the results for neat PVAC could be compared with experimental results of previous researchers in this field [Mikkilineni et al., 1995]. Coatings utilize a variety of fillers, additives, and optical brighteners. Calcium carbonate is a typical filler and it was chosen for use in this work. The results of this work were compared with known models for mass transfer in filled polymers.

CHAPTER II

BACKGROUND ON DIFFUSION OF PENETRANTS IN POLYMERS

The first section of this chapter contains a discussion of experimental methods for obtaining sorption data, with particular emphasis on the quartz crystal microbalance method used in this study. The next section contains a discussion of methods of analysis for the quartz crystal microbalance in order to obtain a diffusion coefficient. This is followed by several sections which contain discussions of various behaviors inherent to diffusion in polymers. Major topics discussed are Fickian and anomalous diffusion, the free volume theory of polymer-solvent diffusion, and mass transfer in heterogeneous materials.

Experimental Methods for Obtaining Diffusion Coefficients

Experimental methods for studying the diffusion of gases in polymers have been discussed by Felder and Huvard [1980]. Their historical overview dates back almost 170 years and contains discussions of many diffusion phenomena and methods. Another source, which contains more detailed demonstrations of the theory, is the work of Crank and Park [1968]. This section focuses on methods of greatest relevance to this work.

Fundamental Diffusion Equations

Diffusion of a gas in any material, rubber or plastic, amorphous or crystalline, neat or filled, involves transport of the gas from one part of the material to another. Just as the viscosity is a coefficient that describes the transport of momentum in a gas or liquid in the familiar Newton's law of viscosity, and the

heat transfer coefficient describes the transport of thermal energy in a material according to Fourier's law of heat conduction, the diffusion coefficient describes the transport of mass in a material in accordance with Fick's law of diffusion,

$$J = -D\frac{\partial C}{\partial x}, \tag{1}$$

where J is the rate of transfer of diffusing gas per unit area of a specified sectional area, C is the concentration of diffusing substance, x is the space coordinate measured normal to the section, and D is the diffusion coefficient, or diffusivity. This equation is referred to as Fick's first law of diffusion. The diffusion coefficient has dimensions of length^2 time^{-1} and in this work, has units cm^2 sec^{-1}. From a mass balance on an element of volume containing material, the differential equation of diffusion takes the form

$$\frac{\partial C}{\partial t} = \frac{\partial}{\partial x}\left(D\frac{\partial C}{\partial x}\right) + \frac{\partial}{\partial y}\left(D\frac{\partial C}{\partial y}\right) + \frac{\partial}{\partial z}\left(D\frac{\partial C}{\partial z}\right), \tag{2}$$

where D can be a function of C. If D is constant then equation 2 becomes

$$\frac{\partial C}{\partial t} = D\left(\frac{\partial^2 C}{\partial x^2} + \frac{\partial^2 C}{\partial y^2} + \frac{\partial^2 C}{\partial z^2}\right). \tag{3}$$

If the diffusion is in one direction, equations 2 and 3 simplify to what is commonly referred to as Fick's second law of diffusion,

$$\frac{\partial C}{\partial t} = \frac{\partial}{\partial x}\left(D\frac{\partial C}{\partial x}\right), \tag{4}$$

and, if the diffusion coefficient is constant,

$$\frac{\partial C}{\partial t} = D\frac{\partial^2 C}{\partial x^2}. \tag{5}$$

The equations for one-dimensional diffusion are valid for this work since thin polymer films were used.

General Sorption Methods for Studying Diffusion

In general, there are three experimental techniques from which diffusion coefficients are obtained. These are: sorption into or out of a polymer, permeation

through a membrane into a closed chamber, and permeation through a membrane into a flowing stream. Only sorption is discussed in detail in this thesis since this study used a sorption method.

Sorption methods are mainly used in measurements of equilibrium solubilities, two-stage sorption processes, slow processes, studies of anomalous diffusion, high-pressure measurements and studies of cracking and crazing [Felder and Huvard, 1980]. Categories of sorption measurements include integral sorption, integral desorption, interval sorption, and interval desorption. In integral sorption, the polymer is abruptly exposed to a step change in penetrant concentration at the boundaries of the polymer. In integral desorption, the polymer is initially equilibrated with a penetrant, and abruptly exposed to a penetrant-free atmosphere, usually a vacuum, until no penetrant remains in the polymer. Interval sorption and desorption are the same as integral sorption and desorption, respectively, except that the initial and final penetrant concentrations are greater than zero. In all four categories of sorption measurements, the mass of the penetrant in the polymer is measured as a function of time, either directly, as in gravimetric techniques, or indirectly by measuring a change in properties such as pressure or volume of the atmosphere surrounding the polymer.

The method used in this work involved determining the mass of the penetrant in the polymer indirectly by measuring a change in the frequency of a piezoelectric quartz crystal as a function of time. For both direct and indirect methods, the data usually appear as shown in Figure 1. The variable, M_t/M_∞, is plotted on the ordinate, where M_t is the instantaneous mass sorbed or desorbed and M_∞ is the mass sorbed or desorbed at equilibrium. Time, t or $\sqrt{t}$ is plotted on the absisca. In the integral sorption method, M_∞ is the ultimate final mass of the penetrant in the polymer. In the integral desorption method, M_∞ is the initial mass of the penetrant in the polymer. In the interval sorption or desorption method, M_∞ is the difference between the initial and the final mass of the penetrant in the polymer.

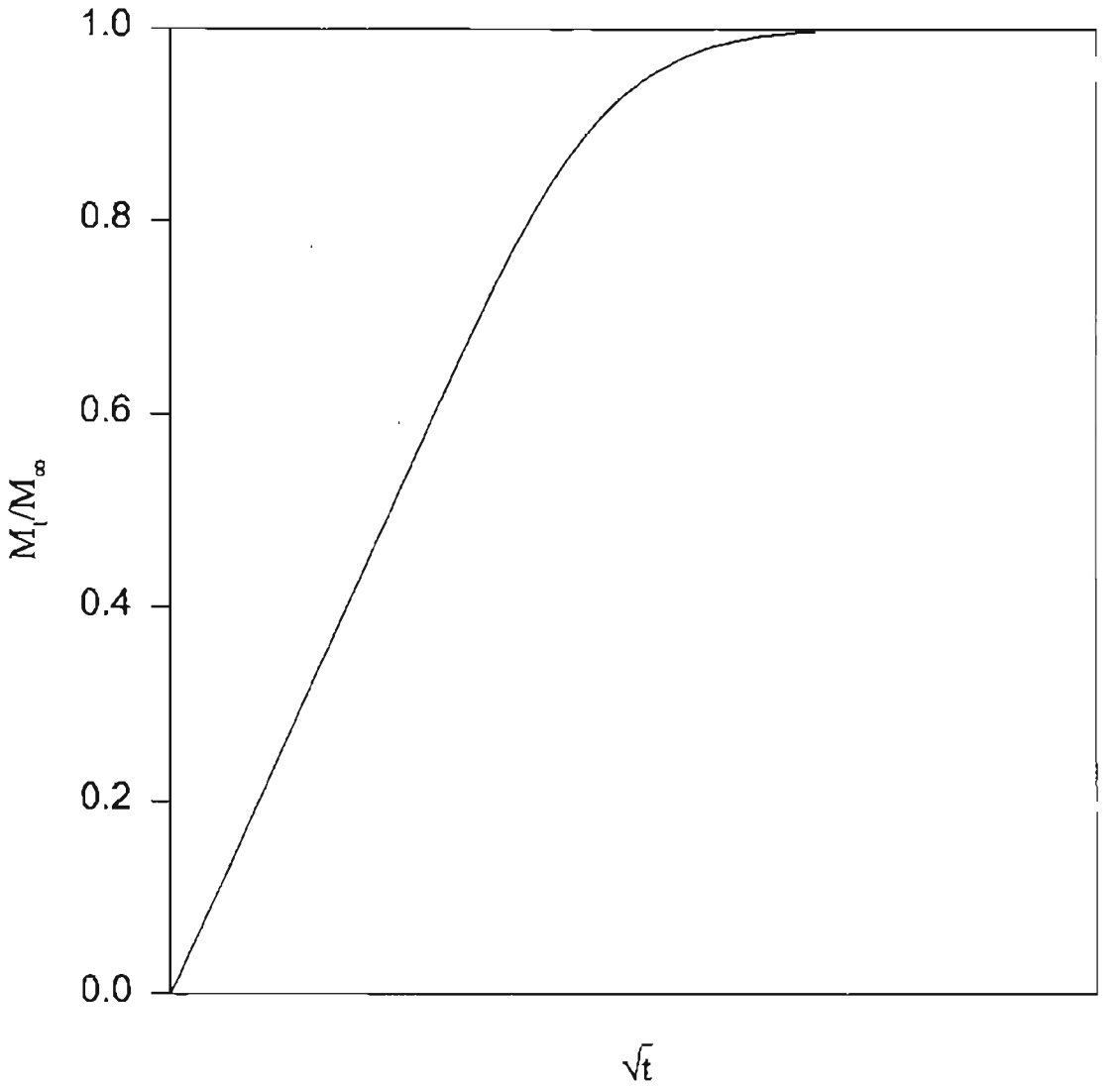

Figure 1. A Typical Reduced Sorption Curve Obtained from a Step-Change Sorption Experiment.

If a sorption experiment was followed by a desorption experiment to the initial penetrant level, one might expect that the sorption and desorption curves would coincide. However, this is only true for Fickian diffusion with a constant diffusion coefficient, D. If D increases with the penetrant concentration, such as toluene in PVAC as is used in this work, the sorption curve lies above the desorption curve. If D decreases with the penetrant concentration, the sorption curve lies below the desorption curve. If swelling is significant and stress relaxation of the polymer controls the penetration rate, the sorption curve is sigmoidal, but desorption from the swollen polymer is Fickian and initially relatively rapid. If relaxation occurs slowly, two stage sorption occurs. Fickian and Non-Fickian diffusion are discussed in a later section.

The Quartz Crystal Microbalance Sorption Apparatus

All data in this work were obtained with a quartz crystal microbalance (QCM). The QCM used in this work was developed by Deshpande [1993] to measure the diffusion characteristics of a penetrant in a polymer film. The QCM was later modified by Mikkilineni to reduce operational difficulties, increase the accuracy of the data, and increase the ease of operation of the apparatus [Mikkilineni, 1995]. This subsection discusses the QCM apparatus as it existed in the work of Mikkilineni [1995].

The principal component of the QCM was a 0.5 inch circular gold coated piezoelectric quartz crystal. A mechanical stress, when applied to a piezoelectric quartz crystal, induces an electric potential across the crystal, or vice versa, an electrical potential applied across a piezoelectric quartz crystal induces a mechanical strain in the crystal. This property of the quartz crystal facilitated extremely accurate measurements of the rate of diffusion of solvents in polymers. By including the quartz crystal in a circuit, a small electric potential was created across the crystal and the crystal vibrated at its resonant frequency.

A 6 MHz gold coated AT-cut piezoelectric quartz crystal was used in the experiments. The crystal was coated with a polymer solution. A penetrant diffusing into this polymer coating decreased the resonant frequency of the crystal. The resonant frequency of the piezoelectric quartz crystal was found to be extremely sensitive to changes in mass on the surface of the crystal. A load as low as 1 nanogram could cause a detectable change in the frequency of the quartz crystal [Mikkilineni, Tree, and High, 1995]. Since the quartz crystal was so sensitive to mass changes, a small change in the concentration of the solvent in the polymer caused a measurable change in the frequency, which allowed diffusion data to be obtained at low and closely spaced solvent concentrations.

The bulk of the QCM was constructed from a stainless steel six way cross chamber (Kurt J. Lesker Co., C6-0600) that had entrances at all six ports. Figure 2 shows a schematic diagram of the QCM. The chamber was operable from 10^{-11} torr to slight positive pressures and up to a maximum temperature of 500°C [Mikkilineni, 1995]. A standard quartz crystal sensor (Leybold Inficon, 750-207-G1) which housed and provided a circuit for the quartz crystal was placed in the right port of the chamber (see Figure 2). A thin-film-deposition controller (Leybold Inficon, XTC/2), interfaced to a computer, monitored the frequency of the crystal. A computer program recorded frequency as a function of time as the penetrant diffused into the polymer.

The QCM was enclosed in a box made of plywood lined with insulating material to accurately control the chamber and polymer film temperature. A heating element mounted on a metallic stand was used to heat the box. A fan was used to circulate the hot air in the box. The fan motor was mounted on the outside of the box to prevent overheating of the motor due to the high operating temperature in the box [Mikkilineni, 1995]. The motor was connected to the fan inside the box by an aluminum shaft and was mounted onto one side of the box.

A temperature controller (LFE Instruments, 2004) was used to regulate the temperature inside the box. A resistance temperature device was also mounted in the back port of the chamber (not shown in Figure 2) to measure the temperature

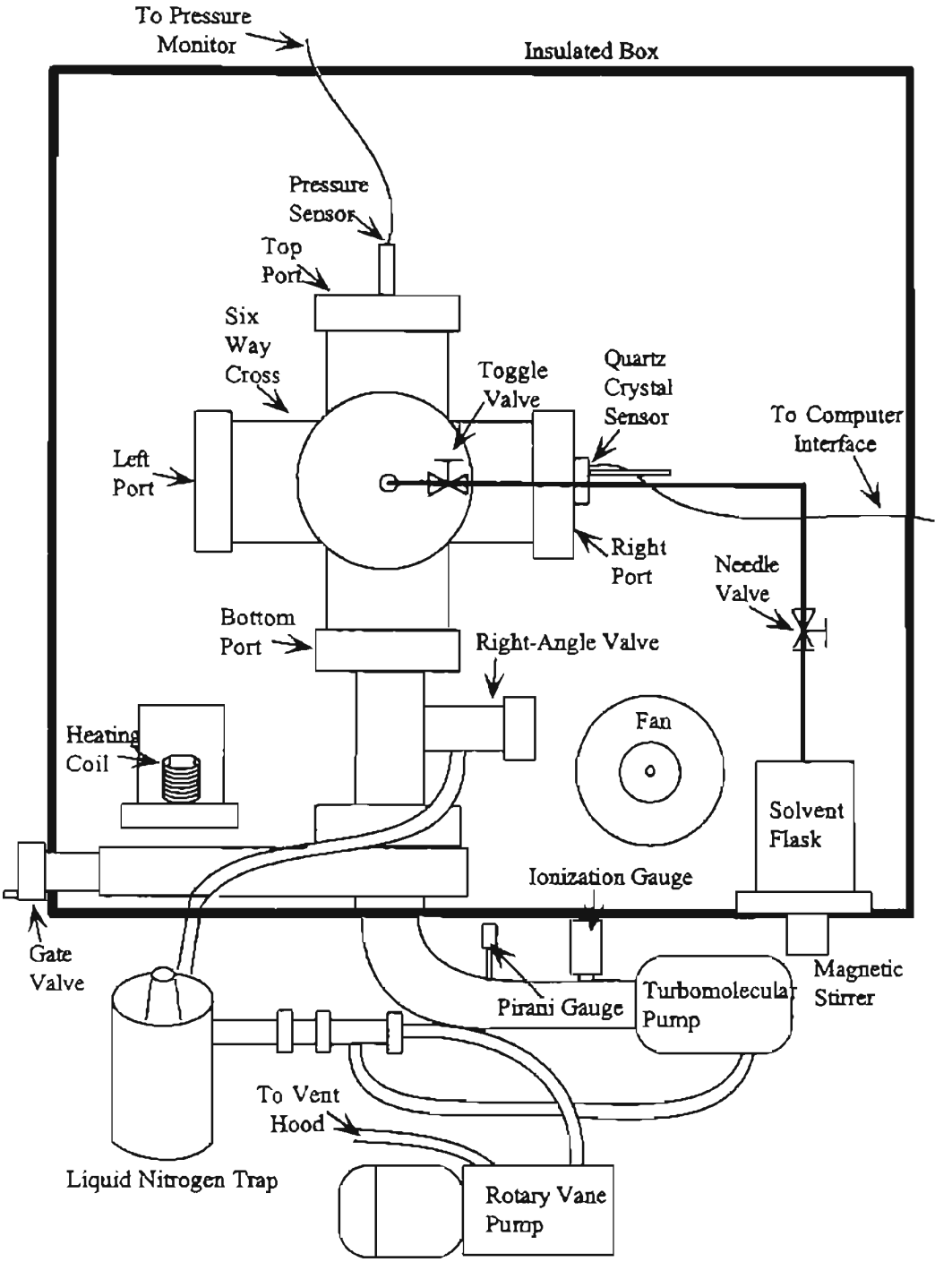

Figure 2. Schematic Diagram of the Quartz Crystal Microbalance.

inside the chamber. Several resistance temperature devices were installed in the box and surface mounted onto the cross chamber to check for temperature gradients in the box and chamber [Mikkilineni, 1995].

The chamber was evacuated to remove any contaminants, such as air or penetrant from previous experiments. The bottom port of the chamber led to two vacuum pumps. A rotary vane pump (Leybold Inficon, Trivac A 4-A) was used to obtain pressures of the order of 10^{-2} torr, and a turbomolecular pump (Leybold Inficon, Turbovac 50) was used to reduce pressures further, to the order of 10^{-7} torr. A liquid nitrogen trap (Kurt J. Lesker Co., LNF 1000) was used in line to keep solvent vapors from entering the pumps and oil vapors from entering the chamber. A gate valve (Kurt J. Lesker Co., SG0400) was connected to the turbomolecular pump and a right angle valve (Huntington Laboratories, EV 150) was connected to the rotary vane pump through the liquid nitrogen trap. The two valves were required to connect the chamber to the rotary vane pump or to the turbomolecular pump, so that vapors would not enter the turbomolecular pump during initial evacuation of the chamber with the rotary vane pump. To prevent the turbomolecular pump from overheating, cold water was circulated through a heat exchanger mounted on the pump casing.

A Pirani gauge (Leybold Inficon, PG3; sensor, TR901) and a hot-cathode ionization gauge (Leybold Inficon, IG3; sensor, 850-675-G5) were connected on the outside of the box to the pipe which connected the chamber with the turbomolecular pump. The gauges measured pressure in the chamber and were used only during the evacuation process. The Pirani gauge measured low vacuum ($\sim 1000 - 10^{-4}$ torr absolute) and the hot-cathode ionization gauge measured high vacuum ($\sim 10^{-2} - 10^{-10}$ torr absolute). A pressure gauge (Druck Instruments, DPI 265) was also mounted in the top port of the chamber to measure pressure in the chamber after the penetrant was introduced. This gauge can be used to measure pressures of solvent vapors in the chamber over the range of $0 - 19.999$ psia and can withstand temperatures up to 300°C [Mikkilineni, 1995].

The front port of the chamber was used to introduce solvent into the chamber. A jacketed metallic flask containing the penetrant was connected to the chamber using 1/4 in. stainless tubing. Water could be circulated through the flask to heat or cool the solvent to a desired temperature. A toggle valve was used to control the flow of penetrant into the chamber. A needle valve was used to isolate the flask. A quick connect coupling was used in the tubing connecting the solvent flask and the chamber to make solvent change in the flask easy [Mikkilineni, 1995]. A magnetic stirrer was used to ensure that the solvent was well mixed throughout the experiment.

Further modifications, made to the QCM for this work, are discussed in the next chapter. A detailed, stepwise experimental procedure is given in Appendix A.

Methods of Analyzing Data Obtained Using the Quartz Crystal Microbalance

Diffusion coefficients for polymer-penetrant systems are typically highly concentration dependent. However, all of the methods discussed in the literature assume that the diffusion coefficients are concentration independent. In order to calculate the concentration dependence, the sorption experiments are performed over small step changes in pressure driving the sorption. Over these small changes in driving force, the concentrations do not change significantly and the methods employing constant diffusion coefficients are valid.

Crank [1956] derived solutions for one-dimensional diffusion in a plane sheet. These solutions apply to diffusion into a sheet of polymer assuming that the edges of the sheet can be ignored and diffusion can be considered as taking place only through the surface of the sheet. Since the polymer films used in this work were about 3 to 5 μm in thickness and about 5 to 8 mm in diameter, this assumption is valid. The derivation starts with the one-dimensional diffusion equation

$$\frac{\partial C}{\partial t} = D\frac{\partial^2 C}{\partial x^2}. \tag{6}$$

The initial and boundary conditions for this equation are

$$C(x,0) = C_1, \tag{7}$$

$$C(L,t) = C_0, \tag{8}$$

$$\frac{\partial C}{\partial x}(0,t) = 0. \tag{9}$$

The initial condition indicates that at $t = 0$ the entire polymer film is at a uniform concentration of C_1. The first boundary condition indicates that at any time after the beginning of diffusion into the polymer film, the concentration at the surface of the film, $x = L$, is maintained constant at C_0. This boundary condition emphasizes the importance of introducing the penetrant into the quartz crystal microbalance chamber instantaneously and, during the sorption experiment, maintaining a constant concentration at the surface of the polymer film. This requires the pressure in the chamber to be constant. Since the QCM is mainly used for step change absorption experiments, C_0 is greater than C_1. The second boundary condition indicates that there is no transport of penetrant through the bottom of the polymer film at $x = 0$. The exact solution of equation 6 subject to equations 7, 8 and 9 is given by Crank [1956] as

$$\frac{C - C_1}{C_0 - C1} = \sum_{n=0}^{\infty}(-1)^n \mathrm{erfc}\frac{(2n+1)L - x}{2\sqrt{(Dt)}} + \sum_{n=0}^{\infty}(-1)^n \mathrm{erfc}\frac{(2n+1)L + x}{2\sqrt{(Dt)}}. \tag{10}$$

The concentration of penetrant in the polymer film according to equation 10 is a function of time and position inside the film. The mass of penetrant in the polymer film at a specified time could be determined by integrating the concentration profile of equation 10 over the thickness of the slab at that time. From this procedure, the ratio of the mass sorbed by the polymer film at time t to the mass sorbed by the film at equilibrium ($t = \infty$) is [Crank, 1956]

$$\frac{M_t}{M_\infty} = 1 - \frac{8}{\pi^2}\sum_{n=0}^{\infty}\frac{1}{(2n+1)^2}\exp\left\{\frac{-D(2n+1)^2\pi^2 t}{4L^2}\right\}. \tag{11}$$

The corresponding solution that is useful for small times is [Crank, 1956]

$$\frac{M_t}{M_\infty} = 2\left(\frac{Dt}{L^2}\right)^{1/2}\left\{\pi^{-1/2} + 2\sum_{n=1}^{\infty}(-1)^n \mathrm{ierfc}\frac{nL}{\sqrt{(Dt)}}\right\}. \tag{12}$$

The important assumptions made in the derivation of equations 11 and 12 are that

1. Diffusion of penetrant into the polymer film occurs in one dimension.

2. Concentration of the penetrant at the surface of the film is constant.

3. The diffusion coefficient is a constant.

The first assumption holds well since the polymer films used in this work had a small thickness compared to the surface area coated on the quartz crystal. The thicknesses of the films were about 3 to 5 μm, while the diameters of the films were about 5 to 8 mm. The second assumption holds well in this work since the pressure of the penetrant in the chamber was increased quickly and leaks in the chamber were small. Since diffusion of a penetrant into a polymer is dependent on the concentration of penetrant in the film, the third assumption can only be satisfied approximately if the sorption experiment is carried out over a small step of change in concentration. This was achieved by introducing small amounts of penetrant into the chamber for a sorption run and performing a series of these small step change absorption experiments over the penetrant concentration range of interest.

Obtaining a Sorption Curve from Frequency Data

As the penetrant diffuses into the polymer film, a computer records the frequency as a function of time. Figure 3 shows a plot of a typical response of crystal frequency to a step change in pressure of the penetrant in the chamber where the polymer coated quartz crystal is housed. From the frequency responce data, graphs of M_t/M_∞ versus t or $\sqrt{t}$ are generated.

Theoretical details of piezoelectric quartz crystals are described in Mikkilineni's thesis [1995]. The essence of the theory is that the change of mass, Δm, on the quartz crystal is proportional to the frequency change, Δf, of the crystal,

$$\Delta m = k\Delta f, \tag{13}$$

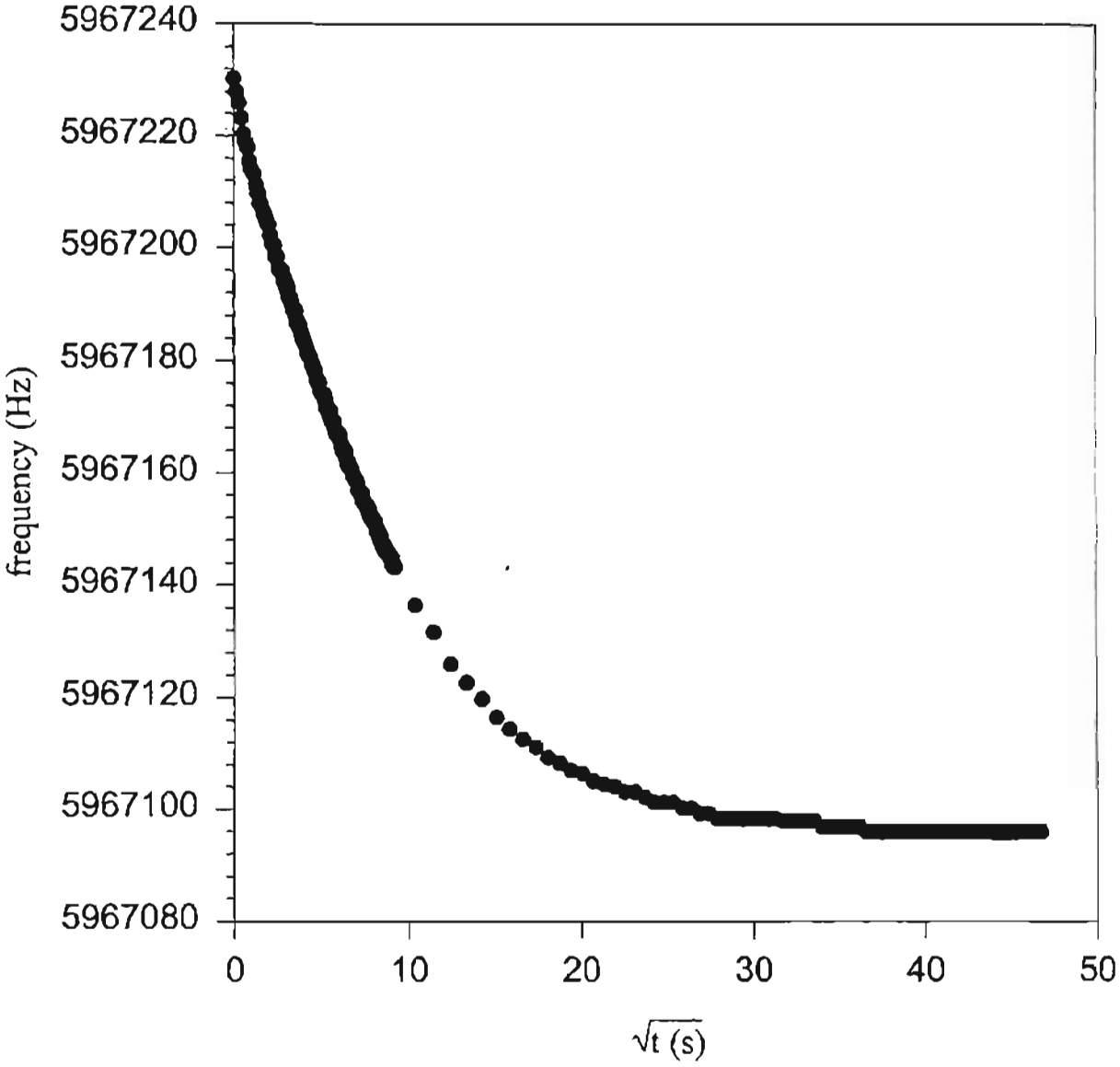

Figure 3. Frequency Response of a Coated Quartz Crystal to a Step Change in Chamber Pressure.

where k is a proportionality constant. The mass change of penetrant in the polymer film at time, t, after the step change in penetrant pressure, is

$$M_t = k(f_t - f_1), \tag{14}$$

where f_1 is the frequency of the coated crystal before the penetrant is allowed into the chamber, and f_t is the frequency of the coated crystal at time t after the penetrant is allowed into the chamber. If only the first step of the sorption experiment is considered, then f_1 is the frequency of the polymer coated, solvent-free crystal and M_t is the total mass of penetrant in the polymer at time t. If the n^{th} step is considered ($n > 1$), then f_1 is the frequency of the polymer coated crystal before the step change and M_t is the change in mass of the penetrant in the polymer from the onset of the step change to time t after the step change in chamber pressure. After sufficiently large time ($\sim$ 15 minutes for unfilled polymer and up to 6 hours for filled polymer), the penetrant comes to equilibrium with the polymer film and the mass of penetrant in the film approaches a constant value. Polymer-solvent equilibrium is established, and equation 14 is still valid as $t \to \infty$. The ratio of the mass sorbed at time t, M_t, to the mass sorbed at equilibrium, M_∞, can be expressed as

$$\frac{M_t}{M_\infty} = \frac{f_t - f_1}{f_\infty - f_1}, \tag{15}$$

where f_∞ is the frequency of the coated crystal at polymer-solvent equilibrium. Figure 4 shows a plot of M_t/M_∞ obtained from equation 15 versus $\sqrt{t}$. Such a plot is called a reduced sorption curve. Once the M_t/M_∞ data are obtained, the diffusion coefficients can be estimated.

Evaluating Diffusion Coefficients Using the Half-Time Method

The simplest technique for estimating the diffusion coefficient is the half-time method. Equation 11 is used, and the value of t/L^2 for which $M_t/M_\infty = 1/2$ is approximately given as

$$\left(\frac{t}{L^2}\right)_{1/2} = -\frac{4}{\pi^2 D} \ln\left\{\frac{\pi^2}{16} - \frac{1}{9}\left(\frac{\pi^2}{16}\right)^9\right\}, \tag{16}$$

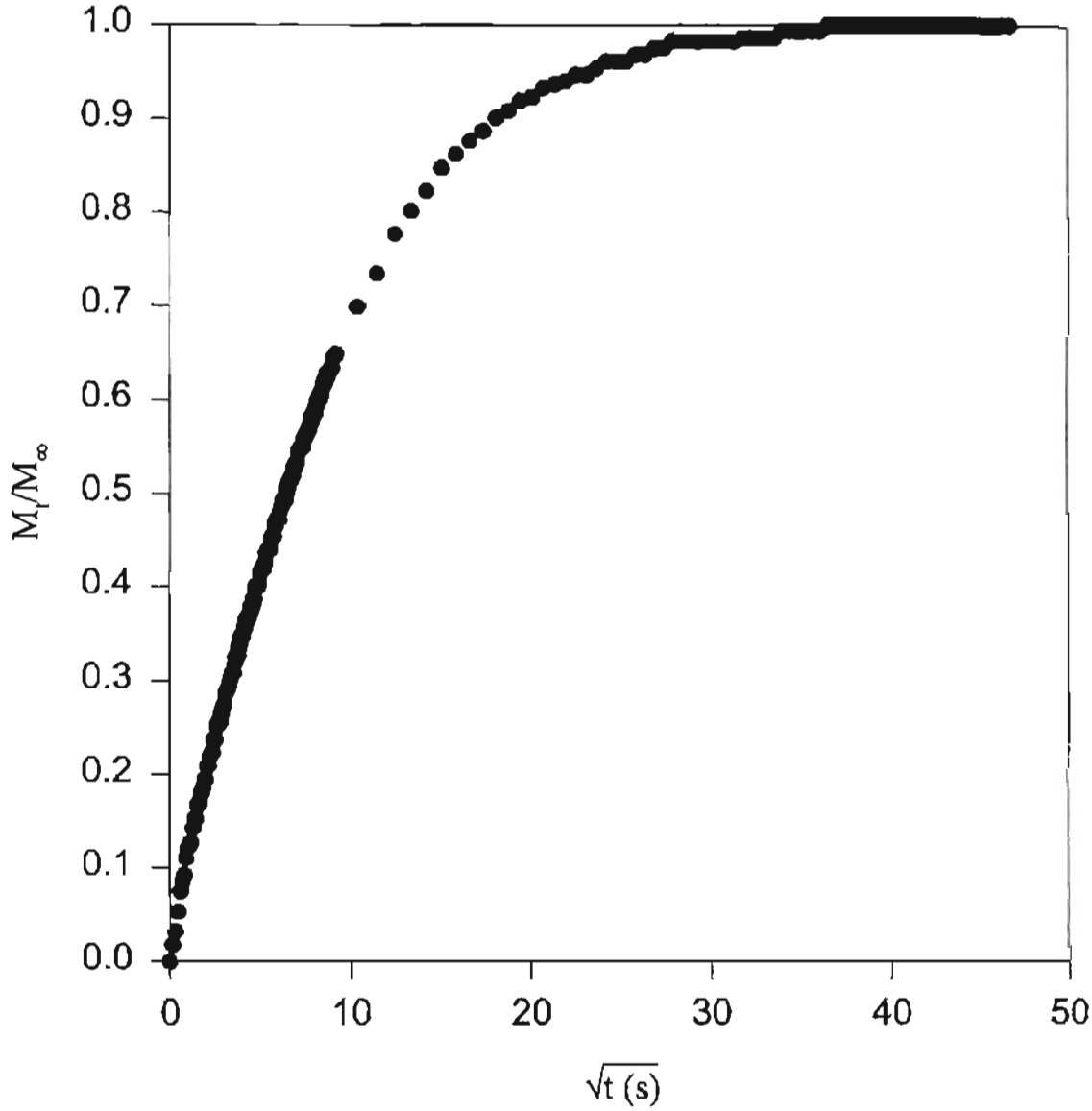

Figure 4. Sorption Curve Obtained from Frequency Measurements.

with an error of about 0.001 per cent [Crank, 1956]. After performing the necessary arithmetic, the time $t_{1/2}$ for which M_t/M_∞ equals 1/2 for a plane sheet is given by

$$D = \frac{0.19675L^2}{t_{1/2}}. \tag{17}$$

Evaluating Diffusion Coefficients Using the Initial Slope Method

The initial slope method was initially used for evaluating the diffusion coefficients from data taken on the quartz crystal microbalance at Oklahoma State University. All the sorption curves obtained by Deshpande [1993] and Mikkilineni [1995] were analyzed with the initial slope method.

During the initial stages of the sorption experiment, the polymer film behaves as a semi-infinite medium and the ratio of the mass uptake at time t to the mass uptake at time $t = \infty$ increases linearly with $\sqrt{t}$, often to as much as 50 per cent of M_t/M_∞ [Crank and Park, 1968]. At small times, the summation term in equation 12 can be neglected, and the equation becomes

$$\frac{M_t}{M_\infty} = \frac{2}{\sqrt{\pi}}\left(\frac{Dt}{L^2}\right)^{1/2}. \tag{18}$$

According to equation 18, the average diffusion coefficient can be calculated as

$$D = \frac{\pi}{4}R_i^2L^2, \tag{19}$$

where R_i is the initial slope of the M_t/M_∞ vs. $\sqrt{t}$ curve. If the sorption curve is approximately linear up to $M_t/M_\infty = 1/2$, equation 17 and equation 19 would yield about the same diffusion coefficient [Crank, 1956]. Figure 5 shows an example of an evaluation of the diffusion coefficient by the initial slope method. The fractional solvent uptake was plotted as a function of the square root of time. Linear regression was used to determine the slope of the initial portion of the sorption, from $M_t/M_\infty = 0$ to 0.5. Equation 19 was used to calculate the diffusion coefficient. The sorption curve in this example is linear well above 50 per cent of M_t/M_∞. Most of the experimental sorption curves obtained in this work were linear to approximately 25 per cent. The length of the initial linear portion of the sorption curve will vary between sorption experiments depending on the concentration dependence of the diffusion coefficient [Crank and Park, 1968].

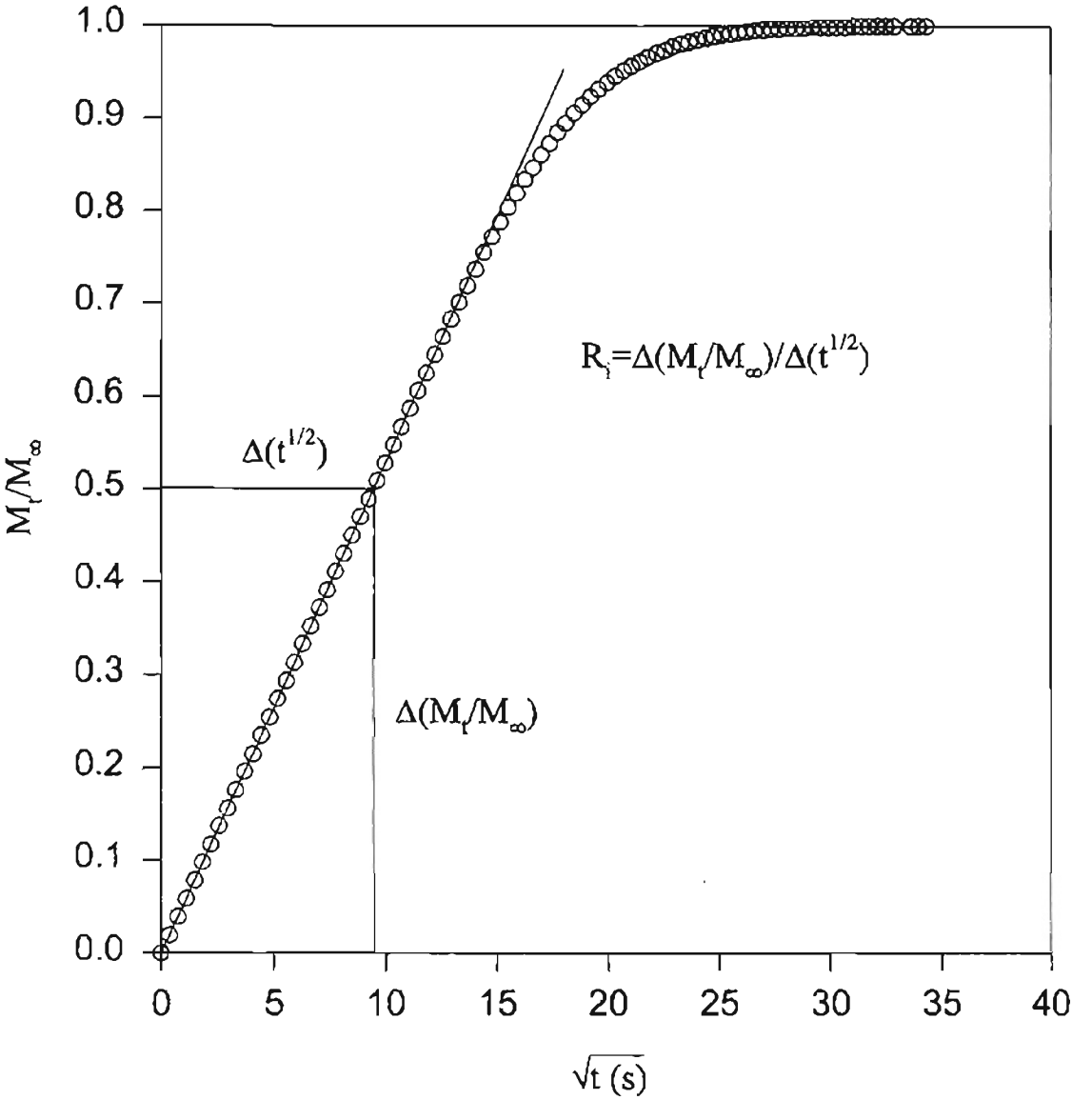

Figure 5. Calculation of Diffusion Coefficients Using the Initial Slope Method.

Evaluating Diffusion Coefficients Using the Limiting Slope Method

The limiting slope method [Balik, 1996; Palekar, 1995] uses only the first term of the series in equation 11. At large times, a plot of $\ln\{1 - M_t/M_\infty\}$ versus time approaches a straight line, and the average diffusion coefficient can be calculated as

$$D = -\frac{4R_l L^2}{\pi^2}. \tag{20}$$

R_l is the limiting slope of the $\ln\{1 - M_t/M_\infty\}$ vs. t curve. Figure 6 shows an example of an evaluation of the diffusion coefficient by the limiting slope method. $\ln\{1 - M_t/M_\infty\}$ was plotted as a function of time. Linear regression was used to determine the limiting slope, from $M_t/M_\infty = 0.99$ to 0.996. Equation 20 was used to calculate the diffusion coefficient.

Evaluating Diffusion Coefficients Using the Moment Method

In this work, the moment method was used to evaluate the diffusion coefficients. The moment method [Felder and Huvard, 1980; Palekar, 1995] is advantageous since the entire sorption curve is used instead of just the initial or final portion as in the methods discussed above. The quantity

$$\tau_s = \int_0^\infty \left[1 - \frac{M_t}{M_\infty}\right] dt \tag{21}$$

is first calculated by numerical integration, where τ_s is the first moment of the monotonically increasing curve, M_t/M_∞ versus time. Then, the average diffusion coefficient is calculated by

$$D = \frac{L^2}{3\tau_s}. \tag{22}$$

Details of the derivation of equation 22 are given in Appendix B. Figure 7 shows an example of the evaluation of the diffusion coefficient by the moment method. To calculate τ_s, a plot was made of $1 - \frac{M_t}{M_\infty}$ vs t as shown in Figure 7. The first moment, τ_s, is the area under the curve of Figure 7 and was found by numerical integration. The trapezoidal rule was used in this work to find the area under the curve.

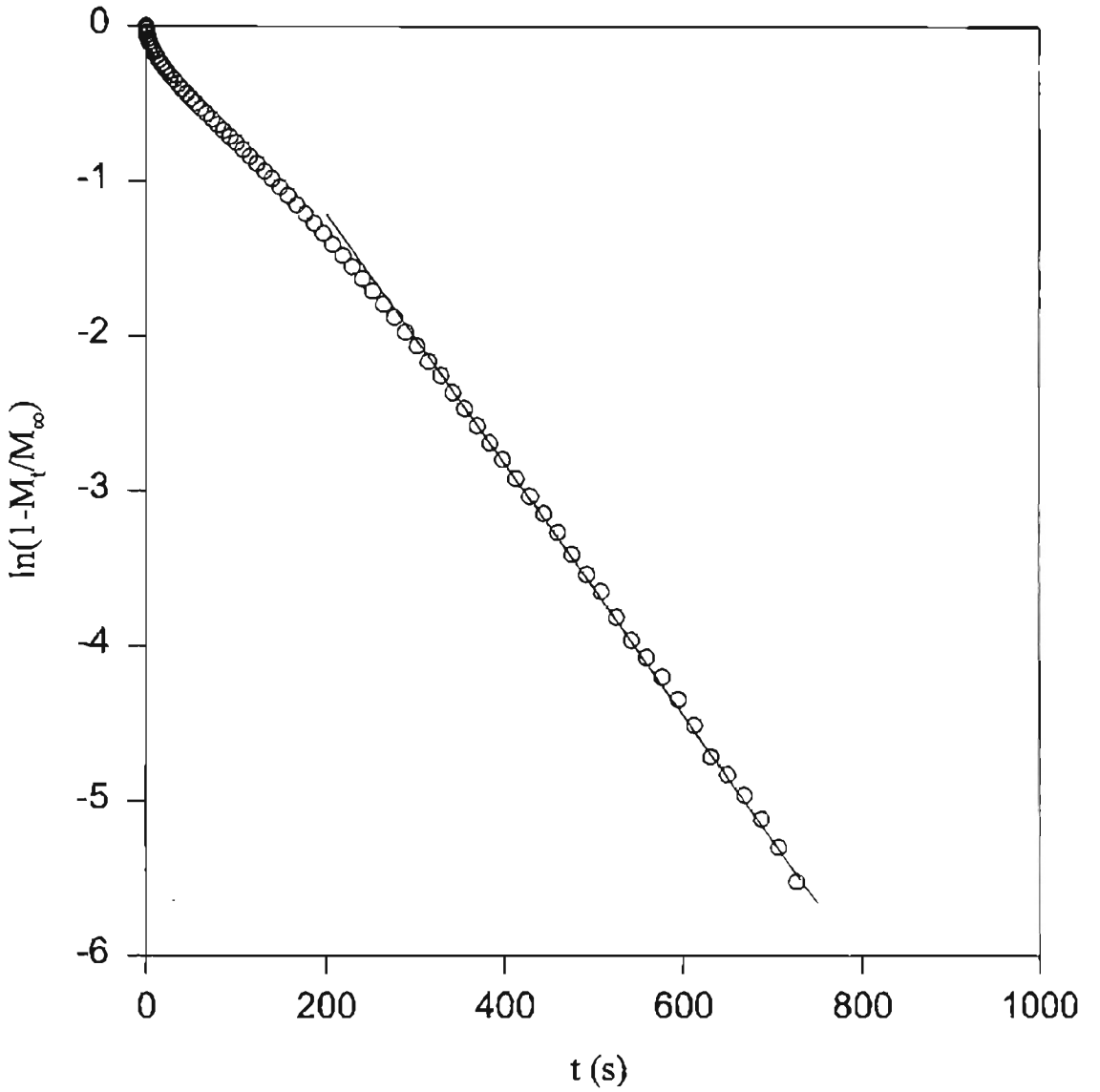

Figure 6. Calculation of Diffusion Coefficients Using the Limiting Slope Method.

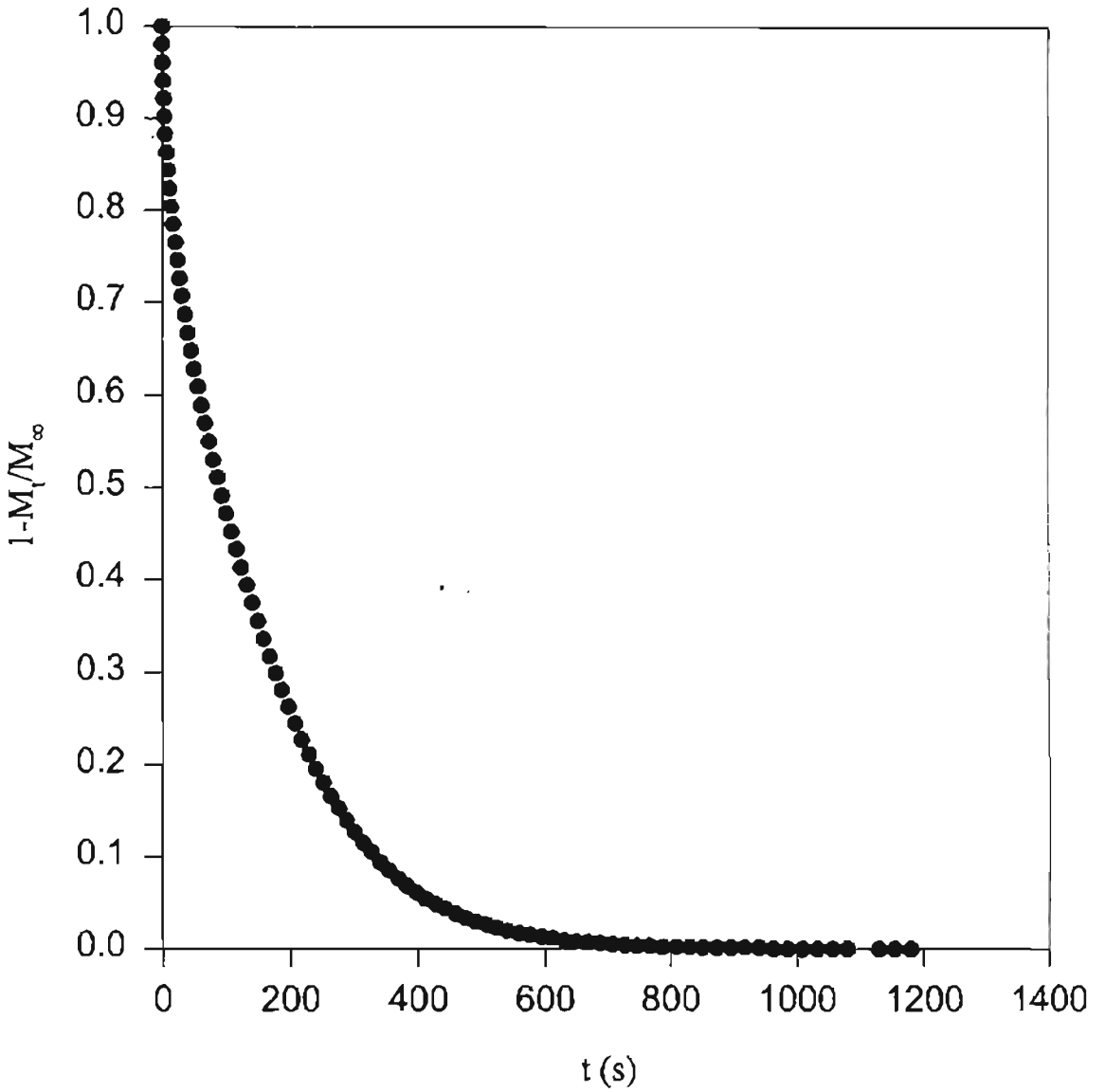

Figure 7. Calculation of Diffusion Coefficients Using the Moment Method.

Evaluating the Weight Fraction of Penetrant in the Polymer Film

Since the diffusion coefficient is a function of the concentration of the penetrant in the polymer film, equations 17, 19, 20 and 22 give average diffusion coefficients over the concentration range. Vrentas et al. [1977] has concluded that the average diffusion coefficient obtained from a step-change sorption experiment is equal to the diffusion coefficient at a concentration which is 0.7 of the way across the concentration interval, with less than 5% error. (See Equation 25.)

The equilibrium weight fraction of the penetrant in the polymer film, w_1^{eq}, is the ratio of the mass of the penetrant at equilibrium, M_∞, to the total mass of the polymer-solvent mixture at equilibrium, M_∞^{tot},

$$w_1^{eq} = \frac{M_\infty}{M_\infty^{tot}}. \tag{23}$$

Since, according to equation 13, the change of mass on a quartz crystal is proportional to the change in crystal frequency, equation 23 becomes

$$w_1^{eq} = \frac{f_\infty - f_1}{f_\infty - f_0}. \tag{24}$$

where f_0 is the frequency of the bare, uncoated crystal. The weight fraction which corresponds to the average diffusivity can be calculated by

$$w_1^{av} = w_{1i} + 0.7(w_{1f} - w_{1i}), \tag{25}$$

where w_{1i} is the weight fraction of penetrant before introducing more penetrant, and w_{1f} is the weight fraction of penetrant at equilibrium after introducing the penetrant.

Diffusion of Organic Penetrants into Polymers at Temperatures above the Glass Transition Temperature, T_g

Diffusion in polymer-penetrant systems do not follow the laws of the classical theory of molecular diffusion [Crank and Park, 1968]. There has been considerable interest in understanding the anomalous behavior of diffusion in polymer-penetrant systems [Vrentas et al., 1986]. However, it is also of interest to discover

the circumstances under which polymer-penetrant systems can be analyzed using classical or Fickian theory. Generally, Fickian theory can be used to describe diffusion in polymer-penetrant systems which have high temperatures and concentrations, since the polymer-penetrant system behaves as a purely viscous fluid under these conditions. Diffusion at low concentrations and temperatures below the glass transition temperature can also be analyzed with the classical theory since the system has properties of an elastic solid [Vrentas et al., 1986]. At intermediate temperatures and concentrations, diffusion in the polymer-penetrant system can have anomalous or non-Fickian behavior which are caused by viscoelastic effects [Vrentas et al., 1986]. This section discusses the mechanisms of diffusion of penetrants into polymers at temperatures above the glass transition temperature, and discusses typical Fickian sorption features.

Diffusion of simple gases such as hydrogen, argon, nitrogen and carbon dioxide requires a limited rotational oscillation of only one or two monomer units in order to translate from one position to a neighboring one since the molecular size of such gases is small compared to the monomer unit of a polymer, however if a gas has a molecular size comparable or larger than the monomer unit of the polymer, a cooperative movement by the Brownian motion of several monomer units, i.e. a polymer segment, must take place during diffusion [Fujita, 1968]. Organic vapors, such as toluene which was used in this work, are among such large molecular size penetrants. The diffusion of organic vapors in polymers exhibit different features in the regions above and below the glass transition temperature, T_g, of a polymer. These features are simple at temperatures above T_g and complex at temperatures below T_g [Fujita, 1968].

At temperatures well above the glass transition temperature, polymers are in a rubbery state and diffusion of penetrants in polymers usually follow Fick's law. The presence of the penetrant weakens the molecular interaction between adjoining chains, increasing the magnitude of Brownian motion within the polymer and therefore increases the rate of penetrant diffusion [Felder and Huvard, 1980]. This effect increases with the amount of penetrant present, so the diffusion

coefficient of organic vapors in rubbery polymers usually exhibits a concentration dependence [Felder and Huvard, 1980].

In Fickian diffusion in a polymer film during sorption, the distribution of penetrant, and the change of penetrant concentration with time, are governed by Fick's one-dimensional, differential equation for diffusion. The space coordinate is taken in the direction normal to the polymer film. The solution of this equation depends on the initial and boundary conditions for the penetrant concentration, C, and on how the diffusion coefficient, D, varies with C. Solutions for constant D were shown earlier. Solutions for a concentration dependent D are given by Crank [1956]. Mathematical studies of Crank and coworkers have developed the following summary of sorption features which are Fickian or normal type [Fujita, 1968].

1. Both absorption and desorption curves are linear in the initial stage. For absorption, the linear region extends over 60% or more of M_∞, where M_∞ is the amount of vapor absorbed per gram of dry polymer until the sorption equilibrium is reached. For $D(C)$ increasing with C the absorption curve is linear almost up to the final sorption equilibrium.

2. Above the linear portions both absorption and desorption curves are concave to the abscissa axis, irrespective of the form of $D(C)$.

3. When the initial concentration C_i and the final concentration C_f are fixed, a series of absorption curves for films of different thicknesses are superposable to a single curve if each curve is replotted in the form of a reduced curve, i.e. M_t is plotted against $t^{1/2}/L$. This same applies to the corresponding series of desorption curves.

4. The reduced absorption curve so obtained always lies above the corresponding reduced desorption curve if D is an increasing function of C between C_i and C_f. Both reduced curves coincide over the entire range of t when D is

constant in this concentration interval. The divergence of the two curves becomes more marked as D increases more strongly with C in the concentration range considered.

5. For absorptions from a fixed C_i to different C_f's, the initial slope of the reduced curve becomes larger as the concentration increment $C_f - C_i$ becomes larger, provided that D increases monotonically with C in the range considered. This same applies to the reduced desorption curves which start from different C_i's to a fixed C_f.

Criteria 1, 2 and 3 are independent of how D varies with C. Therefore, these three criteria are checked to determine whether a given polymer-penetrant system exhibits Fickian diffusion. Criteria 1 and 2 can be checked easily by inspecting the appearance of the sorption curves. Since criterion 3 requires sorption measurements to be made with films of different thicknesses, a system is often regarded as Fickian if experimentally determined sorption curves have appearances consistent with criteria 1 and 2 [Fujita, 1968].

Free Volume Theory

A theory that has been well accepted for describing the temperature and concentration dependence of the mutual diffusion coefficient in polymer-solvent systems is the free-volume theory of transport developed by Vrentas and Duda [Duda et al., 1982]. Vrentas and Duda [Vrentas and Duda, 1976; Vrentas et al., 1985] proposed the following equation for the solvent self-diffusion coefficient, D_1, in a polymer-solvent system,

$$D_1 = D_0 \exp\left(-\frac{E}{RT}\right) \exp\left(-\frac{\gamma(w_1\hat{V}_1^* + w_2\xi\hat{V}_2^*)}{\hat{V}_{FH}}\right), \tag{26}$$

$$\frac{\hat{V}_{FH}}{\gamma} = w_1\frac{K_{11}}{\gamma}(K_{21} + T - T_{g1}) + w_2\frac{K_{12}}{\gamma}(K_{22} + T - T_{g2}). \tag{27}$$

In equations 26 and 27, D_0 is a constant preexponential factor, E is the energy per mole of molecules to overcome intermolecular attractive forces, R is the ideal gas constant, T is the temperature, w_I is the mass fraction of component I ($I = 1$ for solvent; $I = 2$ for polymer), $\hat{V}_I^*$ is the specific critical hole free volume of component I required for a jump, ξ is the ratio of the critical molar volume of the solvent jumping unit to the critical molar volume of the polymer jumping unit, K_{11} and K_{21} are free-volume parameters for the solvent, K_{12} and K_{22} are free-volume parameters for the polymer, γ is an overlap factor which is introduced because the same free volume is available to more than one molecule, $\hat{V}_{FH}$ is the average hole free volume per gram of mixture, and T_{gI} is the glass transition temperature of component I.

Since this theory presents an expression for the self-diffusion coefficient, D_1, expressing the mutual diffusion coefficient, D (measured in the sorption experimental apparatus, and required for process calculations), in terms of D_1 is desirable. Duda et al. [1979] proposed an approximation for low solvent concentrations which couples D to the self-diffusion coefficient for polymer solvent systems,

$$D = \frac{D_1 w_1 w_2}{RT} \left(\frac{\partial \mu_1}{\partial w_1} \right)_{T,p} . \tag{28}$$

In this equation, μ_1 is the chemical potential of the solvent. The Flory-Huggins theory was used to determine the concentration dependence of the solvent chemical potential [Duda et al., 1982]. The Flory-Huggins equation can be written as

$$\mu_1 = \mu_1^0 + RT \left(\ln \phi_1 + \chi (1 - \phi_1)^2 + (1 - \phi_1) \right), \tag{29}$$

where ϕ_1 is the solvent volume fraction in the solution and χ is the polymer-solvent interaction parameter, which is assumed to be independent of temperature. Introduction of equations 26, 27, and 29 into equation 28 yields the following expression for the mutual diffusion coefficient, D, in a rubbery polymer-solvent system [Duda et al., 1982]

$$D = D_1 (1 - \phi_1)^2 (1 - 2\chi\phi_1), \tag{30}$$

$$D_1 = D_0 \exp\left(-\frac{E}{RT}\right) \exp\left(-\frac{\gamma(w_1\widehat{V}_1^* + w_2\xi\widehat{V}_2^*)}{\widehat{V}_{FH}}\right) \tag{31}$$

$$\frac{\widehat{V}_{FH}}{\gamma} = w_1\frac{K_{11}}{\gamma}(K_{21} + T - T_{g1}) + w_2\frac{K_{12}}{\gamma}(K_{22} + T - T_{g2}). \tag{32}$$

$$\phi_1 = \frac{w_1\widehat{V}_1^0}{w_1\widehat{V}_1^0 + w_2\widehat{V}_2^0}, \tag{33}$$

where $\widehat{V}_I^0$ is the specific volume of pure component I.

In this version of the free volume theory, there are 13 independent parameters to be evaluated. Grouping some of them together leaves only 10 parameters which are required to determine the mutual diffusion coefficient, D: K_{11}/γ, $K_{21} - T_{g1}$, K_{12}/γ, $K_{22} - T_{g2}$, $\widehat{V}_1^*$, $\widehat{V}_2^*$, D_0, E, ξ and χ.

The parameters $\gamma\widehat{V}_1^*/K_{11}$ and $K_{21} - T_{g1}$ can be determined from data for solvent viscosity as a function of temperature, $\eta_1(T)$, by using a non-linear regression to correlate the viscosity data with

$$\ln\eta_1 = \ln A_1 + \frac{(\gamma\widehat{V}_1^*/K_{11})}{(K_{21} - T_{g1}) + T}, \tag{34}$$

where the parameters, A_1, $\gamma\widehat{V}_1^*/K_{11}$ and $K_{21} - T_{g1}$ are assumed to be independent of temperature [Duda, 1983].

The parameters $\gamma\widehat{V}_2^*/K_{12}$ and $K_{22} - T_{g2}$ can be determined from polymer melt viscosity data as a function of temperature, $\eta_2(T)$, by using a non-linear regression to correlate the data with [Duda, 1983]

$$\ln\eta_2 = \ln A_2 + \frac{(\gamma\widehat{V}_2^*/K_{12})}{(K_{22} - T_{g2}) + T}. \tag{35}$$

The critical volumes, $\widehat{V}_1^*$ and $\widehat{V}_2^*$, can be estimated to be the specific volumes of the solvent and polymer at 0 K. Molar volumes at 0 K can be estimated using group contribution methods developed by Sugden and Biltz [Duda, 1983].

The parameter χ can be determined from solubility data in which the equilibrium weight fraction of the penetrant in the polymer is known as a function of the solvent vapor pressure, p_1, using the Flory-Huggins equation [Duda, 1983],

$$\frac{p_1}{p_1^0} = \phi_1 \exp\{(1 - \phi_1) + \chi(1 - \phi_1)^2\}, \tag{36}$$

where p_1^0 is the penetrant saturation vapor pressure.

Lumping the parameters D_0 and E into the parameter D_{01} gives

$$D_{01} = D_0 \exp\left(-\frac{E}{RT}\right), \tag{37}$$

which is the Arrhenius form of temperature dependence. The parameters D_{01} and ξ can be determined by correlating diffusion coefficient data with a nonlinear regression analysis of equation 30 [Duda, 1983].

Anomalous Diffusion of Penetrants into Polymers

Deviations from the Fickian type of process are generally described as anomalous or "non-Fickian" and are almost always observed when the polymer is studied at temperatures below T_g, or within roughly 10°C above T_g [Felder and Huvard, 1980]. In general, the polymers in which anomalies are observed are hard and glassy while normal sorption is observed in soft and rubbery materials. Polymeric materials in the rubbery state respond rapidly to changes in condition, but polymers in the glassy state take longer to come to equilibrium. For example, as the concentration in a polymer solution changes with time, the system must adjust to new conformations consistent with new values of concentration. Anomalous mass transfer processes are associated with the sluggish relaxation of large polymer molecules; however, in rubbery polymers which follow a Fickian diffusion process, relaxation of polymer molecules is fast compared to the diffusion process [Vrentas and Duda, 1979].

Fickian diffusion at temperatures above the glass transition, T_g, has been designated as case I diffusion and D depends only on concentration. As the glass transition temperature, T_g, of the polymer is approached, D begins to depend on time explicitly as well as on concentration. At moderate penetrant activities when swelling is appreciable and the temperature is less than, but within about 10°C of T_g, the mechanism of penetration may change from Fickian diffusion to a stress relaxation-controlled process in which the penetrant advances in a sharply

defined front at a nearly uniform velocity. This mechanism is designated as case II transport [Felder and Huvard, 1980]. The two modes of transport are easily distinguished from the sorption results. In both modes at small times t,

$$M_t = kt^n, \tag{38}$$

where M_t is the cumulative mass absorbed at time t. For case I (Fickian) transport $n = 1/2$, and for case II transport $n = 1$. On a plot of M_t vs. $\sqrt{t}$, case I transport would be linear at small times and case II transport would be sigmoidal. A mode designated "super-case II transport" has also been observed [Felder and Huvard] which has a sorption curve convex to the time axis at large times on a plot of M_t vs. t, where a similar plot would be linear for case II transport and concave for case I transport. Another anomaly which can occur is two stage sorption in which swelling penetrants are sorbed by glassy polymers and a rapid approach to an apparant equilibrium state, followed by a gradual shift to the true equilibrium state is observed. This phenomenon has been attributed to a gradual relaxation of the elastic cohesive force in the polymer, and to a time-varying surface concentration of penetrant [Felder and Huvard, 1980].

Diffusion anomalies also occur in polymers at temperatures well above T_g when crystallites or fillers are present [Park, 1968]. Fillers can lead to differences between diffusion coefficients obtained by steady-state and transient methods. Such differences have been reported for filled rubber [Barrer et al., 1963] at temperatures well above the glass transition temperature (T_g + 100°C) [Park, 1968]. These anomalies are not due to time effects, but are due to the complicated effect of microheterogeneities discussed in the next section.

In crystalline polymers, sigmoidal sorption curves are obtained at temperatures well above T_g and the sigmoidal character is more marked at higher crystalline-amorphous ratios. The effects in crystalline polymers are thought to result from slow responses to external changes in the crystalline regions, which could lead to a time-dependence in the crystalline-amorphous ratio and so produce time-dependent diffusion coefficients leading to sigmoidal sorption curves [Park, 1968].

Mass Transfer in Heterogeneous Systems

Diffusion in Filled Polymers

This discussion of diffusion in filled polymers begins with the effect of fillers in elastomers, since rubber products have been the most frequently studied filled polymer system [Barrer et al., 1962; Carpenter and Twiss, 1940; Morris, 1931; Smith, 1953; van Amerongen, 1947]. This discussion is, therefore, appropriate to introduce the present work since at the temperatures at which the experiments in this study were performed, the polymer, PVAC, is an elastomer. Most rubber compounds contain considerable amounts of fillers [van Amerongen, 1964]. The fillers may be spherical or non-spherical, and they may be reinforcing or non-reinforcing. Also, certain fillers could have a major effect on the diffusivity, solubility and permeability. Diffusion as mentioned above is the transport of a molecule from one part of a material to another. The solubility of foreign molecules in an elastomer is defined by a state of equilibrium between the molecules inside and outside of the polymer [van Amerongen, 1964]. In the equilibrium state the polymer has taken up as many penetrant molecules by dissolution as can be expected thermodynamically. As long as equilibrium has not been reached, the elastomer continues to absorb or desorb the foreign molecules, which involves transport by diffusion.

Permeation is more complex than diffusion since it involves the absorption of the gas on one side of a membrane, diffusion of the gas to the other side of the membrane, and finally evaporation or extraction from the other side of the membrane. The simplest solution-diffusion theory would be if the sorption of the gas at the surface of the membrane exposed to the gas obeyed Henry's law

$$C = \sigma p, \tag{39}$$

where C is the dissolved species concentration in equilibrium with a gas whose partial pressure is p and σ is the solubility coefficient, and that the absorbed gas diffuses through the membrane in accordance with Fick's law

$$J = D\nabla C, \tag{40}$$

where J is the flux of gas through the membrane and D is the diffusion coefficient or diffusivity. In these equations, the solubility and diffusion coefficients σ and D are assumed independent of concentration. If the above equations are valid, the steady-state permeation rate per unit area through a membrane of thickness L is

$$J = \sigma D \frac{\delta p}{L} = \frac{P}{L} \delta p, \tag{41}$$

where δp is the partial pressure difference across the membrane, and the product $P = \sigma D$ is the permeability of the membrane to the gas. Since permeation is experimentally easier to study than diffusion [van Amerongen, 1964], much of the work on filled rubbers has focussed on the process of permeation instead of pure diffusion. A good discussion on the subject of diffusion and permeation in heterogeneous media is given by Barrer [1968]. Barrer describes the derivation of differential diffusion equations taking into account the volume fractions of polymer, filler and vacuoles. These equations and the concept of vacuoles will be discussed later.

Most of the early studies of diffusion and permeation of gases in filled elastomers used gases with low molecular weight such as hydrogen, nitrogen, oxygen and air [Morris, 1931; Smith, 1953; van Amerongen, 1947, 1955]. This was a logical choice since the production of automotive tires is a major use of rubber and the permeability of air in tires was of great concern. Also, experimentation using gases with low molecular weight was easier since solute condensation was not a significant problem as when using high molecular weight condensable vapors. Van Amerongen [1955, 1964], showed that the diffusion coefficients of hydrogen, nitrogen and oxygen in natural rubber were greatly modified by the presence of fillers.

Many mineral fillers, lamellar fillers and carbon black fillers were used in van Amerongen's work [1955, 1964]. All of the rubber mixtures contained about 20% filler by volume. Mineral fillers such as whiting, aluminum oxide and barium sulfate reduced the diffusivity by about 10 to 15% at a temperature of 25°C and 15 to 25% at a temperature of 50°C. Mineral fillers such as hi-sil and durosil

reduced the diffusivity by about 40 to 65% at temperatures of 25°C and 50°C. Fillers such as aerosil and teg-N reduced the diffusivity by about 30 to 40% at the same temperatures. Lamellar fillers such as aluminum powder and mica powder reduced the diffusivity by about 60 to 75% at the same temperatures. At the same two temperatures, carbon black fillers reduced the diffusivity approximately 15 to 30% for thermax and P 33, 50 to 80% for slatex K and Vulcan 3, and 75 to 90% for spheron 9 and spheron 4.

One explanation for a reduction in diffusivity with the addition of fillers was that the fillers behave as a geometric obstruction to the path of gas through the rubber. The average diffusion path length was increased by the presence of the filler particles and the localized direction of flow was in general not normal to the geometrical cross section of the membrane. While the tortuosity of diffusion paths might account for some reduction in diffusivity, some of the reductions noted above were quite large, which implied that the phenomenon was more than just a geometrical effect of impermeable fillers.

As well as a modification in the diffusion coefficients, the values of the solubility coefficients, σ, in van Amerongen's work [1955] were considerably increased by the addition of filler. The solubility coefficients were found from the ratios of permeability and diffusion coefficients ($P = \sigma D$), and in some cases by direct measurements. The increase in solubility due to the added filler could have meant that a part of the gas diffusing into the polymer was adsorbed by the filler particles. Assuming that transport was restricted to the polymer phase only, the gas once adsorbed by the filler particles was rendered immobile and no longer participated in the diffusion process. The measured effective diffusion coefficient was then an average value between the diffusivity in the polymer phase and the zero diffusivity of the gas adsorbed on the filler particles.

Barrer, Barrie, and Raman [1962] studied the diffusion of higher molecular weight gases such as n-butane, iso-butane, n-pentane and neo-pentane in silica filled silicone rubbers. The filler used was Santocel CS, a relatively porous amorphous form of silica. Studies were performed over a temperature range of 30 to 70°C in

the neat rubber and at volumes of filler of 5.6, 10.6, 14.9 and 19.1%. Reported reductions in diffusivity with addition of filler were 15 to 38% for 5.6% filler, 23 to 39% for 10.6% filler, 32 to 53% for 14.9% filler, and 32 to 61% for 19.1% filler. The percent reduction in diffusivity due to the added filler was found to increase with temperature and size of the penetrant molecule.

Barrer, Barrie, and Rogers [1963] studied the diffusion of propane and benzene in membranes of natural rubber with zinc oxide filler. The volumes of filler were 0, 5, 10, 20, 30, and 40% for diffusion of propane, and 0, 10, and 40% for diffusion of benzene. For diffusion of propane at 40°C, the reduction in diffusivity ranged from 3 to 26% over the volumes of filler given. The results of the filler reducing the diffusion of benzene in the membranes were reported for three temperatures, 30, 40, and 50°C, for 10% ZnO, and for one temperature, 40°C, for 40% ZnO. Results were also reported for various concentrations of benzene up to 0.10 volume fraction. For the membrane with 10% ZnO, the reduction in diffusivity was about 16 to 57% at 30°C, 22 to 56% at 40°C, and 19 to 26% at 50°C. For the membrane with 40% ZnO, the reduction in diffusivity was about 42 to 72% at 40°C.

A filled polymer may contain two disperse phases, the filler and small vacuoles. Vacuoles are small gaps in the structure which are filled with the diffusing gas and usually occur at very high volume fractions of filler (above 50%) where incomplete wetting of the filler by the polymer is extensive [Barrer, 1968]. The following derivation of an effective diffusion coefficient which takes into account these disperse phases was developed by Barrer and Chio [1965].

The solubility of a gas in the polymer-filler system can be considered to be composed of three factors. The first is related to the solubility in the polymer, σ_p. The second is related to the gas adsorption by the filler, σ_f. The third is related to filling of gas pockets or vacuoles, σ_v. If the distribution of gas in each phase obeys Henry's law, $C = \sigma p$, where p is the pressure of the gas at the surface of the

polymer, then the three factors are defined as

$$\sigma_p = \frac{C'_p}{p}; \quad \sigma_f = \frac{C'_f}{p}; \quad \sigma_v = \frac{C'_v}{p}, \tag{42}$$

where C'_p, C'_f and C'_v are the concentrations in molecules per cm^3 of pure polymer, of filler particles and of vacuoles, respectively, and the solubility of the gas in the polymer-filler system becomes

$$\sigma = \sigma_p v_p + \sigma_f v_f + \sigma_v v_v, \tag{43}$$

where v_p, v_f and v_v are volume fractions of polymer, filler and vacuoles, respectively. If there were no vacuoles present and the filler was non-adsorbing or fully wetted, then equation 43 would become

$$\sigma = \sigma_p v_p. \tag{44}$$

If equation 44 is valid, solubility should decrease linearly with increasing filler volume fraction, which is not the case for some polymer-filler systems studied [Barrer et al., 1962, 1963]. Barrer [1965, 1968] states that for one dimensional flow in the x direction, a differential equation of diffusion can be written as

$$\frac{\partial C_p}{\partial t} + \frac{\partial C_f}{\partial t} + \frac{\partial C_v}{\partial t} = (\kappa D_p)\frac{\partial^2 C_p}{\partial x^2} + D_f \frac{\partial^2 C_f}{\partial x^2} + D_v \frac{\partial^2 C_v}{\partial x^2}, \tag{45}$$

where, C_p, C_f and C_v are the numbers of molecules of diffusant per cm^3 of membrane which are present in the polymer, on or in the filler and in the vacuoles, respectively. The terms κD_p, D_f and D_v are the effective diffusion coefficients in the polymer, on or in the filler and across the vacuoles, respectively. D_p is the diffusion coefficient in the pure polymer. The value κ in the polymer effective diffusion coefficient is a structure factor which takes into account the tortuosity of diffusion paths. Defining C as the total number of molecules per cm^3 of filled polymer gives

$$C = C_p + C_f + C_v = \sigma p. \tag{46}$$

Combining equations 42, 43, 45 and 46 gives

$$\frac{\partial C}{\partial t} = \left(\frac{(\kappa D_p)\sigma_p v_p + D_f \sigma_f v_f + D_v \sigma_v v_v}{\sigma_p v_p + \sigma_f v_f + \sigma_v v_v} \right) \frac{\partial^2 C}{\partial x^2}. \tag{47}$$

The term in brackets is the overall effective diffusion coefficient, D_{eff}, in the filled polymer. Barrer [1968] also defines a diffusion coefficient, D'_{eff}, by the flux, J, through unit area and the concentration gradient in the polymer phase only,

$$J = -D'_{eff}\frac{dC_p}{dx}. \tag{48}$$

The effective diffusion coefficients are related by

$$D'_{eff} = D_{eff}\frac{\sigma_p v_p + \sigma_f v_f + \sigma_v v_v}{\sigma_p v_p}. \tag{49}$$

If transport is restricted to the polymer phase ($D_f = 0$, $D_v = 0$), the effective diffusivity reduces to

$$D_{eff} = \kappa D_p \sigma_p \frac{v_p}{\sigma_p v_p + \sigma_f v_f + \sigma_v v_v}. \tag{50}$$

In the absence of vacuoles, equation 50 reduces to

$$D_{eff} = \kappa D_p \frac{v_p}{v_p + v_f(\sigma_f/\sigma_p)}. \tag{51}$$

For zero sorption by the filler ($\sigma_f = 0$), equation 51 can be reduced to

$$D_{eff} = \kappa D_p. \tag{52}$$

Equations 50, 51 and 52 are the forms frequently found in literature [Barrer et al., 1962, 1963; van Amerongen, 1964].

Of interest in the study of diffusion in filled polymers is the extent to which the polymer wets the filler. Assuming no vacuoles are present, two extreme cases for the solubility of a polymer-filler system are

$$\sigma = \sigma_p v_p + \sigma_f v_f, \tag{53}$$

and

$$\sigma = \sigma_p v_p. \tag{54}$$

In equation 53, σ_f has the value for the unwetted filler powder. In equation 54, σ_f has a value of zero implying that the filler is completely wetted by the polymer. The parameter σ_f usually has values between the two limits of equation 53 and 54

since the filler must be at least partly wetted by the polymer and is by no means always fully wetted [Barrer, 1968; Barrer, Barrie, and Raman, 1962]. To illustrate this, Figure 8 shows solubility data taken from Barrer, Barrie, and Rogers [1963] The solubility coefficients are for propane in natural rubber filled with ZnO. To compare the data to the two extreme cases mentioned above, equation 53 and 54 were plotted. Curve (a) is a plot of equation 53 with $\sigma_p = 0.0495$ and $\sigma_f = 0.0305$, solubility coefficients of propane in rubber with no filler and in bulk filler, respectively. Curve (b) is a plot of equation 54 with $\sigma_p = 0.0495$ and $\sigma_f \simeq 0$, which would imply complete wetting of the filler by the rubber. At low filler volume fractions the solubility coefficients follow a slope closer to that of curve (b) (complete wetting of filler), but at higher filler volume fractions the solubility coefficients are closer to curve (a) (no wetting of filler). As mentioned above, expectations are that the filler in the rubber have solubilities less than that of a free filler since the polymer should at least partially wet the filler, and that the polymer will not always fully wet the filler. This would lead to solubility coefficients lying between curves (a) and (b). To complicate matters, vacuoles may also be present, which was neglected here for simplification.

Since the rate of decrease of solubility falls off with increasing filler content in Figure 8, more filler surface is probably available for sorption of penetrant. A possible explanation of this and the drastic reductions in diffusivity with added filler is non-uniform dispersion of the filler particles [Barrer, Barrie, and Rogers, 1963]. If particle conglomerates are formed, gaps are created between some of the particles and two processes could occur which reduce diffusivity. Gas may occupy the void volume created and be rendered immobile. Moreover, since the filler surface in the conglomerates will not be completely wetted by polymer, a larger fraction of the conglomerate is available for gas adsorption.

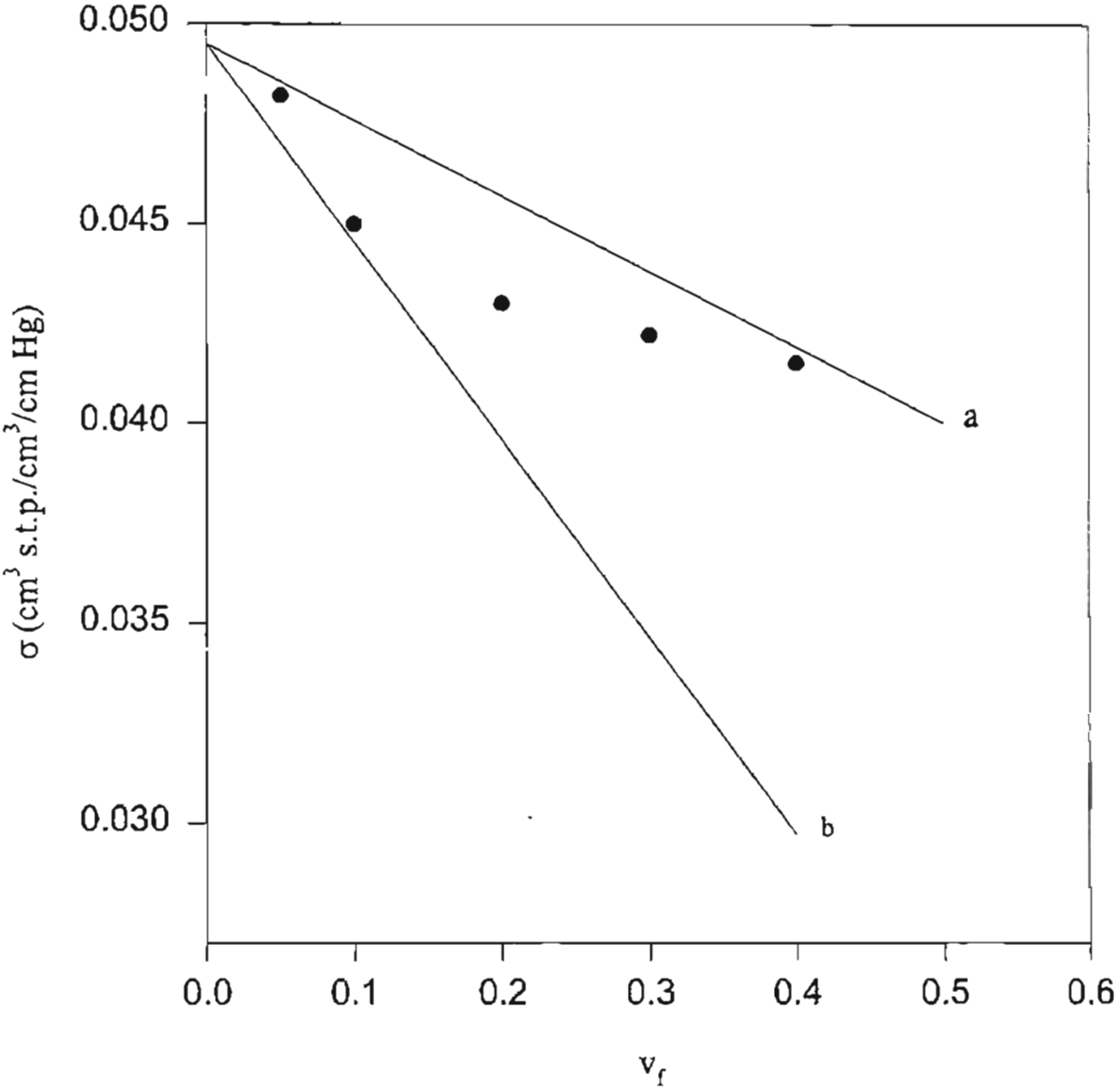

Figure 8. Solubility Coefficient, σ, of Propane in Natural Rubber Filled with ZnO Vs Volume Fraction Filler. Curve (a), $\sigma = \sigma_p v_p + \sigma_f v_f$ with $\sigma_f = 0.0305$; Curve (b), $\sigma = \sigma_p v_p$, $\sigma_f = 0$. Taken from Barrer, Barrie, and Rogers [1963].

Diffusion in Crystalline Polymers

A description of some of the work done in the area of diffusion in crystalline polymers is included in this section since the effect of crystals in crystalline polymers is similar to that of fillers in filled polymers.

Solution of a penetrant in perfectly crystalline regions is not to be expected [Barrer, 1968], and usually, σ decreases linearly with increasing crystalline fraction, v_c (subscript c and a will replace f and p, respectively since the subject is now diffusion in crystalline polymers which have a crystal and an amorphous phase) [Michaels et al., 1964] as

$$\sigma = \sigma_a v_a, \tag{55}$$

where v_a is the volume fraction of amorphous polymer and $v_a + v_c = 1$. The diffusion coefficient of a penetrant in a polymer crystal is expected to be very small; therefore, crystals act similarly to impermeable filler particles [Barrer, 1968]. The difference is that the degree of crystallinity may be changed by heating, cooling and annealing and that the crystals should always be fully wetted by the polymer chains in the amorphous regions [Barrer, 1968]. Crystals only act as a geometrical obstruction which increases the diffusion path length.

The effective diffusion coefficient can be expressed similarly as was for filled polymers,

$$D_{eff} = \kappa D_a, \tag{56}$$

where D_a is the diffusion coefficient in the completely amorphous polymer. However, most forms [Hedenqvist and Gedde, 1996] use a tortuosity factor, τ, such as the relationship proposed by Michaels and Bixler [1961], who interpreted κ as the product of a geometrical impedance factor, τ, and a chain immobilization factor, β [Barrer, 1968],

$$D_{eff} = \frac{D_a}{\tau\beta}. \tag{57}$$

Initially, suggestions were made that β described the reduced segmental mobility of polymer molecules in the vicinity of crystalline surfaces [Michaels and Bixler,

1961]. If the crystalline surface area is large, then β may be large. Later, findings were that β depends more on the size of the penetrant molecule and only weakly on the crystallinity [Michaels et al., 1964].

Peterlin [1975, 1984] has a slightly different form for the effective diffusivity

$$D_{eff} = \frac{\psi D_a^*}{B}, \tag{58}$$

where ψ is a detour factor describing the physical obstruction of the crystallites, which takes values between 0 and 1, B (≥ 1) is a blocking factor, and D_a^* is the diffusion coefficient in the "relaxed" region of the amorphous phase of the crystalline polymer [Hedenqvist and Gedde, 1996]. The amorphous phase is a complex network of tortuous very thin and broad flat channels, and the amorphous chains are restrained in mobility by their ends fixed in the adjacent crystals [Peterlin, 1975]. Therefore, diffusion in the amorphous phase is anisotropic and the effective diffusion coefficient D_{eff} of the crystalline polymer will be smaller than D_a^*. The effect of the restraint on chain mobility increases with a smaller thickness of amorphous layers. An increase in the amorphous component implies an increased thickness of such a layer and an increase in the diffusion coefficient D_a^* [Peterlin, 1975]. Therefore, D_a^* is strongly dependent on crystallinity. The blocking factor, B, in equation 58 describes the geometrical blocking that occurs when the penetrant molecules are too large to be able to enter the amorphous interlayers. The immobilization factor, β, in equation 57 is analogous to the blocking factor, B. It takes into account the constraining effect of the crystals on the amorphous phase and is included in the crystallinity dependence of D_a^* in equation 58. The detour factor, ψ, and the tortuosity factor, τ, are both purely geometrical factors [Hedenqvist and Gedde, 1996].

Several other models have been used to describe the diffusion in crystalline polymers [Hedenqvist and Gedde, 1996]. Some are empirical and some are based on physical and chemical processes involving the penetrant and the polymer. The models listed above (equations 57 and 58) do not include a dependence on the

concentration of the penetrant. In most polymers, the diffusivity is greatly dependent on concentration. This concentration dependence is sometimes expressed as [Hedenqvist and Gedde, 1996]

$$D_{eff} = D_0 e^{\gamma C}, \tag{59}$$

where D_0 is the diffusivity at zero penetrant concentration and γ is a constant. A linear dependence of diffusivity on concentration was used for poly(ethylene terephthalate) and 4-nitro-4′-hydroxyazobenzene in an aqueous solution [Iijima and Chung, 1973]

$$D_{eff} = D_0(1 + \gamma C). \tag{60}$$

A polynomial was used to fit the diffusivity of water in PA-6 [Hanspach and Pinno, 1992]

$$D_{eff} = D_0 + \gamma_1 C + \gamma_2 C^2, \tag{61}$$

where γ_1 and γ_2 are constants.

Equations based on the free volume theory have also been used to explain diffusion in crystalline polymers. In simple terms the free volume theory is expressed as [Hedenqvist and Gedde, 1996]

$$D \propto e^{-\frac{B}{f}}, \tag{62}$$

where B is a constant and f is the fractional free volume of the system. An equation based on the free volume theory was used to fit the diffusivity of various gases into polyethylene [Kulkarni et al., 1983; Stern et al., 1972, 1983, 1986]

$$D_T = RTA_d e^{-\frac{B}{f_a v_a}}, \tag{63}$$

where A_d is a constant which depends on the size of the penetrant, and f_a is the amorphous fractional free volume,

$$f_a = f_1 v_1 + f_2 v_2. \tag{64}$$

The quantities v_1 and v_2 are the volume fractions of the penetrant and the polymer in the amorphous phase, respectively. The values f_1 and f_2 are the corresponding

fractional free volumes. D_T in equation 63 is the thermodynamic diffusivity and is related to the effective mutual diffusion coefficient, D_{eff}, through [Hedenqvist and Gedde, 1996]

$$\frac{D_{eff}}{1-v_1} = D_T \frac{\partial(\ln a_1)}{\partial(\ln v_1)}, \tag{65}$$

where a_1 is the activity of the penetrant. The quantity v_a in equation 63 corrects the effective diffusivity for crystallinity. A similar correction is shown in this work for filler content. Another equation related to the free volume theory which has been used to fit diffusivity data is [Horas and Rizzotto, 1989]

$$D_{eff} = \frac{D_T}{2 - \frac{D_T}{RTA}}, \tag{66}$$

$$D_T = v_a RTA e^{-\frac{B}{T}}, \tag{67}$$

where A and B are functions of crystallinity.

Structure Factor

The structure factor, κ, takes into account the tortuosity of the diffusion path around the filler particles (or crystals). If the filler or polymer crystals are impermeable and have no vacuoles then

$$\frac{P_{eff}}{P_p} = \kappa v_p; \quad \frac{D_{eff}}{D_p} = \kappa, \tag{68}$$

where the subscript a replaces p for crystalline polymers. The value κ can be found from a plot of P_{eff}/P_p or D_{eff}/D_p versus the volume fraction of filler v_f (or crystals v_c). Many mathematical forms have been derived which give the dependence of κ on the volume fraction of filler. The problem is analogous to the electrical conductance of a heterogeneous medium composed of a dispersion of particles in a continuous medium of different conductivity [Barrer et al., 1962, 1963; van Amerongen, 1964]. Maxwell [1891] considered a suspension of spherical particles so dilute in the medium that the spheres had no effect on one another [van Amerongen, 1964]. Fricke [1931] extended the study to include oblate and prolate spheroids. The expression for κ for these approaches is

$$\kappa = \frac{Y}{Y + v_f}, \tag{69}$$

where Y is a shape factor which is 2 for random spheres and decreases to 1.1 as the shape changes from a sphere to an oblate spheroid with axial ratio 4 : 1 [Barrer, 1968; Barrer, Barrie, and Rogers, 1963]. Lord Rayleigh [1892] and Runge [1925] considered a cubic array of uniform spheres for treating a more concentrated dispersion of particles [Barrer, Barrie, and Rogers, 1963]. The equations for κ are

$$\kappa = \frac{1}{(1 - v_f)} \left[1 - \frac{3v_f}{2 + v_f - 0.392 v_f^{10/3}} \right], \tag{70}$$

for a cubic lattice of spheres, and

$$\kappa = \frac{1}{(1 - v_f)} \left[1 - \frac{3v_f}{2 + v_f - 0.306 v_f^4 - 0.0134 v_f^8} \right], \tag{71}$$

for a cubic lattice of cylinders normal to the direction of flow. Barrer, Barrie, and Raman, [1962] have found in a study of diffusion of hydrocarbon penetrants in various silica-filled rubbers that the influence of the filler in reducing the diffusion coefficients is greater than would be expected for a regular dispersion of nonconducting spheres. They have suggested that a filled polymer is a considerably more complex medium, and if trends of diffusivity reduction with temperature and size of penetrant are significant then these simple models must be modified.

For the crystalline polymers polyethylene terephthalate, polyethylene and Nylon, Lasoski and Cobbs [1959] found that water vapor permeabilities followed the relationship

$$\frac{P_{eff}}{P_a} = v_a^2. \tag{72}$$

If the effective diffusion equation is of the form of equation 56, then up to $v_c = 0.4$ [Barrer, 1968]

$$\kappa \simeq (1 - v_c). \tag{73}$$

In this equation, κ decreases much more rapidly than would be expected from Maxwell's or Rayleigh's equations.

Refering now to equation 57, Michaels and Bixler [1961] determined that the tortuosity factor for a series of polyethylenes with different crystallinities using He as a penetrant followed the equation

$$\tau = v_a^{-n}, \tag{74}$$

where n is a constant which takes different values for different polymers. The immobilization for helium was assumed to be small, hence $\beta = 1$ [Michaels and Bixler, 1961].

Treatment of Adsorption as a Chemical Reaction

The problem of adsorption of a gas on filler particles may also be treated as diffusion combined with a chemical reaction [van Amerongen, 1964]. Physical adsorption of a gas by the filler has a similar effect on diffusion as chemical reaction. In either case the gas is rendered inactive and has the misleading effect of increasing the apparant solubility without increasing the permeability. Permeability is related to diffusivity by

$$P = D\sigma, \tag{75}$$

so the diffusivity will decrease.

A differential equation which could describe diffusion with adsorption is [Crank, 1956]

$$\frac{\partial C}{\partial t} = D\frac{\partial^2 C}{\partial x^2} - \frac{\partial C_f}{\partial t}, \tag{76}$$

where C_f is the concentration of penetrant which is adsorbed on the filler particles, and C is the concentration of penetrant which is free to diffuse. In the simplest case, the concentration of the immobilized penetrant, C_f, is directly proportional to C,

$$C_f = RC. \tag{77}$$

This equation is referred to as a linear adsorption isotherm [Crank, 1956]. Substituting for C_f from equation 77 into equation 76 gives

$$\frac{\partial C}{\partial t} = \frac{D}{R+1}\frac{\partial^2 C}{\partial x^2}, \tag{78}$$

which is the usual form of a diffusion equation with an effective diffusion coefficient

$$D_{eff} = \frac{D}{R+1}. \tag{79}$$

If tortuosity is also a factor, the effective diffusion coefficient becomes

$$D_{eff} = \frac{\kappa D_p}{R+1}, \tag{80}$$

where κ is the tortuosity factor and D_p is the diffusivity in the pure polymer.

Summary

This work uses several methods and equations which were discussed in this chapter. Diffusion coefficients for $CaCO_3$ filled PVAC were evaluated from frequency data obtained with a QCM. Sorption data were calculated by analyzing frequency data using equation 15. Diffusion coefficients were calculated by the moment method, equation 22, and penetrant weight fractions were calculated by equations 24 and 25.

The free-volume equation 30 was used to fit the experimental diffusion coefficient data for toluene diffusion in unfilled PVAC. Several equations were fit to the experimental data for toluene diffusion in filled PVAC, including Barrer's equations 51 and 52, and equation 80 which was derived from reaction principles. The free-volume equation 30 was used for D_p, the unfilled polymer diffusivity, in these equations. Also, fits to filled polymer diffusion coefficient data were done using the structure factor equations 69 and 70 in combination with equation 52.

CHAPTER III

MODIFICATIONS OF EQUIPMENT AND PROCEDURES

The equipment in this work was designed to measure diffusion coefficients of penetrants diffusing into polymers. A description of the experimental apparatus was given in Chapter II and also in the works of Deshpande [1993] and Mikkilineni [1995] from the development stage of the QCM through several modifications. This chapter contains a discussion of additional modifications made to the equipment, changes in the data analysis for determining diffusion coefficients, and procedures for sample preparation.

A schematic of the QCM with modifications is in Figure 9. A sample cylinder was installed between the solvent flask and the six-way cross chamber. The sample cylinder allows an instantaneous step change of pressure in the chamber. The toggle valve and the needle valve described in Chapter II were removed. Three ball valves were used, one to isolate the solvent flask, one to isolate the sample cylinder, and one between the sample cylinder and the six-way cross chamber. New 3/16 inch stainless steel tubing was installed between the solvent flask and the six-way cross chamber to increase the flow rate of vapor. Previously, some of the tubing was 1/4 inch. The ball valves allowed the sample cylinder to be filled with penetrant vapor, then introduced into the chamber when needed. Before installing the sample cylinder, the penetrant was introduced into the chamber too slowly to adequately approximate a step change. Figure 10 shows a typical sorption curve for the experimental setup without the sample cylinder. The rate at which the penetrant was introduced into the chamber is reflected by the slow rate of mass sorption in the initial portion of the curve. This severely affected the accuracy of data analysis since the initial slope method uses the initial portion of the curve and the moment method uses the entire curve. Installing the sample cylinder

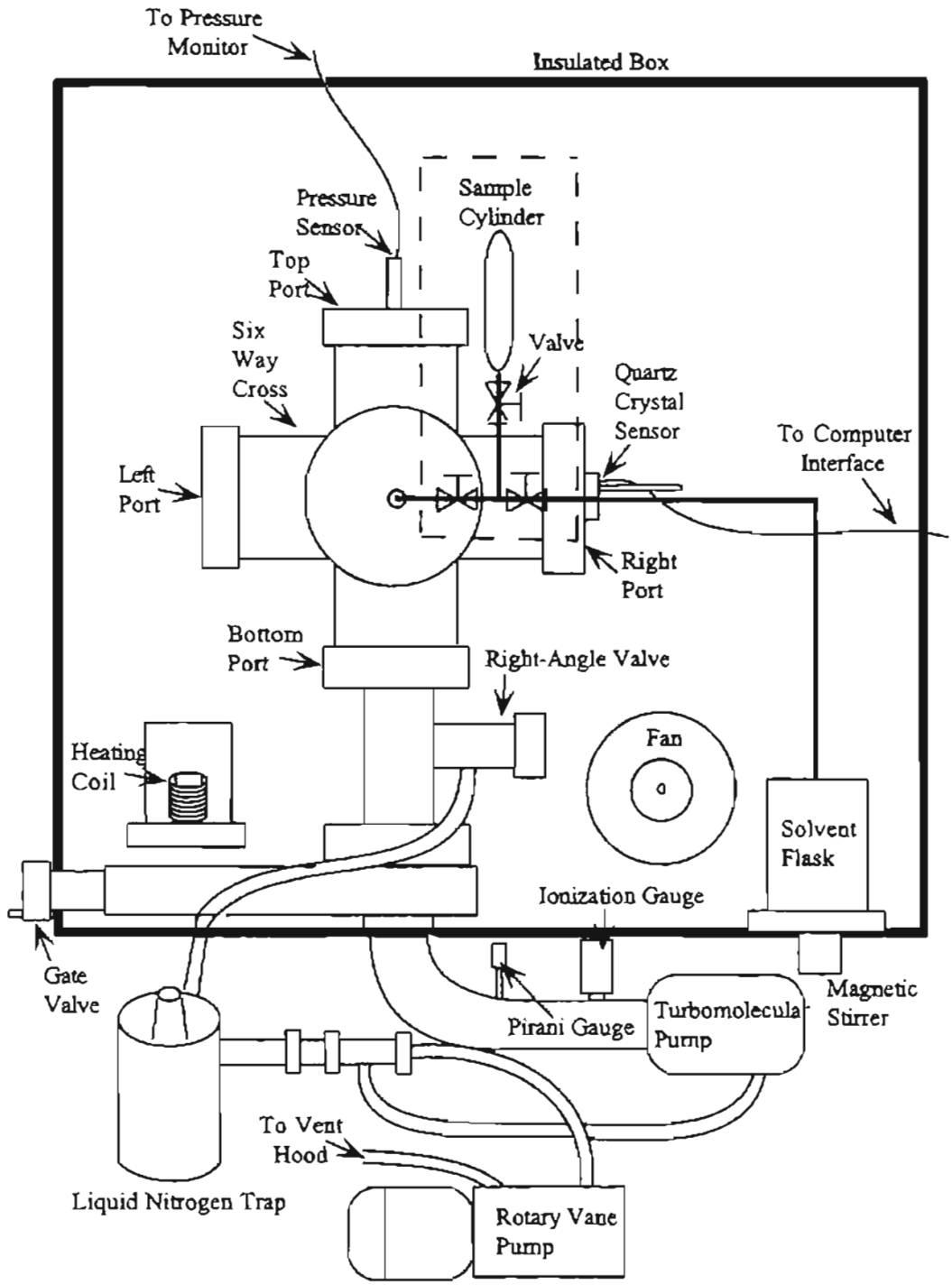

Figure 9. Schematic Diagram of the Quartz Crystal Microbalance Modified Setup.

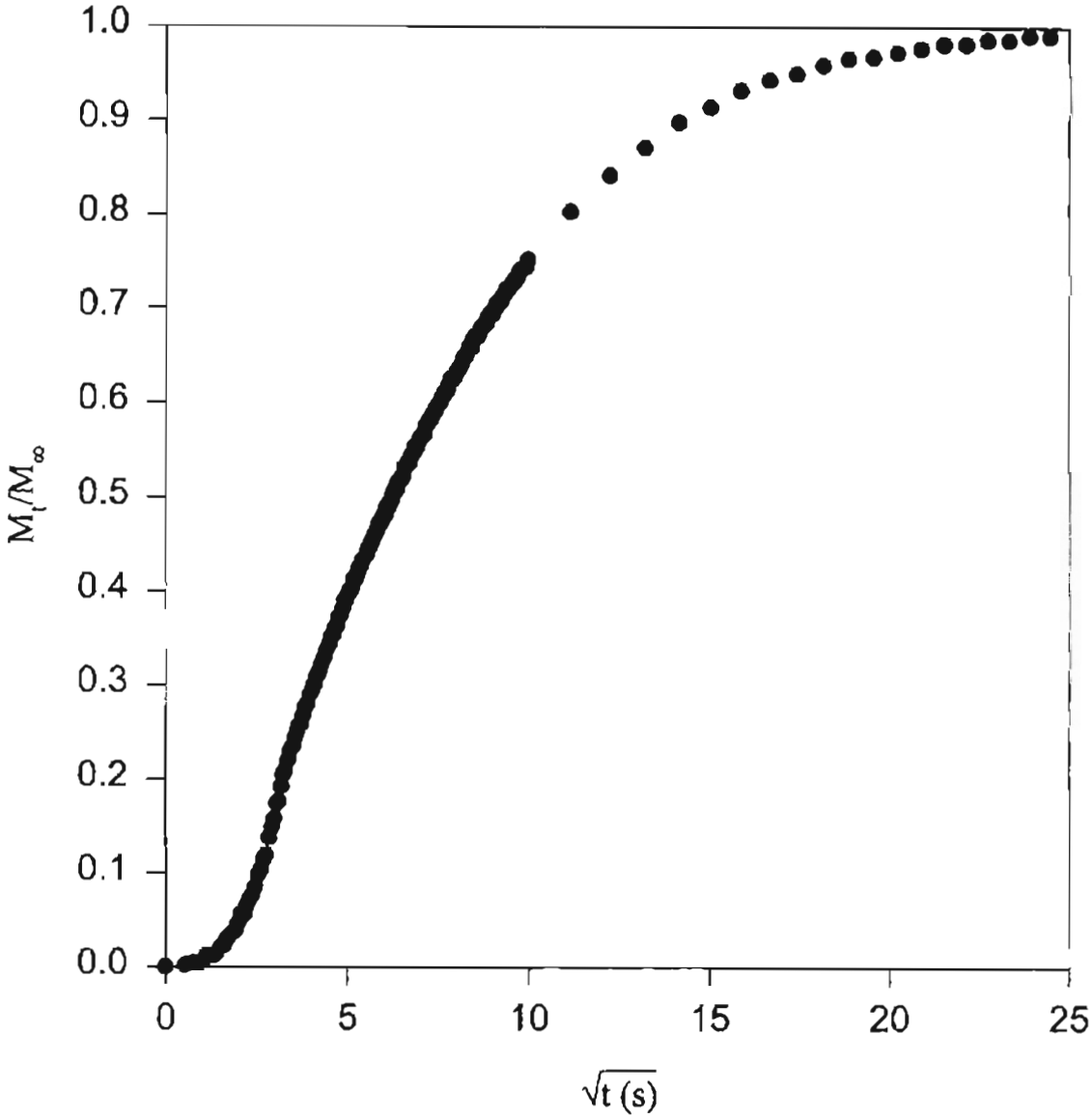

Figure 10. Sorption Curve Before the Sample Cylinder was Installed.

solved this problem. The sample cylinder allows the penetrant to be introduced into the chamber almost instantaneously. Figure 11 shows a sorption curve for the experimental set up with the sample cylinder. Notice that the initial portion of the curve has a shorter tail since the pressure was increased almost instantaneously.

The next change to the QCM was not a modification of the equipment, but a replacement of the gaskets in both the right angle valve and the gate valve. The gaskets were made of rubber and were deteriorated due to the organic vapors used in the QCM chamber. The leakage from the valves led to unreliable data.

The plastic tubing which was used for circulating cold water to the turbomolecular pump was replaced with 1/4 inch copper tubing, decreasing the chances of a water leak. A water circulation line constructed of 1/4 inch copper tubing was connected to the solvent flask. A centrifugal pump was used to circulate water through the solvent flask from a water bath heated by a constant circulation immersion heater.

The computer program recording the frequency data from the deposition monitor was modified to record the data at smaller time intervals. The previously used IBM XT computer was replaced by a Gateway computer with a 33 MHz 486 CPU. This also allowed for data collection at smaller time intervals.

The moment method, discussed in Chapter II, was used to analyze the experimental sorption data in this work. Previously [Deshpande, 1993; Mikkilineni, 1995], the initial slope method, also discussed in Chapter II, was used to analyze the sorption data from the QCM. The initial slope method is very sensitive to the position on the curve at which the slope is calculated. Also, diffusion is sometimes so fast that there are a limited amount of data in the initial portion of the sorption curve, making analysis with the initial slope method even more difficult. The moment method uses the entire sorption curve; thus, is not as sensitive to the initial portion of the sorption curve. An Excel spreadsheet was developed to evaluate the area under the sorption curve using the trapeziodal rule.

In this work, samples were prepared by dissolving a known weight of polymer (PVAC) and filler ($CaCO_3$) in a known volume of solvent (tetrahydrofuran)

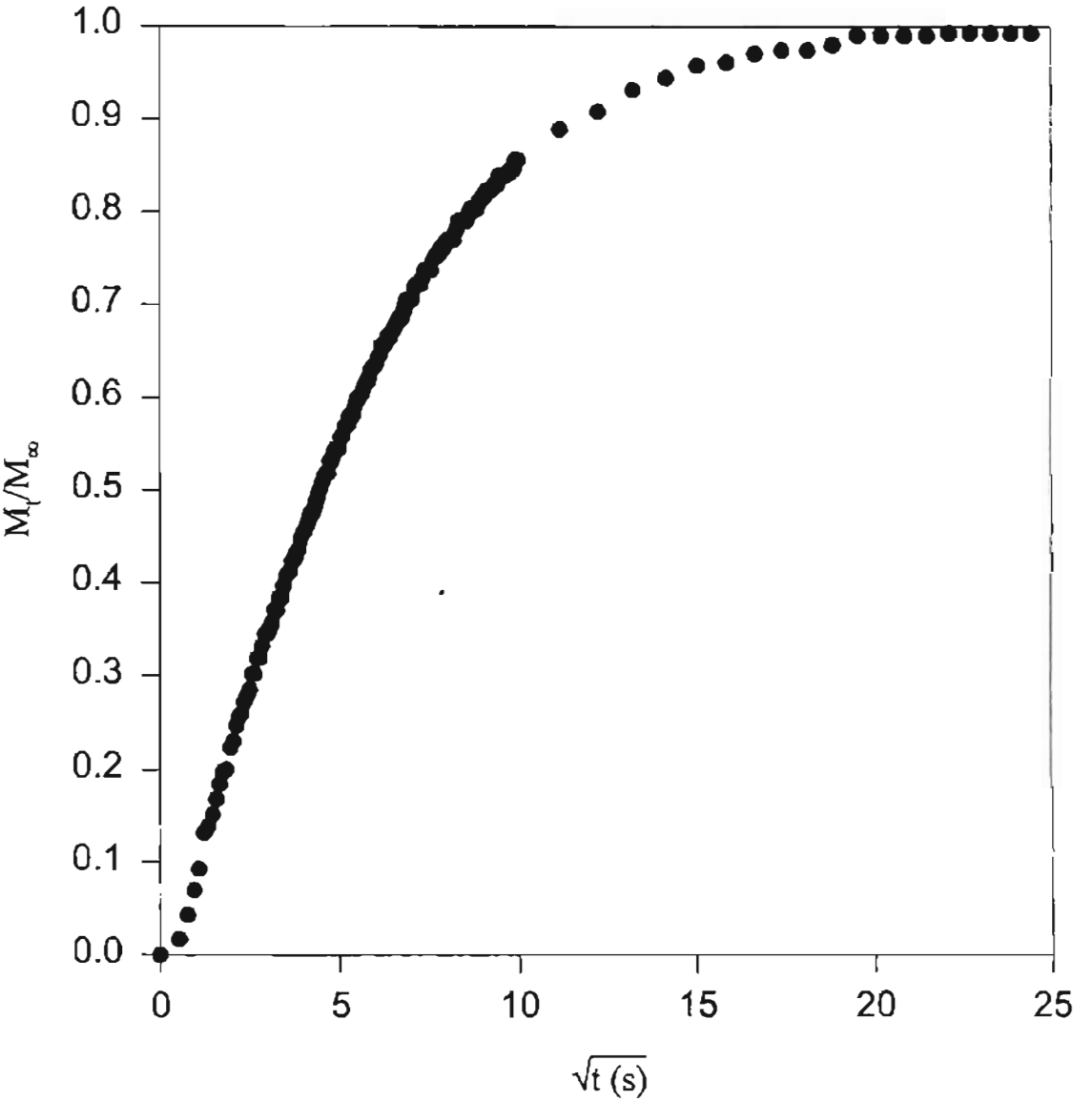

Figure 11. Sorption Curve After the Sample Cylinder was Installed.

to make a very dilute solution ($\sim$ 3% polymer and $\sim$ 0.1% filler). The crystals were coated from a micropipette by dropping a known volume (typically 7μl) of the polymer solution onto the crystal surface and spreading it with the tip of the micropipette. After drying, the diameter of the polymer film was measured with a ruler. The thickness of the polymer film was calculated from the surface area of the film, the volume of the solution used to coat the crystal, and the weights and densities of the polymer, filler and solvent used to make the polymer solution. Weights were recorded with a mass balance; of the empty bottle, after adding polymer, after adding filler, and after adding solvent. The diameter of the film was measured at several locations. The average diameter was used to calculate the area of the polymer film by using the formula for the area of a circle. Detailed procedures for preparing polymer solutions, coating crystals, and calculating film thickness are given in Appendix A.

Since the design phase of the QCM, many improvements have been made. Continual improvement of the equipment and procedures will lead to more accurate data, more ease of operation, and perhaps more uses for the QCM. Suggested improvements are below. All of the monitors for measuring pressure, temperature, and frequency are separate devices. Also, data must be copied from the data acquisition computer and analyzed as a separate step. To make the apparatus and data analysis less cumbersome, a graphical instrumentation program such as LabVIEW should be set up on the data acquisition computer. This program could be used to imitate the appearance and operation of actual instruments, such as pressure and temperature monitors. All of the measured properties, pressure, temperature, and frequency, could be monitored at one location, the computer. Such a program can also produce live graphs of data during an experimental run. All calculations involved in determining the diffusion coefficient could be performed by the graphical instrumentation program. The box surrounding the QCM is made of insulated plywood, but this does not stop all of the heat loss. The quartz crystal microbalance should be fitted inside an insulated oven to better control the temperature of the ambient air and the chamber.

CHAPTER IV

EXPERIMENTAL RESULTS

This chapter presents the results of the sorption experiments performed with the quartz crystal microbalance to obtain effective diffusion coefficients of toluene diffusing into $CaCO_3$ filled PVAC. The diffusion coefficients of toluene diffusing into PVAC with 0.0% $CaCO_3$ (neat PVAC) are compared with the results of other researchers [Mikkilineni, 1995 and Hou, 1986] in Chapter V.

The effective diffusion coefficients of toluene diffusing into $CaCO_3$ filled PVAC were measured at temperatures of 60°C and 80°C for 0, 3.3, 4.9, and 10% (by weight) $CaCO_3$. The diffusion coefficients were obtained at low concentrations of toluene, less than 0.15 weight fraction for 60°C data and less than 0.10 weight fraction for 80°C data. Effective diffusion coefficients were calculated by using the moment method. Effective diffusion coefficients and toluene weight fractions are given in Tables I through VIII. The tabulated diffusion coefficients are plotted as a function of toluene weight fraction in Figure 12 for the 60°C data and Figure 13 for the 80°C data. To verify the reproducibility, each set of experimental data was replicated using the same quartz crystal and polymer film.

Equilibrium sorption solubility data for toluene in $CaCO_3$ filled PVAC were also measured at temperatures of 60°C and 80°C for 0, 3.3, 4.9, and 10% (by weight) $CaCO_3$. Equilibrium toluene vapor pressures, p_1, were measured, and solubility data in the form of p_1/p_1^0, where p_1^0 is the toluene saturation vapor pressure, were calculated. The solubility data and equilibrium toluene weight fractions are given in Tables I through VIII. The solubility data are plotted as a function of toluene weight fraction in Figure 14 for the 60°C data and Figure 15 for the 80°C data. The solubility data are also plotted on a "filler free basis" in Figure 16 for the 60°C data and Figure 17 for the 80°C data, in which the toluene

weight fraction is calculated on a filler free basis, i.e., $M_S/(M_S + M_P)$, where M_S is the mass of the toluene solvent and M_P is the mass of the PVAC polymer.

TABLE I

SOLUBILITY DATA AND DIFFUSION COEFFICIENTS OF TOLUENE IN PVAC WITH 0.0% $CaCO_3$ AT 60°C

w_1^{eq}	p_1/p_1^0	w_1^{av}	$D \times 10^9$ (cm^2/s)
		Run #1	
0.0121	0.0737	0.0085	0.218
0.0253	0.1406	0.0213	0.536
0.0380	0.2028	0.0342	1.26
0.0506	0.2593	0.0468	2.82
0.0634	0.3114	0.0596	4.83
0.0754	0.3583	0.0718	8.81
0.0878	0.4022	0.0841	14.1
0.1000	0.4431	0.0963	24.1
0.1122	0.4811	0.1085	34.2
0.1243	0.5168	0.1207	44.1
0.1380	0.5540	0.1339	53.7
		Run #2	
0.0081	0.0904	0.0057	0.170
0.0176	0.1585	0.0147	0.353
0.0291	0.2221	0.0257	0.687
0.0404	0.2776	0.0370	1.57
0.0519	0.3285	0.0485	2.89
0.0631	0.3754	0.0597	5.38
0.0744	0.4190	0.0710	9.23
0.0855	0.4599	0.0822	17.2
0.0963	0.4964	0.0931	25.7
0.1239	0.5834	0.1157	24.8
0.1375	0.6210	0.1335	44.8

TABLE II

SOLUBILITY DATA AND DIFFUSION COEFFICIENTS OF TOLUENE IN PVAC WITH 3.3% $CaCO_3$ AT 60°C

w_1^{eq}	p_1/p_1^0	w_1^{av}	$D \times 10^9$ (cm^2/s)
		Run #1	
0.0082	0.0766	0.0058	0.882
0.0148	0.1459	0.0129	1.40
0.0218	0.2050	0.0198	2.02
0.0289	0.2530	0.0268	3.54
0.0364	0.2951	0.0341	5.65
0.0452	0.3416	0.0425	7.34
0.0538	0.3855	0.0512	11.0
0.0624	0.4242	0.0599	16.8
0.0802	0.4975	0.0777	35.5
0.0880	0.5295	0.0857	65.7
		Run #2	
0.0086	0.0696	0.0060	1.57
0.0168	0.1306	0.0144	1.58
0.0254	0.1909	0.0228	2.69
0.0341	0.2426	0.0315	4.52
0.0428	0.2913	0.0402	7.41
0.0521	0.3397	0.0493	8.46
0.0607	0.3814	0.0581	13.9
0.0706	0.4443	0.0677	21.9
0.0788	0.4856	0.0764	29.2
0.0867	0.5224	0.0843	44.3

TABLE III

SOLUBILITY DATA AND DIFFUSION COEFFICIENTS OF TOLUENE IN PVAC WITH 4.9% $CaCO_3$ AT 60°C

w_1^{eq}	p_1/p_1^0	w_1^{av}	$D \times 10^9$ (cm^2/s)
		Run #1	
0.0086	0.0681	0.0060	0.392
0.0172	0.1325	0.0146	0.538
0.0258	0.1950	0.0232	1.16
0.0341	0.2534	0.0316	1.82
0.0422	0.3125	0.0397	3.16
0.0504	0.3624	0.0479	4.25
0.0586	0.4033	0.0561	6.70
0.0669	0.4472	0.0644	8.62
0.0874	0.5231	0.0847	17.3
0.0956	0.5548	0.0931	24.6
0.1047	0.5871	0.1019	33.1
0.1133	0.6176	0.1107	40.5
0.1213	0.6418	0.1189	54.9
0.1296	0.6664	0.1271	64.5
		Run #2	
0.0080	0.0841	0.0056	0.325
0.0154	0.1522	0.0132	0.505
0.0230	0.2125	0.0207	0.917
0.0311	0.2619	0.0286	1.27
0.0398	0.3085	0.0372	2.09
0.0487	0.3546	0.0461	3.20
0.0575	0.3937	0.0549	4.53
0.0667	0.4305	0.0639	6.15
0.0767	0.4737	0.0737	8.91
0.0865	0.5090	0.0836	13.1
0.0965	0.5451	0.0935	16.9
0.1058	0.5756	0.1030	27.5
0.1148	0.6020	0.1121	33.0
0.1238	0.6270	0.1211	43.5
0.1334	0.6541	0.1305	64.0

TABLE IV

SOLUBILITY DATA AND DIFFUSION COEFFICIENTS OF TOLUENE IN PVAC WITH 10% $CaCO_3$ AT 60°C

w_1^{eq}	p_1/p_1^0	w_1^{av}	$D \times 10^9$ (cm^2/s)
		Run #1	
0.0114	0.0633	0.0080	0.104
0.0245	0.1213	0.0206	0.133
0.0366	0.1797	0.0330	0.259
0.0482	0.2337	0.0447	0.448
0.0602	0.2820	0.0566	0.662
0.0741	0.3308	0.0699	0.918
0.0895	0.3747	0.0849	1.60
0.1065	0.4190	0.1014	1.89
0.1267	0.4573	0.1206	4.59
0.1403	0.4900	0.1362	6.17
0.1536	0.5243	0.1496	12.0
		Run #2	
0.0085	0.0703	0.0059	0.287
0.0213	0.1343	0.0175	0.134
0.0342	0.1890	0.0303	0.264
0.0473	0.2355	0.0434	0.390
0.0650	0.2832	0.0597	0.676
0.0818	0.3271	0.0768	0.981
0.1064	0.3702	0.0990	1.76
0.1229	0.4085	0.1179	2.85
0.1397	0.4491	0.1346	4.26
0.1530	0.4867	0.1490	10.8

TABLE V

SOLUBILITY DATA AND DIFFUSION COEFFICIENTS OF TOLUENE IN PVAC WITH 0.0% $CaCO_3$ AT 80°C

w_1^{eq}	p_1/p_1^0	w_1^{av}	$D \times 10^9$ (cm^2/s)
		Run #1	
0.0071	0.0559	0.0050	0.624
0.0143	0.1186	0.0121	1.04
0.0206	0.1660	0.0187	1.23
0.0275	0.2113	0.0254	1.48
0.0345	0.2535	0.0324	2.24
0.0413	0.2917	0.0392	3.54
0.0477	0.3242	0.0458	3.86
0.0537	0.3526	0.0519	5.44
0.0604	0.3821	0.0584	7.18
		Run #2	
0.0077	0.0439	0.0054	0.600
0.0149	0.0859	0.0128	0.961
0.0218	0.1225	0.0197	1.38
0.0293	0.1612	0.0270	1.71
0.0379	0.2058	0.0353	2.45
0.0456	0.2420	0.0433	3.00
0.0532	0.2752	0.0509	3.47
0.0605	0.3071	0.0583	5.57
0.0681	0.3380	0.0658	4.80

TABLE VI

SOLUBILITY DATA AND DIFFUSION COEFFICIENTS OF TOLUENE IN PVAC WITH 3.3% $CaCO_3$ AT 80°C

w_1^{eq}	p_1/p_1^0	w_1^{av}	$D \times 10^9$ (cm^2/s)
		Run #1	
0.0057	0.0245	0.0040	0.540
0.0156	0.0698	0.0126	1.19
0.0263	0.1120	0.0231	1.76
0.0397	0.1605	0.0356	2.42
0.0515	0.2006	0.0479	4.24
0.0624	0.2377	0.0591	9.46
		Run #2	
0.0069	0.0302	0.0048	0.972
0.0158	0.0666	0.0131	1.27
0.0274	0.1111	0.0239	1.74
0.0388	0.1511	0.0353	2.67
0.0509	0.1909	0.0473	4.15
0.0615	0.2280	0.0583	10.2

TABLE VII

SOLUBILITY DATA AND DIFFUSION COEFFICIENTS OF TOLUENE IN PVAC WITH 4.9% $CaCO_3$ AT 80°C

w_1^{eq}	p_1/p_1^0	w_1^{av}	$D \times 10^9$ (cm^2/s)
		Run #1	
0.0059	0.0311	0.0041	0.534
0.0135	0.0659	0.0112	0.632
0.0211	0.1019	0.0188	0.901
0.0319	0.1466	0.0286	1.14
0.0420	0.1853	0.0389	1.67
0.0563	0.2367	0.0490	3.04
0.0698	0.2825	0.0657	5.11
0.0797	0.3158	0.0767	10.6
0.0906	0.3524	0.0874	18.8
0.0907	0.3869	0.0960	45.5
		Run #2	
0.0060	0.0291	0.0042	0.551
0.0148	0.0685	0.0121	0.643
0.0247	0.1120	0.0217	0.839
0.0351	0.1571	0.0320	1.16
0.0464	0.2026	0.0430	1.89
0.0566	0.2406	0.0536	2.90
0.0663	0.2736	0.0634	4.40
0.0758	0.3052	0.0729	7.07
0.0848	0.3361	0.0821	16.1

TABLE VIII

SOLUBILITY DATA AND DIFFUSION COEFFICIENTS OF TOLUENE IN PVAC WITH 10% $CaCO_3$ AT 80°C

w_1^{eq}	p_1/p_1^0	w_1^{av}	$D \times 10^9$ (cm^2/s)
		Run #1	
0.0113	0.0282	0.0079	0.463
0.0282	0.0692	0.0232	1.10
0.0410	0.1087	0.0371	1.48
0.0562	0.1573	0.0516	2.59
		Run #2	
0.0164	0.0369	0.0114	0.559
0.0341	0.0820	0.0288	1.28
0.0509	0.1307	0.0459	1.88
0.0638	0.1715	0.0599	3.78

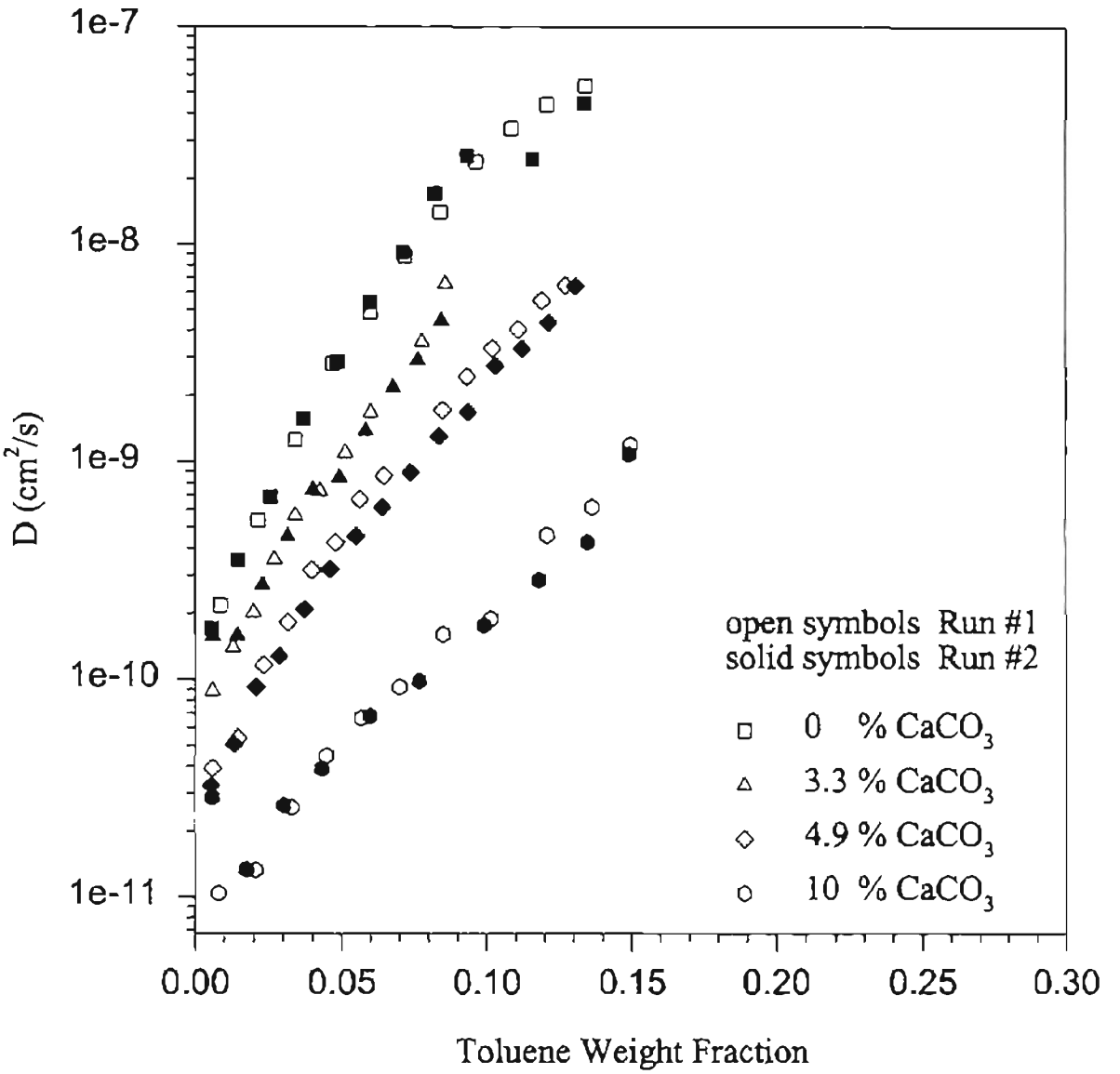

Figure 12. Effective Diffusion Coefficients of Toluene in $CaCO_3$ Filled PVAC at 60°C.

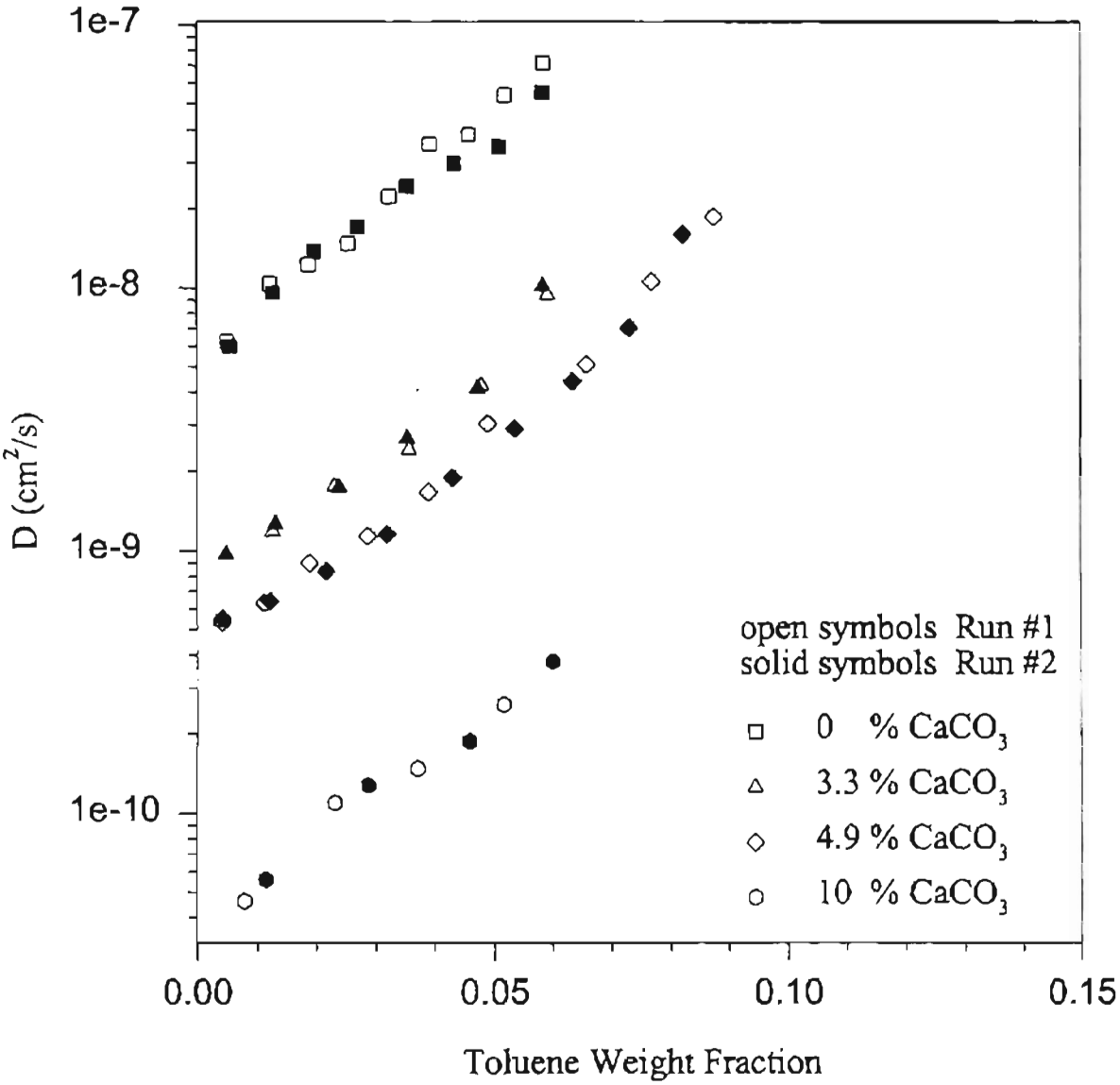

Figure 13. Effective Diffusion Coefficients of Toluene in $CaCO_3$ Filled PVAC at 80°C.

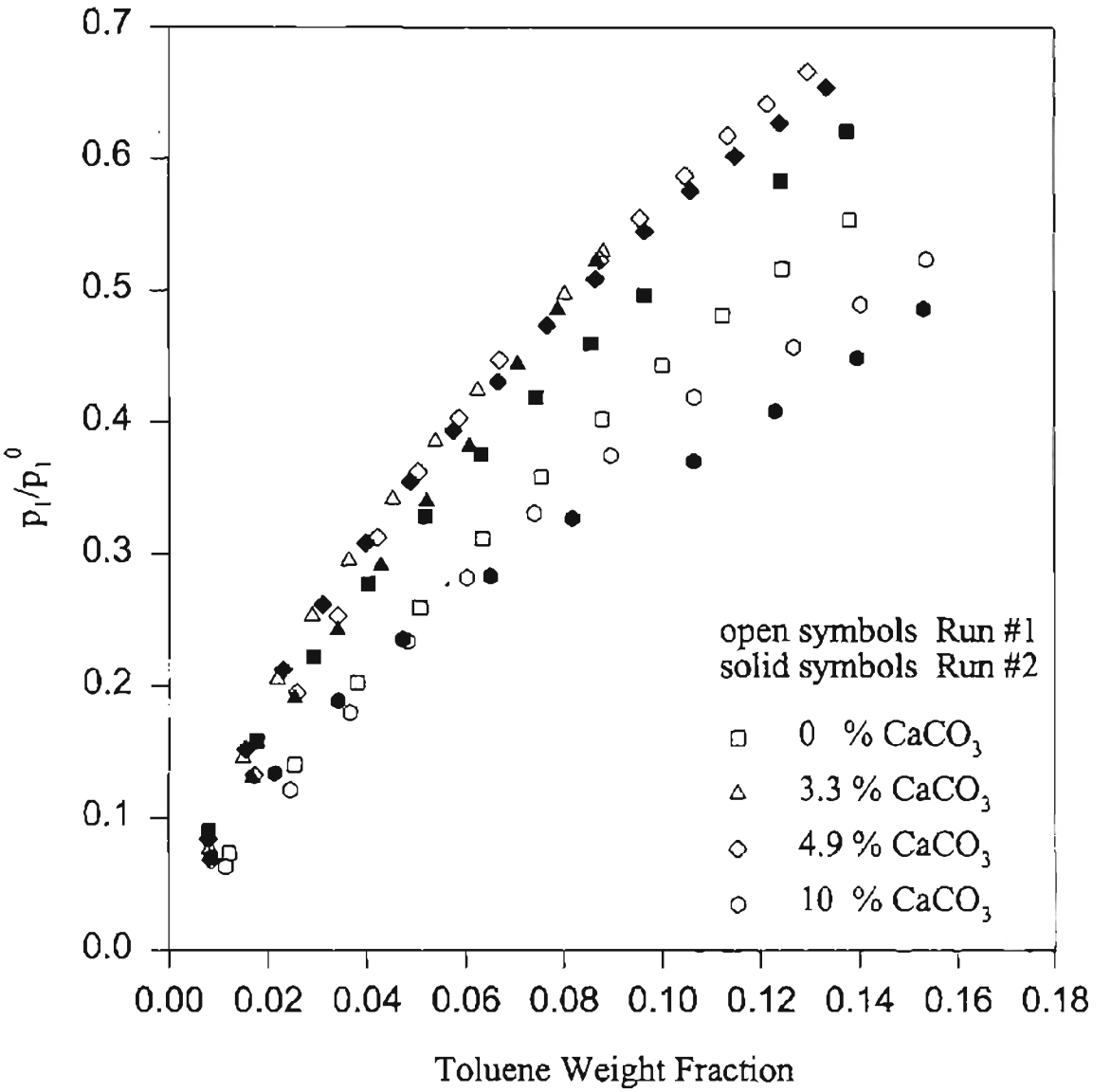

Figure 14. Solubility Data of Toluene in $CaCO_3$ Filled PVAC at 60°C.

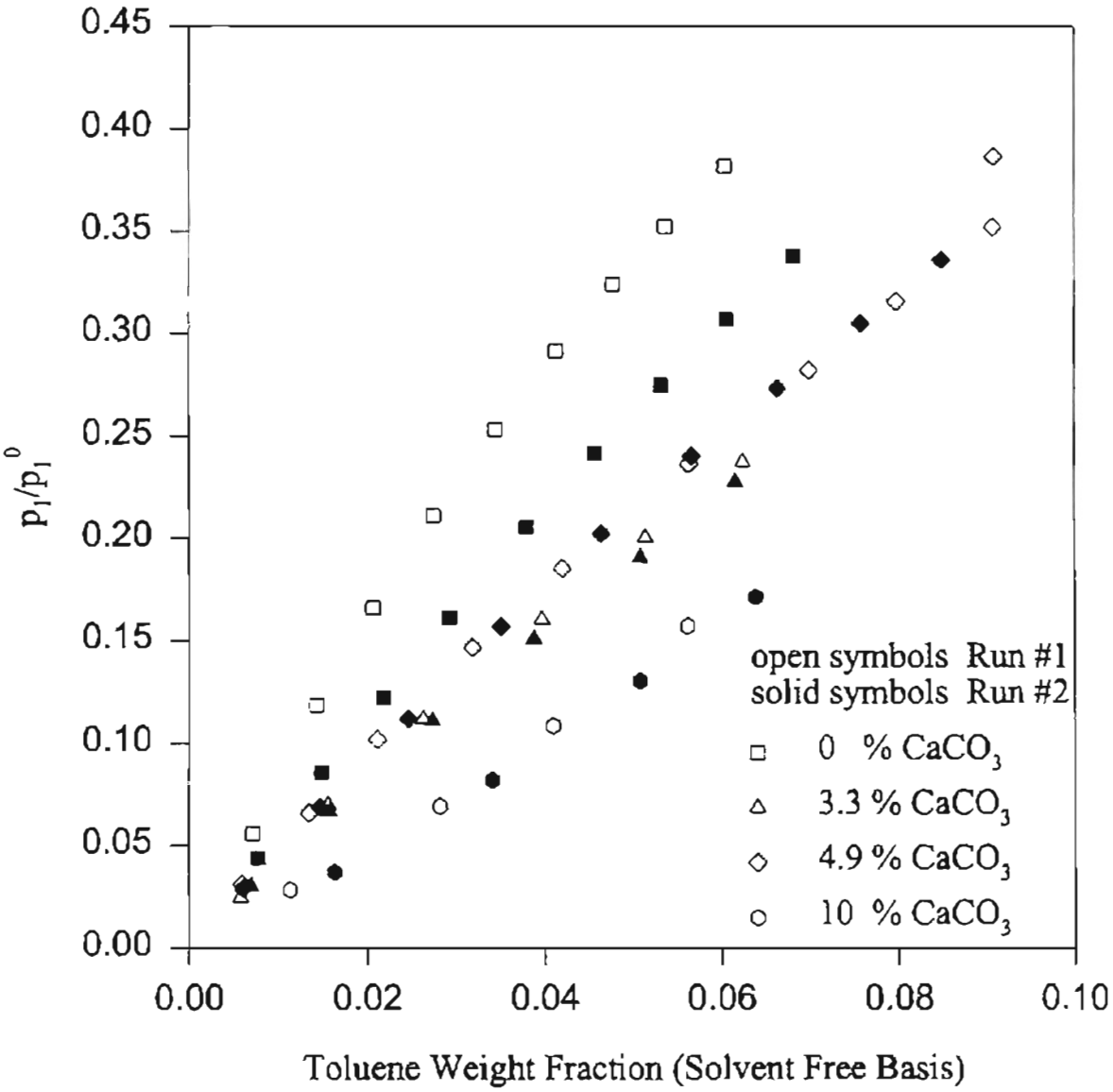

Figure 15. Solubility Data of Toluene in $CaCO_3$ Filled PVAC at 80°C.

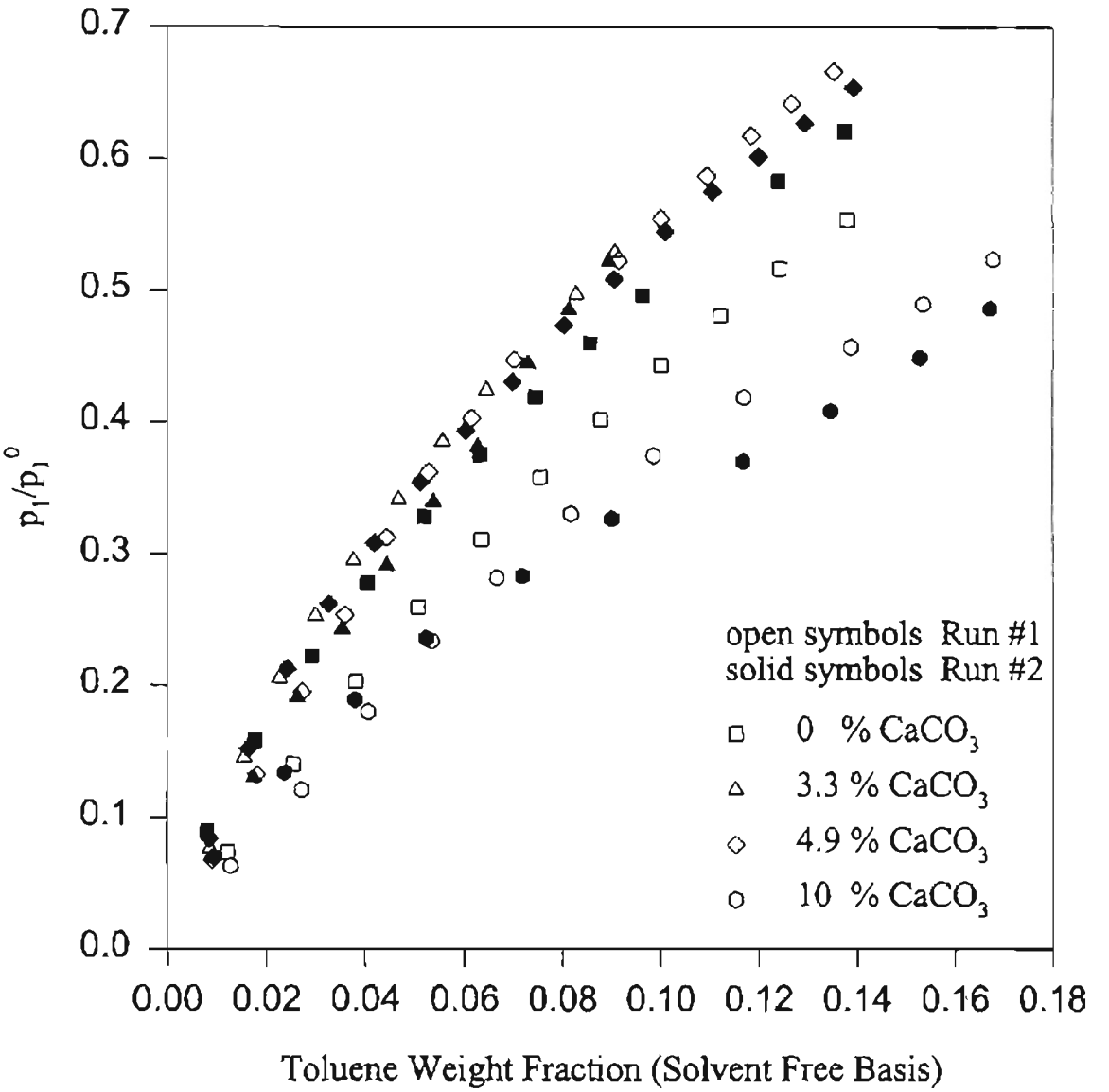

Figure 16. Solubility Data on a Filler Free Basis of Toluene in $CaCO_3$ Filled PVAC at 60°C.

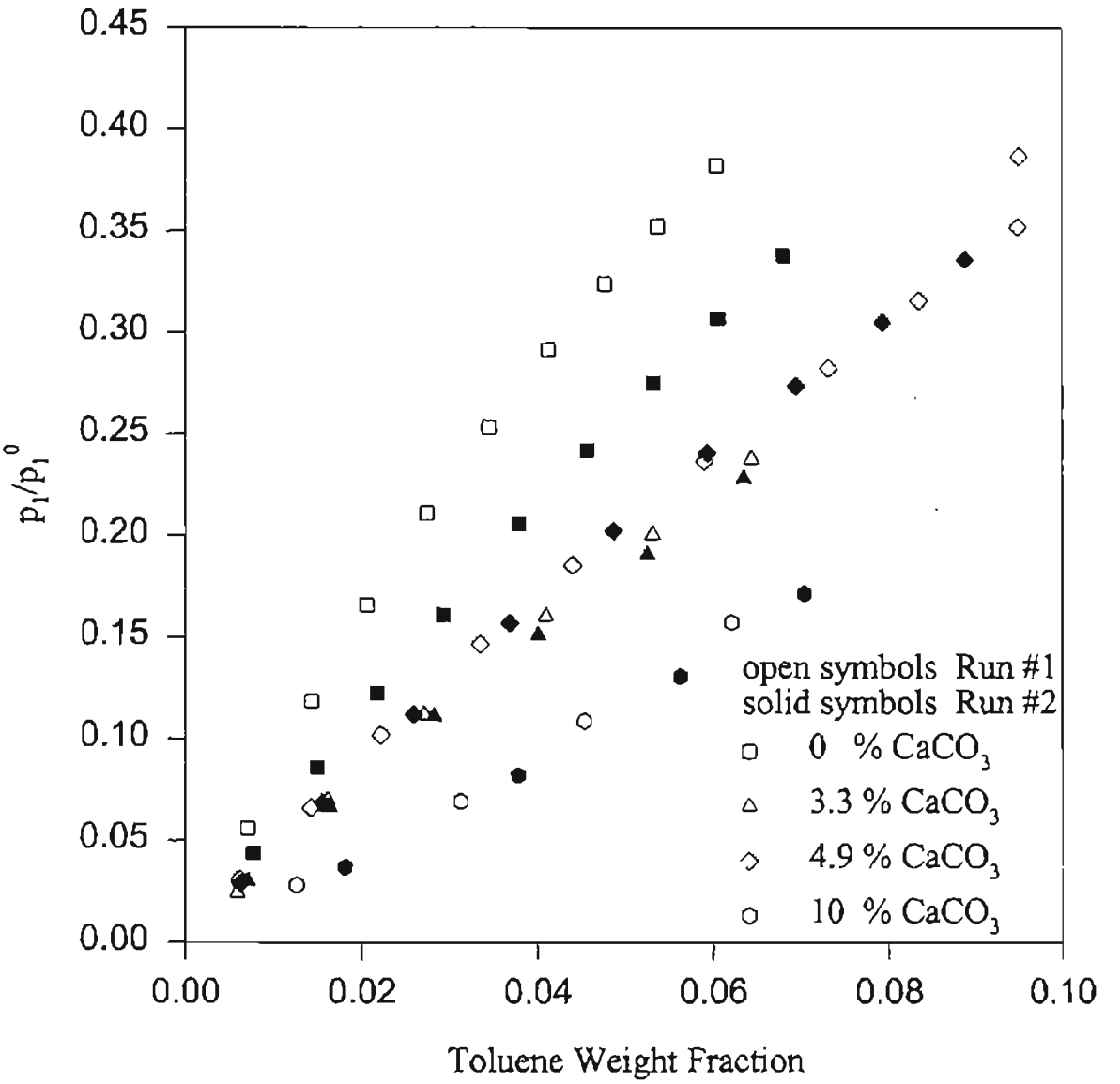

Figure 17. Solubility Data on a Filler Free Basis of Toluene in $CaCO_3$ Filled PVAC at 80°C.

CHAPTER V

DISCUSSION OF RESULTS

In this chapter, the experimental data presented in Chapter IV are discussed. The diffusion coefficients of toluene diffusing into PVAC with 0.0% $CaCO_3$ (neat PVAC) are compared with the results of other researchers [Mikkilineni, 1995 and Hou, 1986] and with the free-volume theory correlation of Vrentas and Duda. The methods discussed in Chapter II for determining diffusion coefficients are compared by analyzing a set of sorption curves with each method. The experimental data for filled PVAC are compared with a free-volume theory correlation modified to account for the added filler and to other correlative equations discussed in Chapter II.

Diffusion coefficients for toluene diffusing into neat PVAC were compared to the data of Mikkilineni [1995] and Hou [1986] at temperatures of 60°C and 80°C in Figures 18 and 19. The diffusion coefficients obtained in this work compare well with the data of both Mikkilineni and Hou. The data shown are from Table I and V of Chapter IV for this work, Table IX for Mikkilineni, and Table X for Hou.

The largest deviations between the data obtained in this work and the data obtained by Hou occur at the lowest weight fractions for both the 60°C and 80°C data. The apparatus used by Hou for obtaining diffusion coefficients was a quartz spring balance. The quartz crystal microbalance is more sensitive to changes in low values of concentration of toluene ($\sim$ 1 ng of toluene) than the quartz spring balance, while the quartz spring balance could give data points at higher values of concentration of the penetrant by using thicker polymer films than can be used by the quartz crystal microbalance.

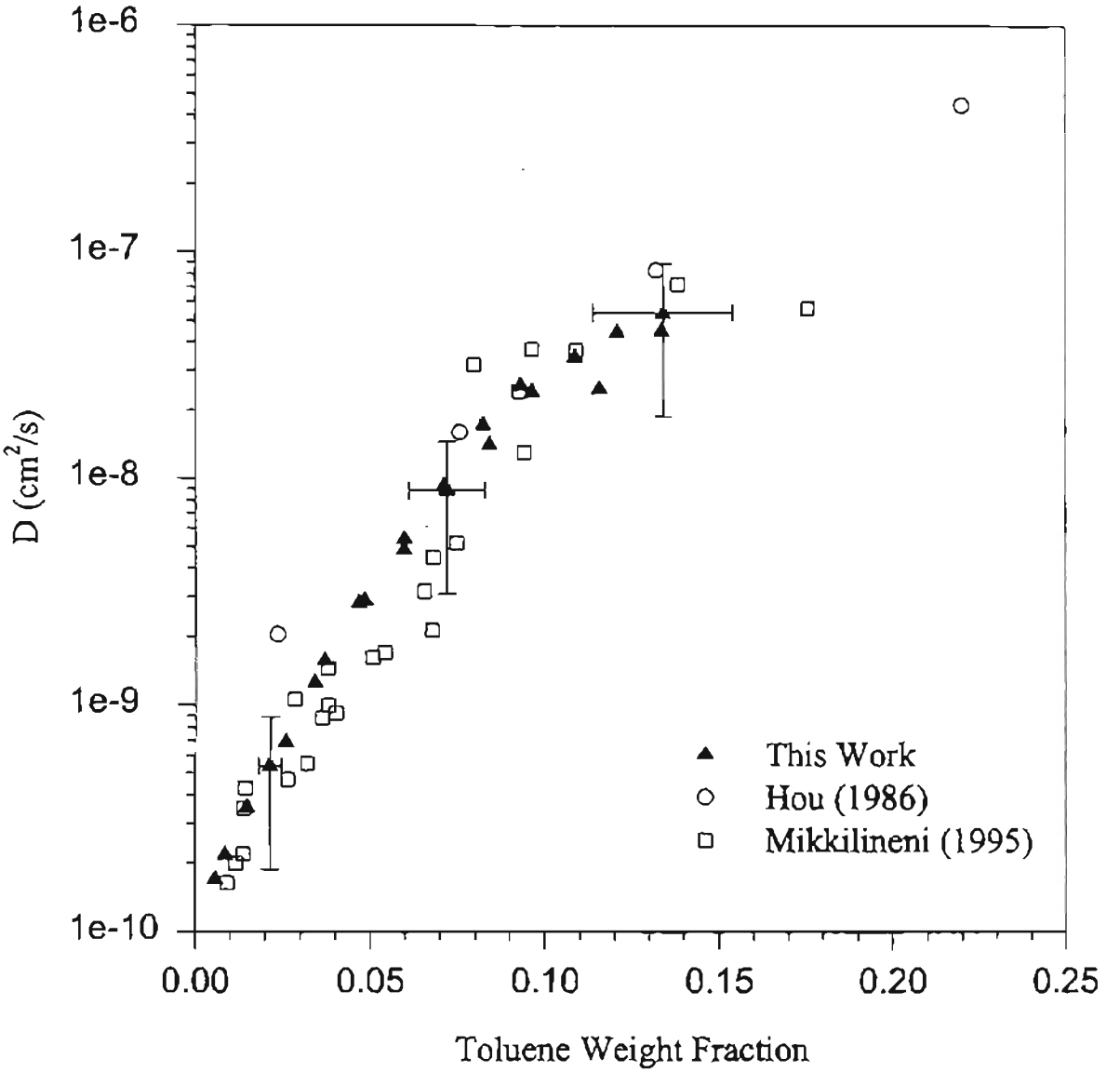

Figure 18. Diffusion Coefficients of Toluene in Neat PVAC at 60°C.

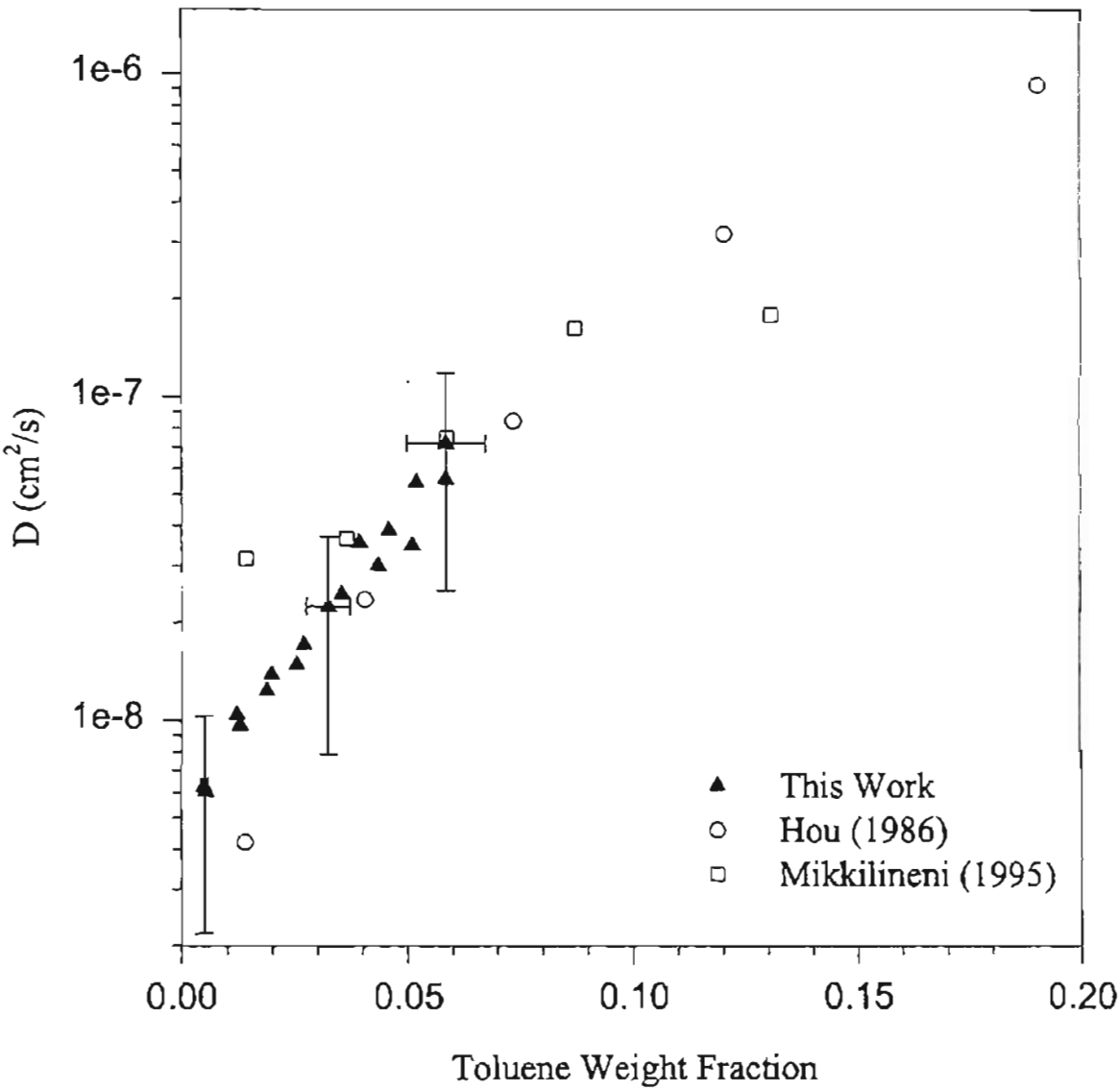

Figure 19. Diffusion Coefficients of Toluene in Neat PVAC at 80°C.

TABLE IX

DIFFUSION COEFFICIENTS OF TOLUENE IN NEAT PVAC FROM MIKKILINENI

Toluene Weight Fraction	D $\times 10^9$ (cm^2/s)
	60°C
0.0091	0.164
0.0264	0.468
0.0508	1.62
0.0680	4.47
0.0963	37.2
0.0136	0.220
0.0402	0.922
0.0746	5.19
0.1088	36.8
0.0116	0.200
0.0321	0.549
0.0677	2.14
0.0941	13.0
0.1382	71.9
0.0144	0.429
0.0397	1.45
0.0138	0.349
0.0363	0.877
0.0654	3.16
0.0283	1.06
0.0795	31.7
0.0541	1.70
0.0380	0.994
0.0928	24.2
0.1756	56.3
	80°C
0.0142	31.5
0.0364	36.5
0.0586	74.8
0.0871	163
0.1305	179

TABLE X

DIFFUSION COEFFICIENTS OF TOLUENE IN NEAT PVAC FROM HOU

Toluene Weight Fraction	D $\times 10^9$ (cm^2/s)
60°C	
0.0234	2.05
0.0755	16.0
0.1320	82.9
0.2199	446
80°C	
0.0140	4.20
0.0404	23.5
0.0734	84.2
0.1202	319
0.1903	921
0.2589	1190

Mikkilineni's data were obtained with the same apparatus as used in this work; however, the methods of analyzing the sorption data were different in this work. Mikkilineni used the initial slope method, and the moment method was used in this work. Also, in this work, the apparatus was modified to include a sample cylinder for quick delivery of the penetrant into the chamber. The use of a sample cylinder was critical for preventing errors which occured from the slow entry of the solvent vapor.

The diffusion coefficients for neat PVAC show greater scatter at larger weight fractions shown, as can be seen in Figures 12 and 13. The reason for increased scatter of data at larger weight fractions was because the diffusion became too fast for enough data to be collected in the beginning stages of diffusion. The faster the diffusion, the fewer the number of data points that were collected in the beginning stages of diffusion. Also, since diffusion at 80°C was faster than diffusion at 60°C, data at 80°C were not obtained at as high of toluene weight fraction. Figure 20 shows an example of a sorption curve that was rejected due to very few data in the initial stages of diffusion. Diffusion coefficients calculated from such a curve would be unreliable since very few data points were collected at the beginning of the curve.

Another phenomena which leads to unreliable diffusion data is the appearance of a hump in the sorption curves for larger toluene weight fractions. Diffusion coefficients obtained from analysis of sorption curves after the appearance of a hump are not shown in Figures 12 and 13 as the scatter of data is too great and the data is considered to be unreliable. The cause of the hump is unknown, but is speculated to be related to "stress effects." Normally, the changes in resonant frequency of the quartz crystal is related to the change in mass on the exposed surface. However, if there is stress in the polymer film on the quartz crystal surface, there is a net force per unit width acting across the polymer film/quartz interface that stress biases the quartz. This stress bias causes the frequency changes referred to as "stress effects" [EerNisse, 1984]. Adding mass or adding stress decreases the resonant frequency of the quartz crystal. Speculations are that, when the coated

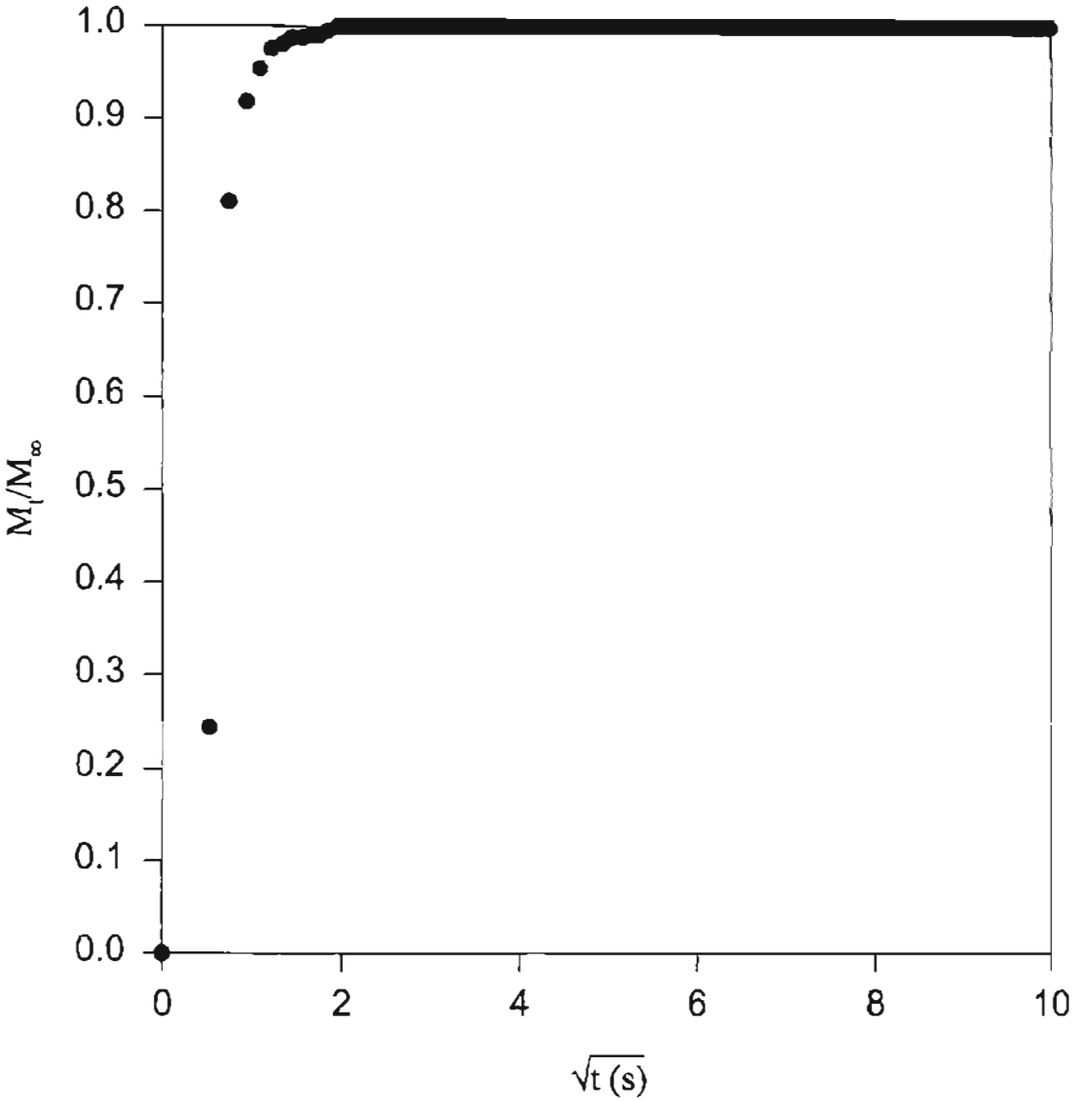

Figure 20. An Example of a Sorption Curve that was Rejected Due to Very Few Data in the Initial Stages of Diffusion.

polymer solution drys, stress builds in the polymer film. During a sorption experiment, adding solvent to the polymer film decreases the resonant frequency of the quartz crystal. The added solvent relaxes the polymer chains, possibly reducing stress at the polymer/crystal interface, which would increase the resonant frequency of the quartz crystal and produce a hump in the sorption curve. Figure 21 shows an example of a sorption curve that was rejected due to a hump in the sorption curve.

Most of the trends of the effective diffusion coefficient data in Figures 12 and 13 are as expected. The diffusion coefficients increase with weight fraction toluene and temperature as is typical of the PVAC-toluene system. Diffusion coefficients decrease with weight percent of $CaCO_3$, which is typical for diffusion in filled rubbery polymers. The diffusion coefficient data are expected to be concave towards the toluene weight fraction axis. The 60°C data appear to follow this trend better than the 80°C data. The data show some upward trends and inflection points, especially for filled PVAC at the larger of the weight fractions. This could be from error in the analysis of the data, due to inaccurate selection of the equilibrium mass uptake. In slower diffusion processes, such as diffusion in filled PVAC compared to diffusion in neat PVAC, the sorption experiment takes a long time to reach equilibrium, and a small error in the equilibrium mass uptake would cause a large error in the first moment calculation of the sorption curve which is used to determine the diffusion coefficient. There could also be errors due to "stress effects" as discussed previously. Although, if "stress effects" are present, they are not noticable enough to form a hump in the sorption data which were analyzed. Replicate experimental runs of each set of data were performed with the same crystal and polymer film for each set in order to verify reproducibility of data. As can be seen from Figures 12 and 13, the data reproduce well. Some scatter is seen, caused by factors such as limited amount of sorption data and inaccurate selection of equilibrium mass uptake, as described above.

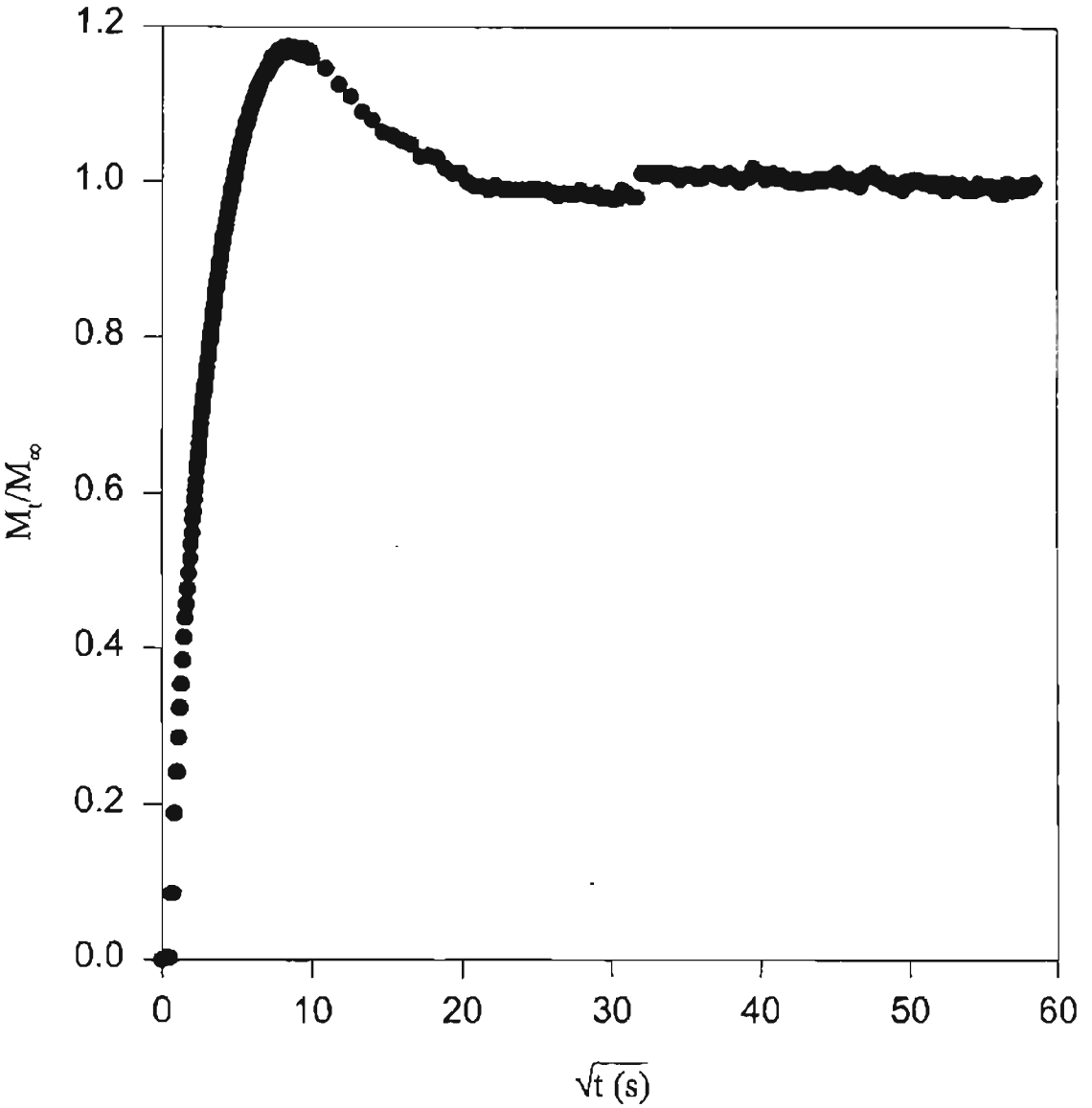

Figure 21. An Example of a Sorption Curve which was Rejected Due to a Hump in the Curve.

The vapor pressure data in Figure 14 through Figure 17 shows the effect of the filler on changing the solubility in the polymer films. The replicate experimental runs compare well for PVAC with 3.3, 4.9, and 10% (by weight) $CaCO_3$ at both 60°C and 80°C. However, there is more error between the replicate experimental runs for neat PVAC at both 60°C and 80°C. The vapor pressure data were plotted against the toluene weight fraction calculated on a filler free basis in Figure 16 and Figure 17 in order to determine effects of adsorption of toluene solvent by the filler. If Henry's law holds, the concentration, C, of the solvent in the polymer film is related to vapor pressure by, $C = \sigma p$. Therefore, the vapor pressure, p_1, is directly proportional to toluene weight fraction, and is indirectly proportional to the solubility coefficient, σ. If p_1 decreases, σ increases. If p_1 increases, σ decreases. The data shown extrapolate to zero vapor pressure at zero toluene weight fraction, as they should. The data also follow different slopes for the different filler contents, as would be expected with different solubility coefficients. Following discussions given in Chapter II, in the absence of vacuoles and for non-adsorbing filler, $\sigma = \sigma_p v_p$, the solubility coefficient would decrease linearly with increasing filler volume fraction. With the exception of the neat PVAC data at 60°C, the general trend in Figures 16 and 17 is a decrease in the vapor pressure with increasing filler content. Therefore, the general trend of the solubility coefficient is to increase with added filler, which means that penetrant adsorption and/or filling of vacuoles with penetrant does occur.

Due to the sensitivity of the quartz crystal microbalance to small changes in concentration of penetrant, the QCM has advantages over other sorption apparatus such as the quartz spring balance since closely spaced diffusion coefficient data can be obtained. The QCM has disadvantages, however, such as the inability to obtain diffusion data at as high of penetrant concentrations as the quartz spring balance, for reasons such as limited sorption data at beginning times and humps in sorption curves, as mentioned above. Yet, these limitations do not pose a problem in the present study, as requirements for model development are satisfied with

low concentration diffusion data and diffusion coefficients with higher penetrant concentrations can be estimated from models.

Another disadvantage of the QCM is the inability to obtain data for highly viscous polymers. As an example, Figure 22 shows a quartz crystal frequency response curve for ethylbenzene diffusing into polybutadiene. The crystal frequency was very unstable during this run. This is due to the viscous nature of polybutadiene. Stress effects are presumed to be great with viscous polymers and the quartz crystal oscillations are damped causing instabilities in the resonant frequency. More examples of trial studies with highly viscous polymers and discussion of the stress effects in piezoelectric quartz crystals are given by Mikkilineni [1995], including interesting examples of polymers so viscous that the quartz crystals ceased to oscillate when coated with the polymer.

The most significant cause of experimental error in this work is believed to be the measurement of the thickness of the polymer film. A possible error is in the measurement of the diameter of the film. The coated films are not perfectly symmetrical; therefore, several measurements of diameter are taken at different orientations and averaged to give the diameter used in the calculations. Another possible error is in the volume measurements with the micropipette. Some of the liquid could adhere to the inner surface of the micropipette tube. Since such a small volume of solution is used, significant error could result. Error also exists due to non-uniformity in the thickness of the polymer films. Visual inspection of the coated films show that the outer edges of the films are usually thicker than the center portion. This is thought to be due to surface tension in the solution while drying. Adhesion of the solution to the surface of the crystal creates forces which move solution to the outer edges of the film. For this same reason, filler particles also tend to be swept to the outer edges of the film. To minimize these effects, the solution is stirred with the tip of the micropipette while being coated.

Appendix C gives and estimate of the error in the diffusion coefficient and penetrant weight fraction due to uncertainties in the thickness of the polymer film

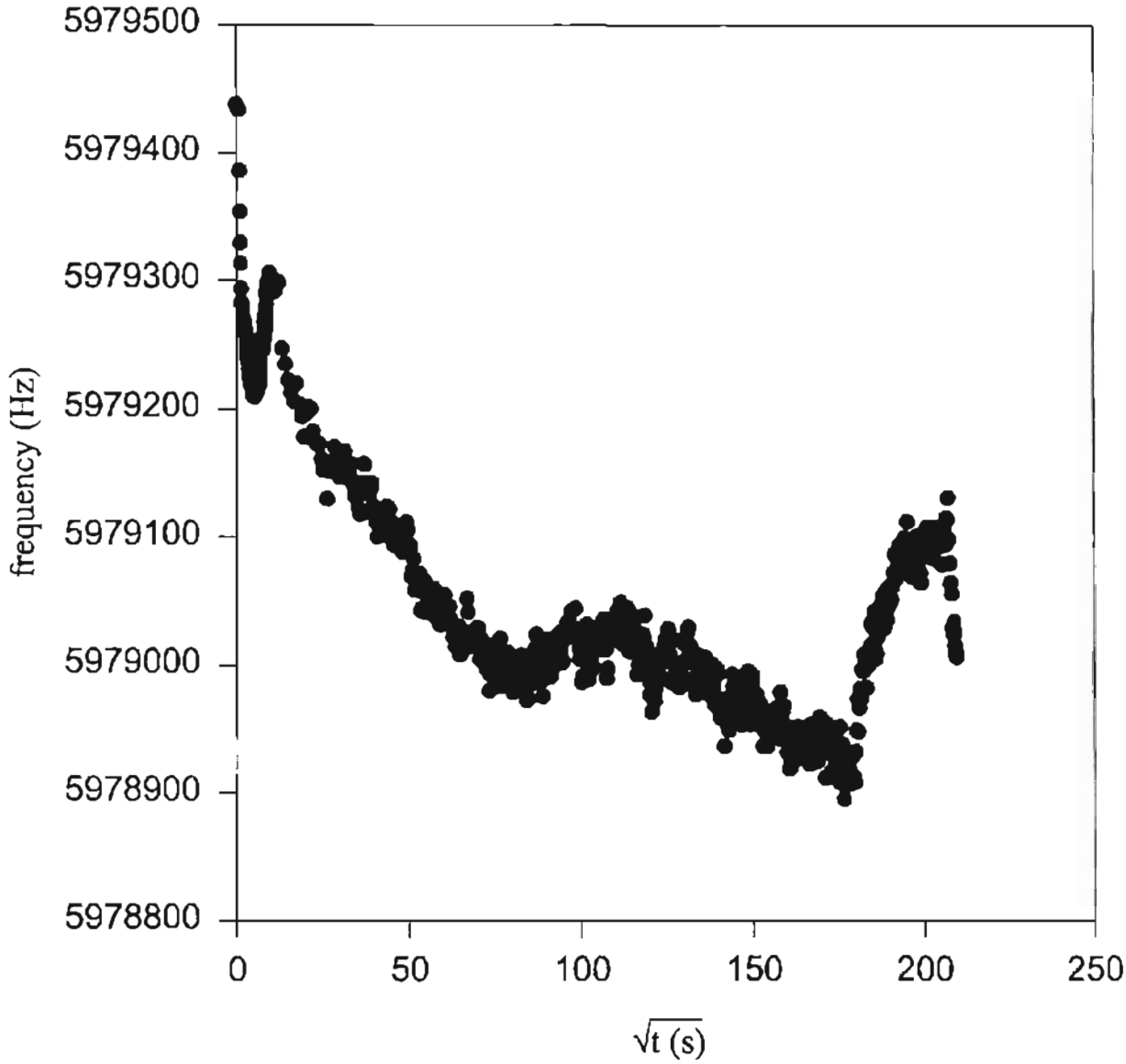

Figure 22. Frequency Curve for Polybutadiene-Ethylbenzene System at 80°C.

and crystal frequencies. The error in the diffusion coefficient was estimated to be 65% and the error in the penetrant weight fraction was estimated to be 15%.

Comparison of Methods for Determining Diffusion Coefficients

There are four well known methods of analyzing sorption data in order to determine diffusion coefficients. The four methods are the half-time method, the initial slope method, the limiting slope method, and the moment method, and have been previously discussed in Chapter II. The moment method was chosen to analyze the sorption data in this work. This section compares the four methods of determining diffusion coefficients by using each method to analyze a set of sorption data.

Sorption data for toluene diffusing into neat PVAC at 60°C was analyzed by the four methods, the half-time method(HT), the initial slope method(ISM), the limiting slope method(LSM), and the moment method(MM). The diffusion coefficients determined by the four methods are shown in Table XI, and compared in Figure 23. The diffusion coefficients determined from the four methods compare well. The diffusion coefficients determined from the limiting slope method has the most scatter. Mass uptake ratios ranging from 0.9 to 1 were used in the limiting slope method, resulting in more random error due to a limited number of data points in such a small range. Mass uptake ratios ranging from 0 to 0.5 or more were used in the initial slope method. The diffusion coefficient data determined from the initial slope method, the half-time method, and the moment method formed smooth curves. Discrepancies in the four methods were more evident at the larger weight fractions shown, since the sorption curves analyzed did not have enough data at the beginning of the curve.

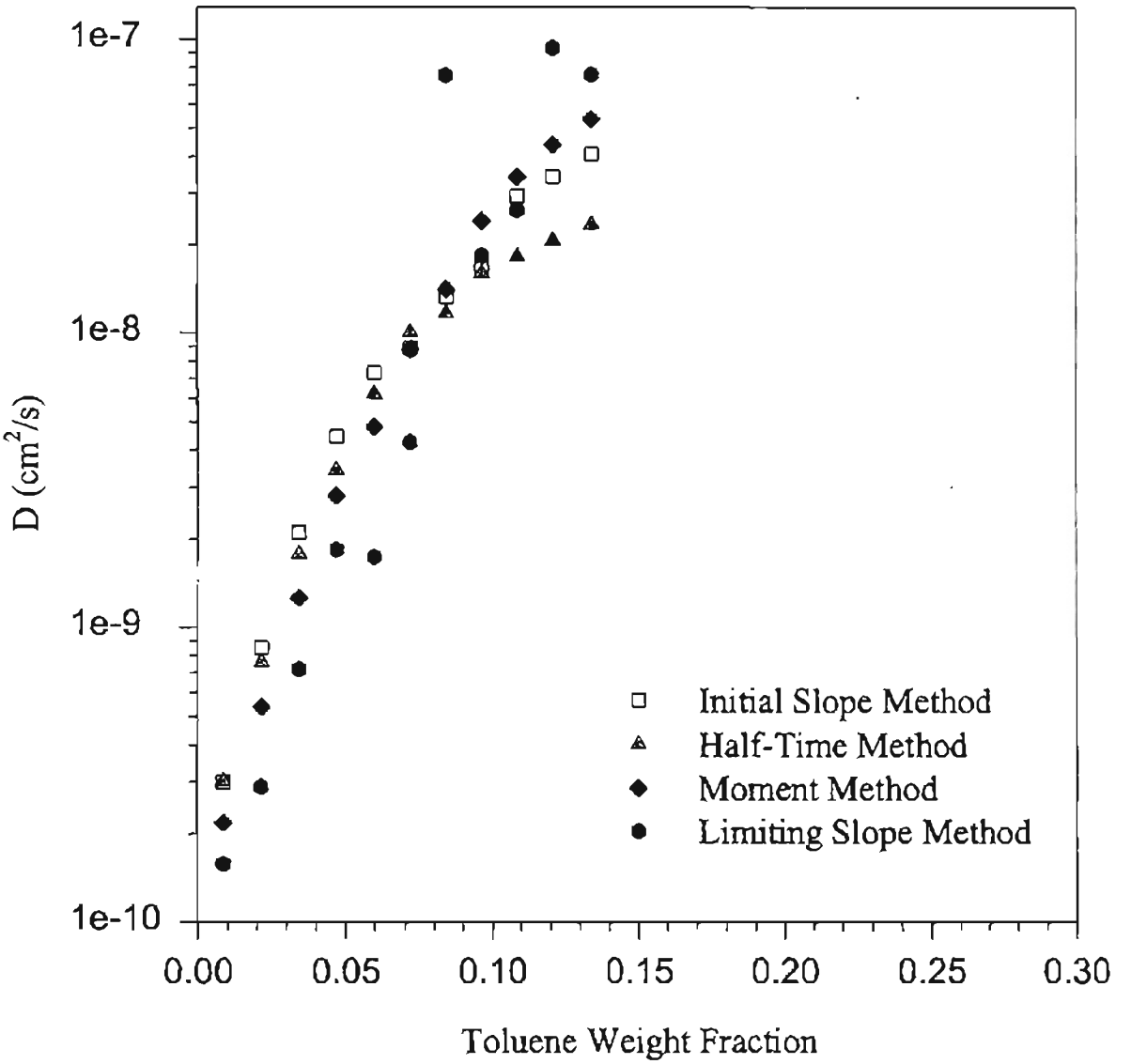

Figure 23. Comparison of Methods for Determining Diffusion Coefficients of Toluene in Neat PVAC at 60°C.

TABLE XI

COMPARISON OF METHODS FOR DETERMINING DIFFUSION COEFFICIENTS OF TOLUENE IN NEAT PVAC AT 60°C

	$D \times 10^9$ (cm^2/s)			
ω_1^{av}	HT	ISM	LSM	MM
0.0085	0.303	0.300	0.158	0.218
0.0213	0.761	0.854	0.289	0.536
0.0342	1.78	2.11	0.720	1.26
0.0468	3.45	4.48	1.84	2.82
0.0596	6.22	7.35	1.74	4.83
0.0718	10.1	8.89	4.28	8.81
0.0841	11.7	13.3	7.57	14.1
0.0963	16.0	16.5	18.4	24.1
0.1085	18.3	29.4	26.3	34.2
0.1207	20.7	34.3	94.0	44.1
0.1339	23.5	41.0	76.1	53.7

Correlating the Experimental Diffusion Coefficient Data

Regressions Using a Modified Free-Volume Equation

Experimental data from this work were compared with effective diffusion coefficient curves obtained from a free-volume equation modified to account for filled polymers. Plots of D vs. volume fraction of filler, v_f, gave insight into how diffusion varies with filler volume fraction. Graphs of D vs. v_f, in semi-log form, are shown in Figure 24 for 60°C data and Figure 25 for 80°C data. These plots are linear, within experimental error; thus, $\log D$ varies linearly with v_f. Models have been developed which describe the penetrant concentration dependence of diffusivity [Duda et al., 1982]. These models are also exponential in form. Combining a model which fits D vs. v_f with a model which fits D vs. w_1 would give a model which describes the dependence of D on both penetrant concentration and filler volume fraction. A linear equation which fits the $\log D$ vs. v_f data may be written as

$$\ln D_{eff} = -mv_f + \ln D_p, \tag{81}$$

where D_{eff} is the effective mutual diffusion coefficient measured in the experiments, D_p is the diffusivity of neat polymer, and m is a positive constant. The negative sign signifies that diffusivity decreases with volume fraction of filler. With $v_f = 0$, this equation simplifies to $D_{eff} = D_p$, as it should. Solving for D_{eff} in equation 81 gives the following equation for diffusion of penetrants in filled polymers,

$$D_{eff} = D_p \exp(-mv_f). \tag{82}$$

An equation which has worked well for many polymer-penetrant systems in describing the concentration dependence of the mutual diffusion coefficient is Vrentas and Duda's [Duda et al., 1982] free-volume theory of transport which was discussed in Chapter II. For this reason, this equation was chosen for D_p. The effective diffusion coefficient in full form can then be given as

$$D_{eff} = D_p \exp(-mv_f), \tag{83}$$

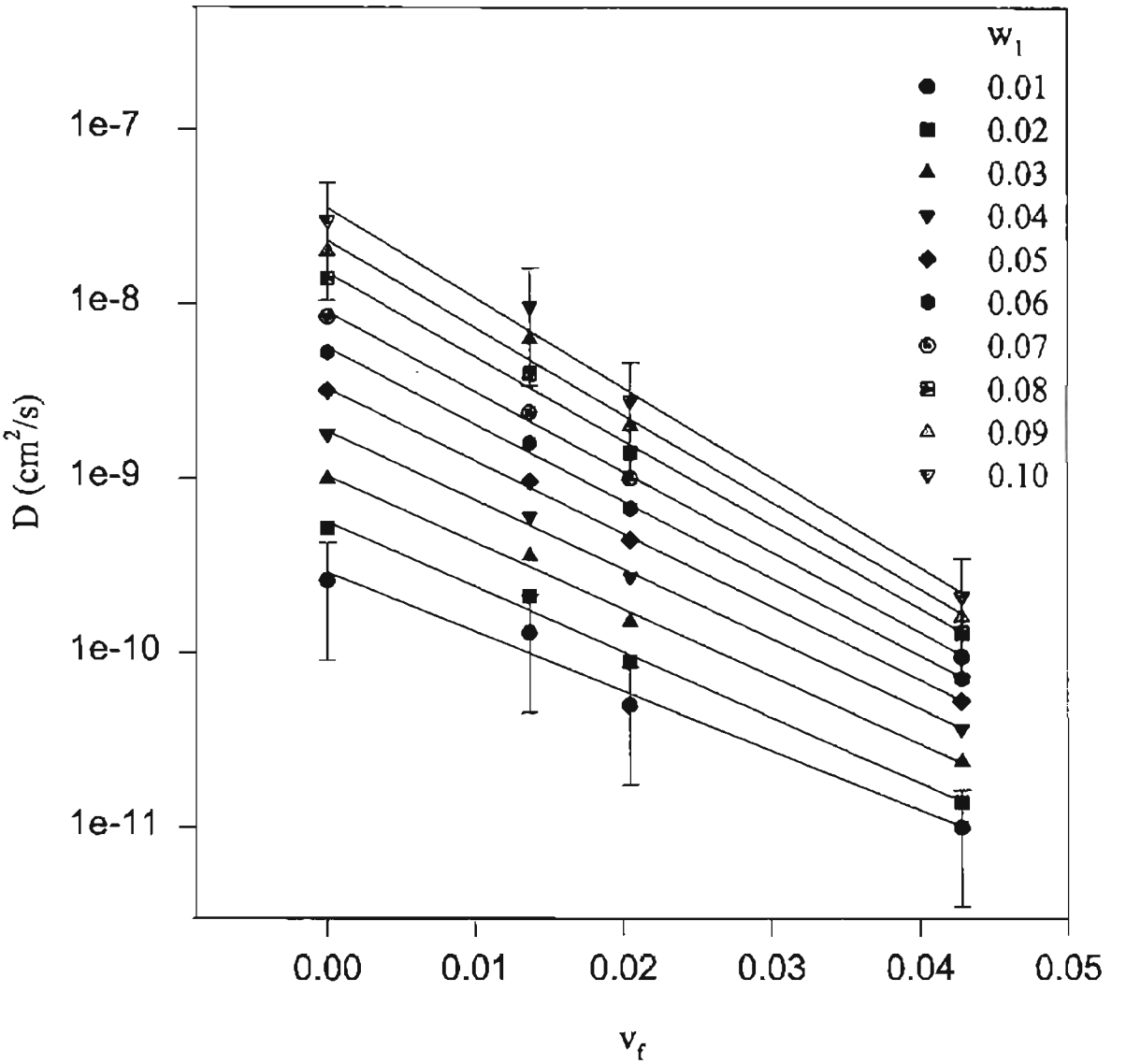

Figure 24. Diffusion Coefficients of Toluene in $CaCO_3$ Filled PVAC as a Function of $CaCO_3$ Volume Fraction at 60°C for Various Toluene Weight Fractions.

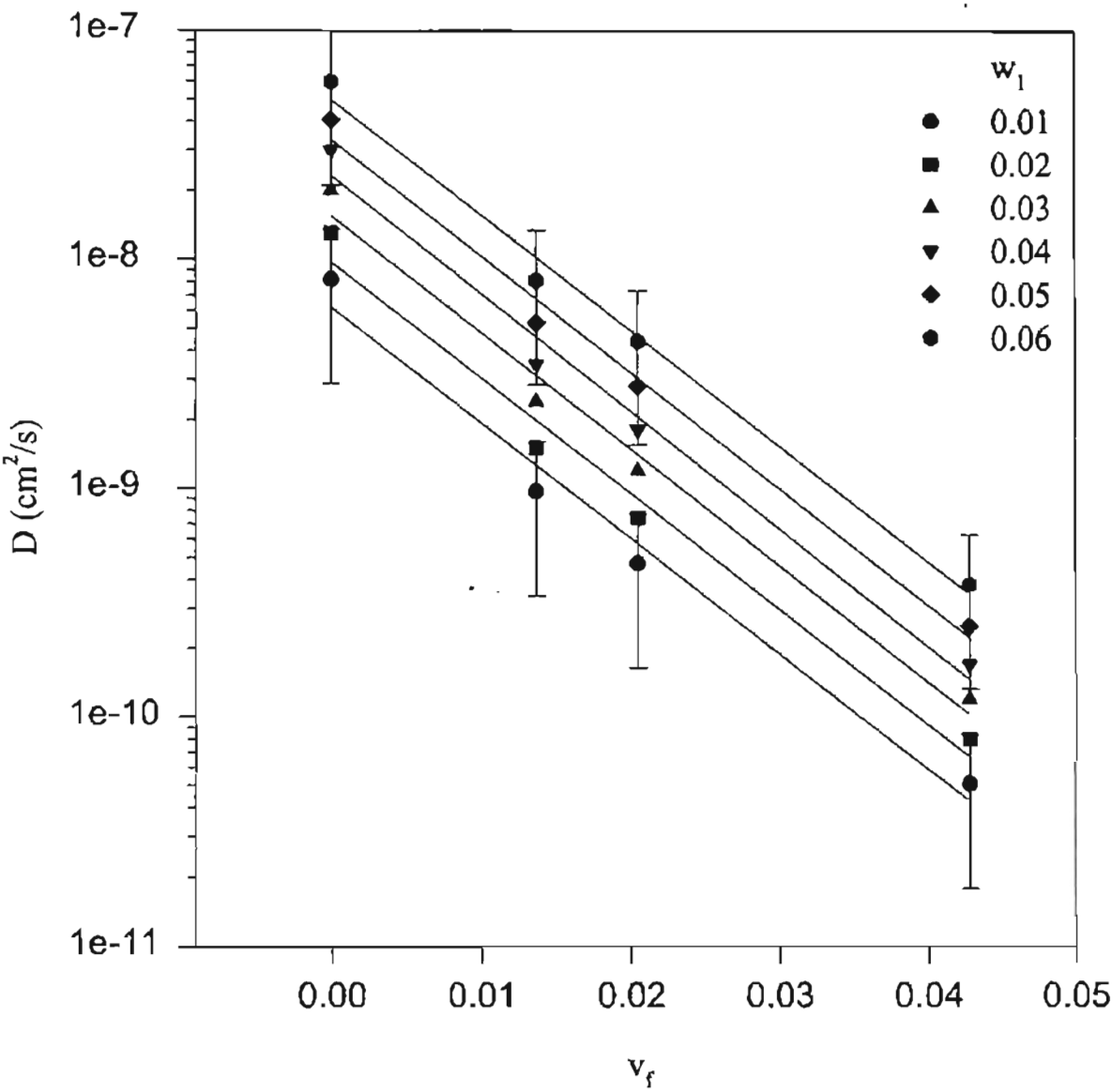

Figure 25. Diffusion Coefficients of Toluene in $CaCO_3$ Filled PVAC as a Function of $CaCO_3$ Volume Fraction at 80°C for Various Toluene Weight Fractions.

$$D_p = D_1(1-\phi_1)^2(1-2\chi\phi_1), \tag{84}$$

$$D_1 = D_{01}\exp\left(-\frac{\gamma(w_1\widehat{V}_1^* + w_2\xi\widehat{V}_2^*)}{\widehat{V}_{FH}}\right), \tag{85}$$

$$\frac{\widehat{V}_{FH}}{\gamma} = w_1\frac{K_{11}}{\gamma}(K_{21}+T-T_{g1}) + w_2\frac{K_{12}}{\gamma}(K_{22}+T-T_{g2}). \tag{86}$$

The preexponential constant, D_0, mentioned in Chapter II is lumped in along with the Arrhenius form of temperature dependence into the term D_{01}. The free volume parameters K_{11}/γ, $K_{21}-T_{g1}$, K_{12}/γ, $K_{22}-T_{g2}$, $\widehat{V}_1^*$ and $\widehat{V}_2^*$ were taken from Hou [1986]. The parameters D_{01}, ξ, χ, and m were obtained from correlations with experimental data from this work, as explained in the following paragraphs.

The interaction parameter, χ, was obtained by fitting the Flory-Huggins equation

$$\frac{p_1}{p_1^0} = \phi_1\exp\{(1-\phi_1)+\chi(1-\phi_1)^2\}, \tag{87}$$

to solubility data in which the equilibrium weight fraction of the penetrant in the polymer was known as a function of penetrant vapor pressure, p_1. The pressure p_1^0 is the penetrant saturation vapor pressure. Table I and Table V of Chapter IV shows the data used for this regression. Figure 26 shows a comparison of solubility data for neat PVAC at 60°C with a theoretical curve calculated by equation 87. Figure 27 shows a similar comparison for 80°C data. The solubility data calculated by equation 87 compare reasonably well with experimental solubility data, with more scatter appearing in the 80°C data. The interaction parameter, χ, is given in Figures 26 and 27 as 0.42 and 0.75 for 60°C and 80°C data, respectively.

The parameters D_{01} and ξ were obtained by fitting equation 83 to experimental diffusion coefficient data for neat PVAC ($v_f = 0$). Figure 28 shows a comparison of experimental diffusion coefficient data for neat PVAC at 60°C with curves calculated by equation 83 with $v_f = 0$. The parameters D_{01} and ξ are given in this figure. The diffusion coefficients calculated by equation 83 compare well with experimental diffusion coefficient data.

The parameter m was obtained by fitting equation 83 to experimental diffusion coefficient data for $CaCO_3$ filled PVAC with a weight of 10% $CaCO_3$

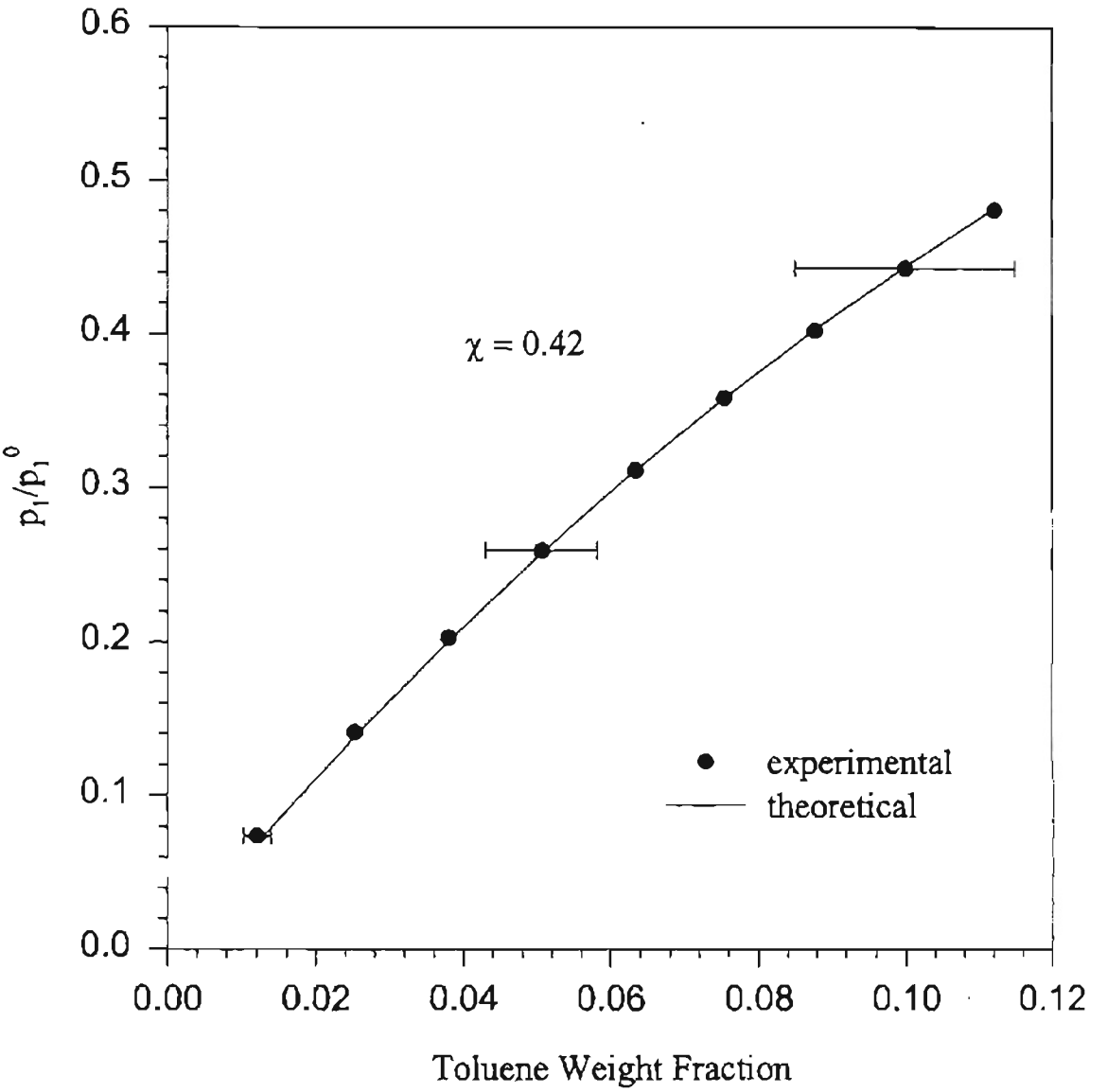

Figure 26. Comparison of Experimental Solubility Data with the Flory-Huggins Equation for PVAC-Toluene at 60°C.

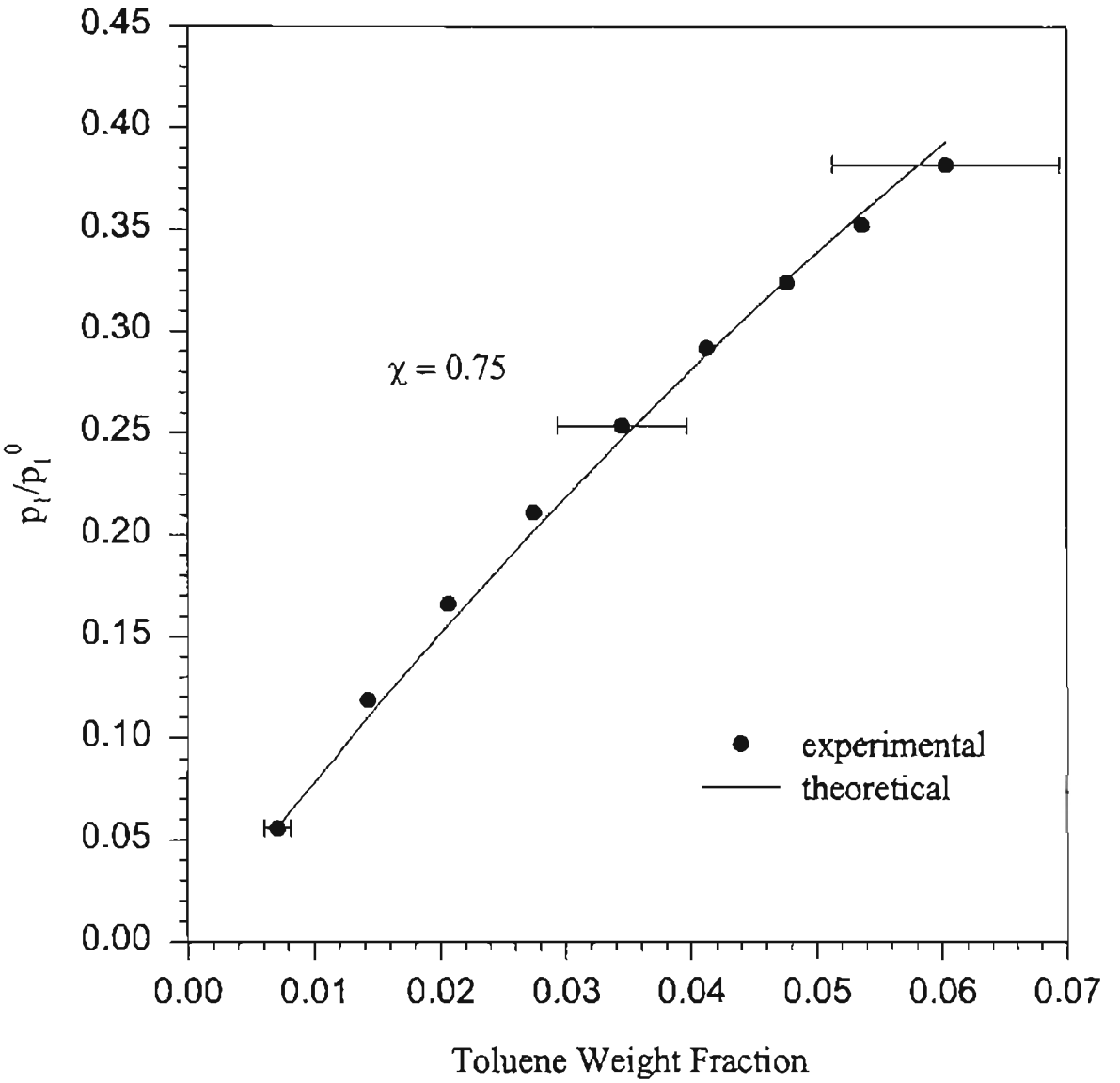

Figure 27. Comparison of Experimental Solubility Data with the Flory-Huggins Equation for PVAC-Toluene at 80°C.

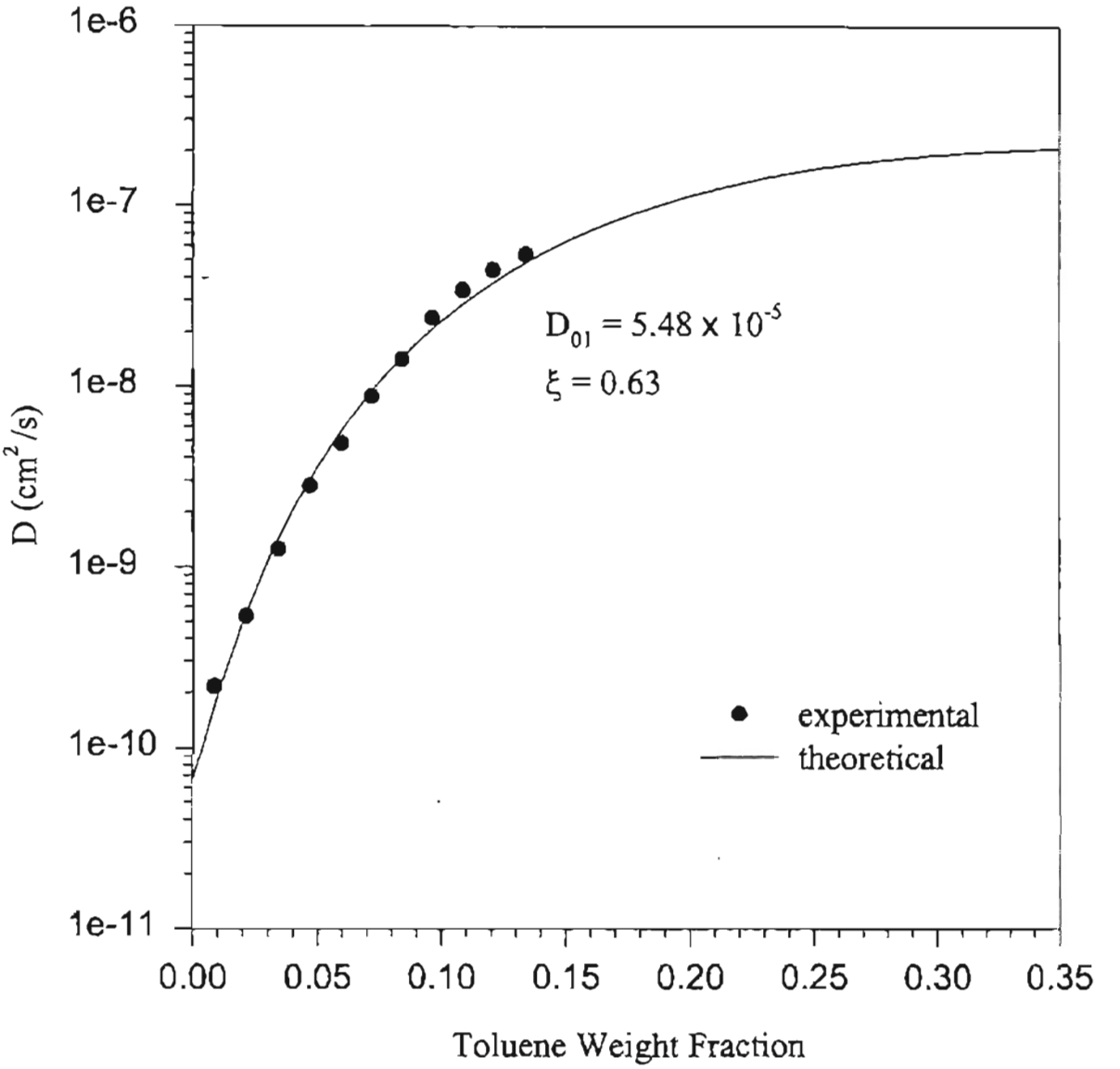

Figure 28. Comparison of Experimental Diffusion Coefficient Data with a Free-Volume Equation for Toluene Diffusing into Neat PVAC ($v_f = 0$) at 60°C.

($v_f = 0.0428$). Figure 29 shows a comparison of the diffusion coefficient data for $CaCO_3$ filled PVAC with a weight of 10% $CaCO_3$ at 60°C with curves calculated by equation 83 with $v_f = 0.0428$. The parameter m is given in this figure. The fit of equation 83 to the experimental diffusion coefficient data in this figure is reasonable, but these data show more scatter than the data for neat PVAC.

Figure 30 shows both of the previous comparisons of the data of neat PVAC and $CaCO_3$ filled PVAC with a weight of 10% $CaCO_3$, as well as comparisons of the diffusion coefficient data of $CaCO_3$ filled PVAC with weights of 3.3% ($v_f = 0.0137$) and 4.9% ($v_f = 0.0205$) $CaCO_3$ at 60°C to predicted curves calculated by equation 83. The curves for data with 3.3% and 4.9% $CaCO_3$ are purely predictive. Only the volume fraction of filler, v_f, in the equation was changed. All other parameters were obtained from previous correlations.

Figure 31 shows similar regressions of neat PVAC data and data of $CaCO_3$ filled PVAC with a weight of 10% $CaCO_3$ using equation 83 as well as predictions of the diffusivity data of $CaCO_3$ filled PVAC with weights of 3.3% and 4.9% $CaCO_3$ at 80°C. As before, the parameters D_{01} and ξ were obtained by fitting the experimental diffusion coefficient data of neat PVAC to equation 83, and the parameter m was obtained by fitting the experimental diffusion coefficient data of $CaCO_3$ filled PVAC with a weight of 10% $CaCO_3$ to equation 83. The predictive curves of the diffusion coefficients of $CaCO_3$ filled PVAC with weights of 3.3% and 4.9% were calculated by equation 83 by changing only the volume fraction of filler, v_f.

The diffusion coefficient curves calculated with equation 83 compare very well with the experimental diffusion coefficient data of neat PVAC and PVAC with 10% $CaCO_3$. Also, the diffusion coefficient curves calculated with equation 83 for PVAC with 3.3% and 4.9% $CaCO_3$ at 60°C and 80°C show a reasonable prediction of the experimental data. The predictions of the diffusion coefficients for PVAC with 4.9% $CaCO_3$ are the better of the two samples. The data for PVAC with 3.3% $CaCO_3$ shows more scatter, showing low predictions of data at 60°C and high predictions of data at 80°C.

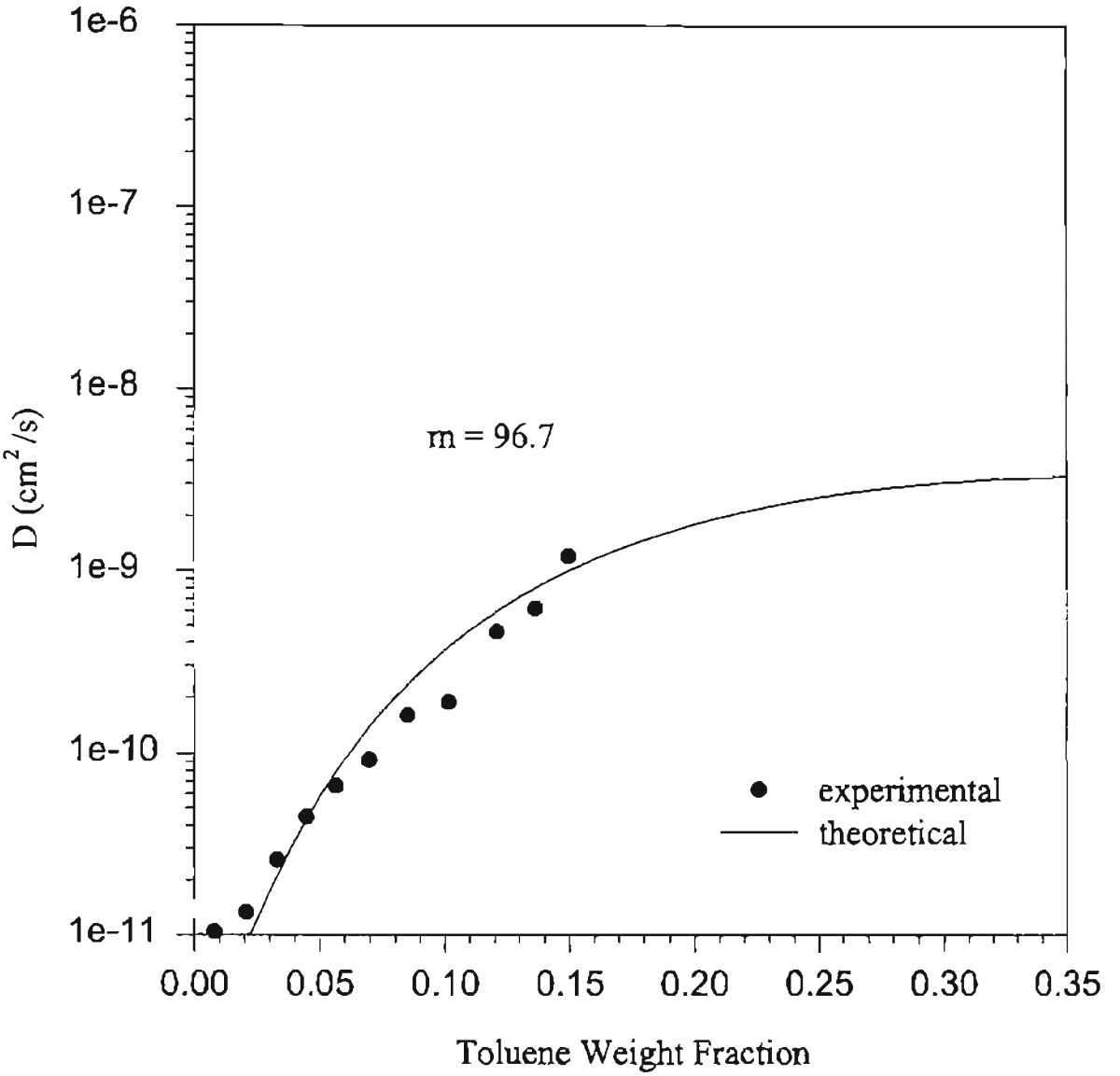

Figure 29. Comparison of Experimental Diffusion Coefficient Data with a Free-Volume Equation for $CaCO_3$ Filled PVAC with a Weight of 10% $CaCO_3$ ($v_f = 0.0428$) at 60°C.

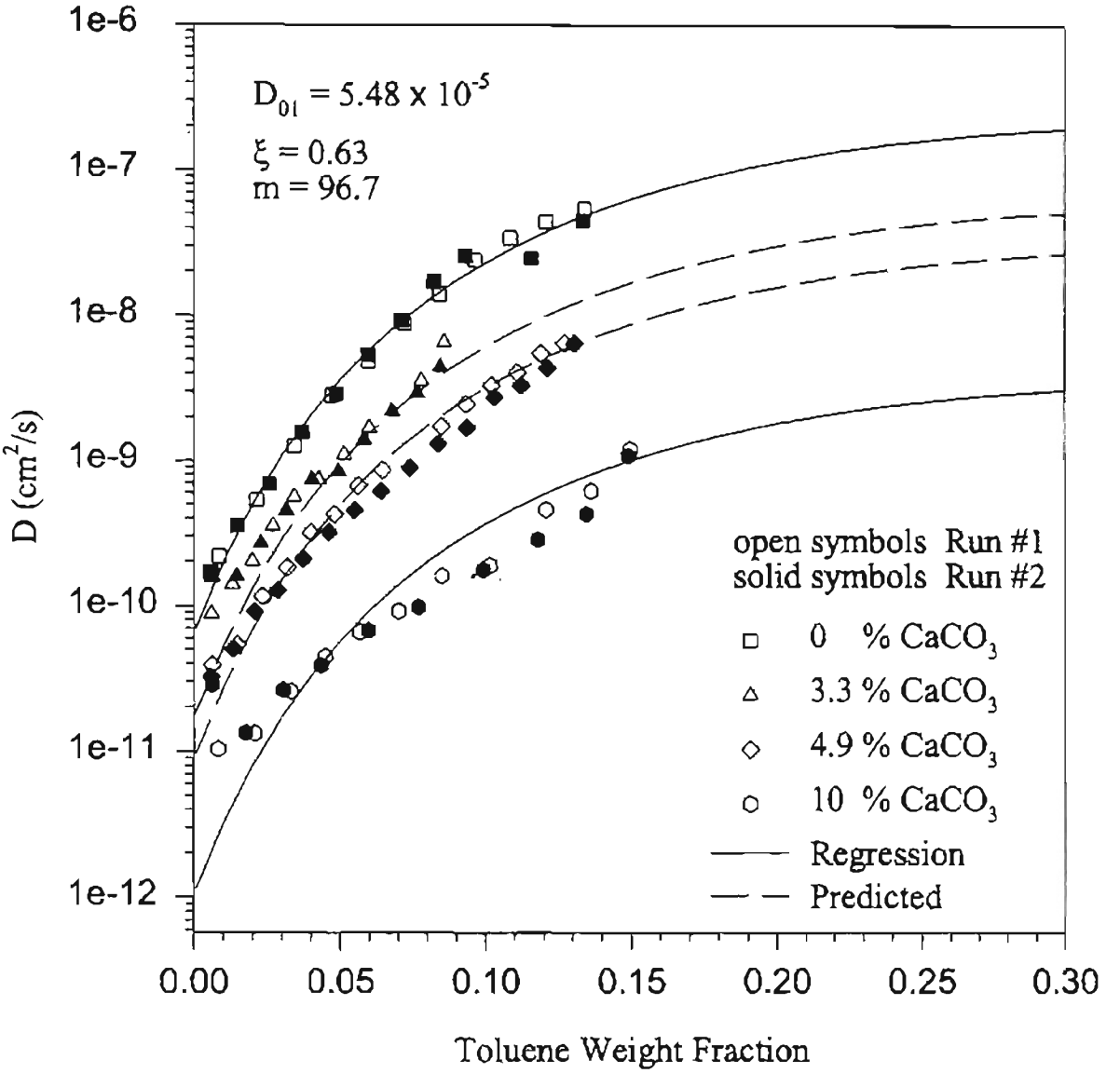

Figure 30. Comparisons of Experimental Diffusion Coefficients with a Free-Volume Equation for $CaCO_3$ Filled PVAC at 60°C.

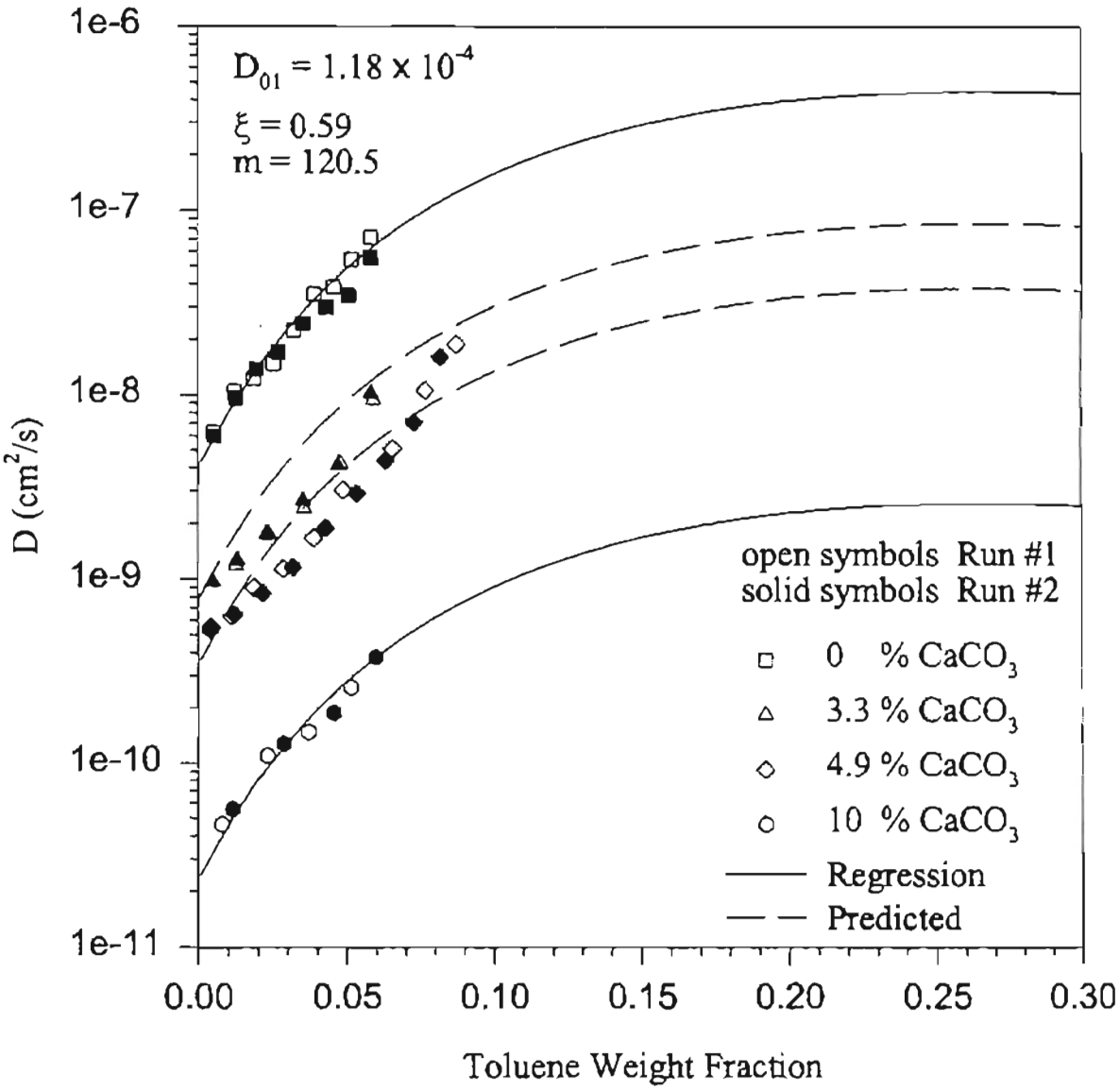

Figure 31. Comparisons of Experimental Diffusion Coefficients with a Free-Volume Equation for $CaCO_3$ Filled PVAC at 80°C.

The free-volume parameters used in this subsection are shown in Table XII. The solubility data regressions show the parameter χ to increase with temperature with a 56% difference between 60°C and 80°C. The parameter, ξ, is usually assumed to be temperature independent [Duda, 1983]. Regressions of diffusion data at 60°C and 80°C show this agreement to within 7%. The parameter, D_{01}, is temperature dependent and is assumed to follow the Arrhenius equation. For positive activation energy, E, the parameter, D_{01}, increases with temperature. Regressions of data verify the increase of D_{01} with temperature. The D_{01} at 80°C was 73% greater than D_{01} at 60°C. The parameter, m, increases with temperature with a 22% difference between the two temperatures. In a study of diffusion of hydrocarbons in silicone rubber, Barrer [1962] reported that the percentage difference in the diffusion coefficient between filled and unfilled rubber increased with temperature. Therefore, from the mathematical form of equation 83, m is expected to increase with temperature.

Regressions Using Equations Derived by Barrer and Chio

Experimental diffusion coefficient data for toluene diffusing into $CaCO_3$ filled PVAC at 60°C was used to test the correlative capabilities of the equations derived by Barrer and Chio [1965], as described in Chapter II. The free-volume equation was used for the unfilled diffusion coefficient, D_p, with parameters as given in the previous subsection.

The first equation used was the simple form in which only the tortuosity of the diffusion paths around the filler particles was considered

$$D_{eff} = \kappa D_p, \tag{88}$$

where κ is the structure factor. The expression of Fricke,

$$\kappa = \frac{Y}{Y + v_f}, \tag{89}$$

TABLE XII

PARAMETERS OF THE MODIFIED FREE-VOLUME EQUATION FOR PVAC-TOLUENE

Free-Volume Parameters from Hou [1986]

Parameter	Value
$\widehat{V}_1^*$ (cm^3/g)	0.917
$\widehat{V}_2^*$ (cm^3/g)	0.728
K_{11}/γ (cm^3/g K)	1.57 $\times 10^{-3}$
K_{12}/γ (cm^3/g K)	4.33 $\times 10^{-4}$
$K_{21} - T_{g1}$ (K)	-90.5
$K_{22} - T_{g2}$ (K)	-256

Regressed Free-Volume Parameters

Parameter	60°C	80°C
χ	0.42	0.75
ξ	0.63	0.59
D_{01} (cm^2/s)	5.48 $\times 10^{-5}$	1.18 $\times 10^{-4}$
m	96.7	120.5

where $Y = 2$ for random spheres was used in equation 89. The expression of Runge,

$$\kappa = \frac{1}{(1 - v_f)} \left[1 - \frac{3v_f}{2 + v_f - 0.392 v_f^{10/3}} \right], \tag{90}$$

for a cubic lattice of spheres was also used. Both of these expressions, equation 89 and equation 90, gave the same value for κ. The smallest value of the structure factor, $\kappa = 0.979$, was for polymer with 10% filler ($v_f = 0.0428$). This value led to only a 2% decrease in the diffusion coefficient. Figure 32 shows this comparison, as well as the previously obtained regression of neat PVAC. The fit using equation 88 is very poor. The values of κ calculated from equations 89 and 90 are used in subsequent calculations.

The next equation used was the more complicated form which takes into account two separate phases, the polymer phase and the filler phase,

$$D_{eff} = \kappa D_p \frac{v_p}{v_p + v_f(\sigma_f/\sigma_p)}, \tag{91}$$

where σ_p is a parameter related to the solubility in the polymer and σ_f is a parameter related to the gas adsorption by the filler. The ratio σ_f/σ_p was obtained by fitting equation 91 to experimental diffusion coefficient data for $CaCO_3$ filled PVAC with a weight of 10% $CaCO_3$ ($v_f = 0.0428$). Figure 33 shows this regression, as well as the previously obtained regression of neat PVAC, and the predictions of the diffusivity data of $CaCO_3$ filled PVAC with weights of 3.3% and 4.9% $CaCO_3$ at 60°C. The diffusion coefficients obtained from the regression using equation 91 compare well with the experimental diffusion coefficients of toluene in 10% $CaCO_3$ filled PVAC, however, equation 91 does not predict well the experimental diffusion coefficients of toluene in 3.3% $CaCO_3$ and 4.9% $CaCO_3$ filled PVAC.

The ratio σ_f/σ_p obtained in the regression using equation 91 is much larger than unity, 1,351.5. However, even assuming independent sorption by filler and rubber phases, Barrer et al. [1962] reported values of the ratio σ_f/σ_p less than unity for hydrocarbons diffusing into silica filled silicone rubber. Therefore, the ratio σ_f/σ_p is unlikely to be as large as that obtained by the regression. Diffusion of toluene in $CaCO_3$ filled PVAC is possibly too complex to model with a diffusion

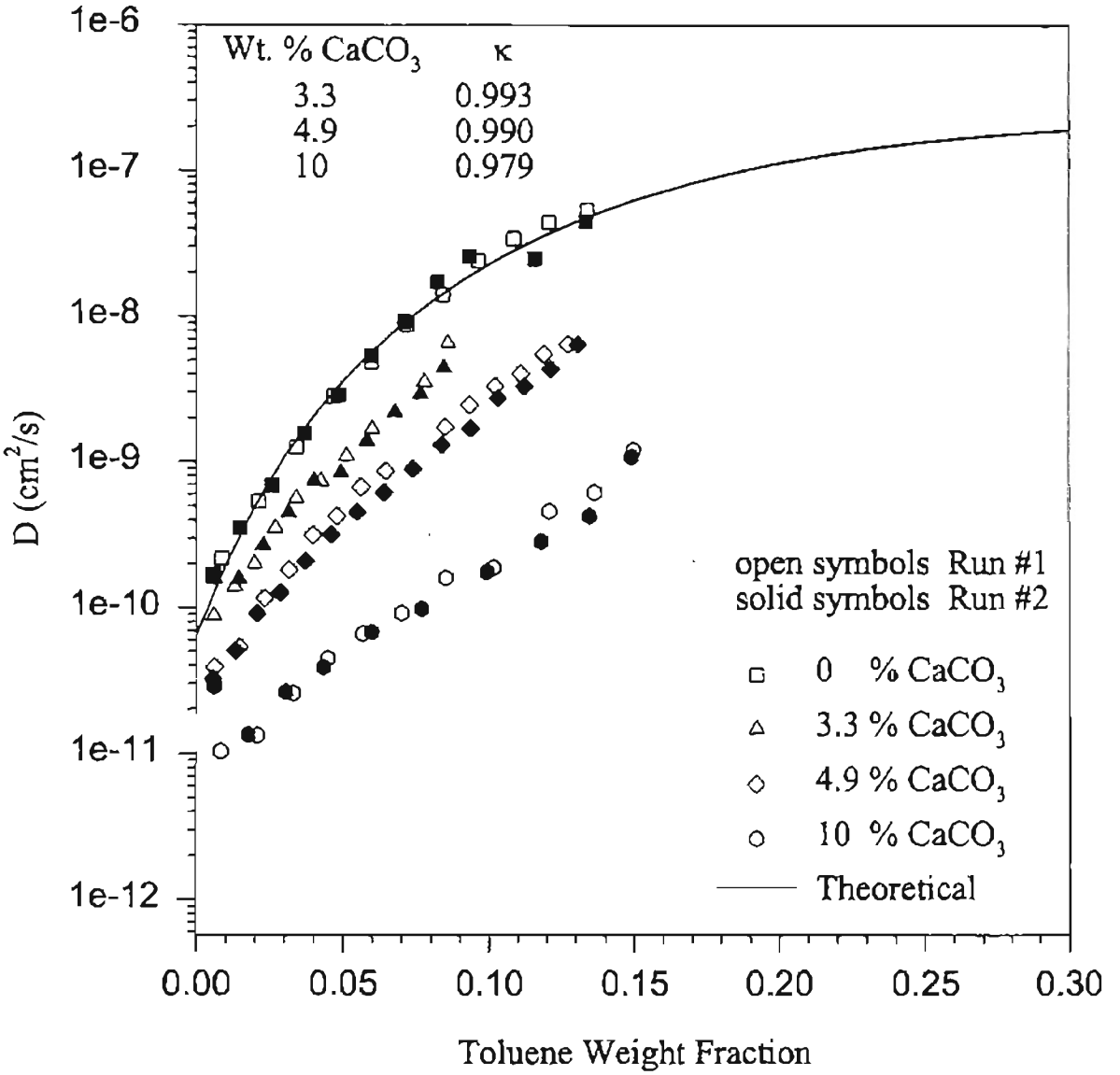

Figure 32. Comparisons of Experimental Diffusion Coefficients with a Simple Structure Factor Equation for $CaCO_3$ Filled PVAC at 60°C.

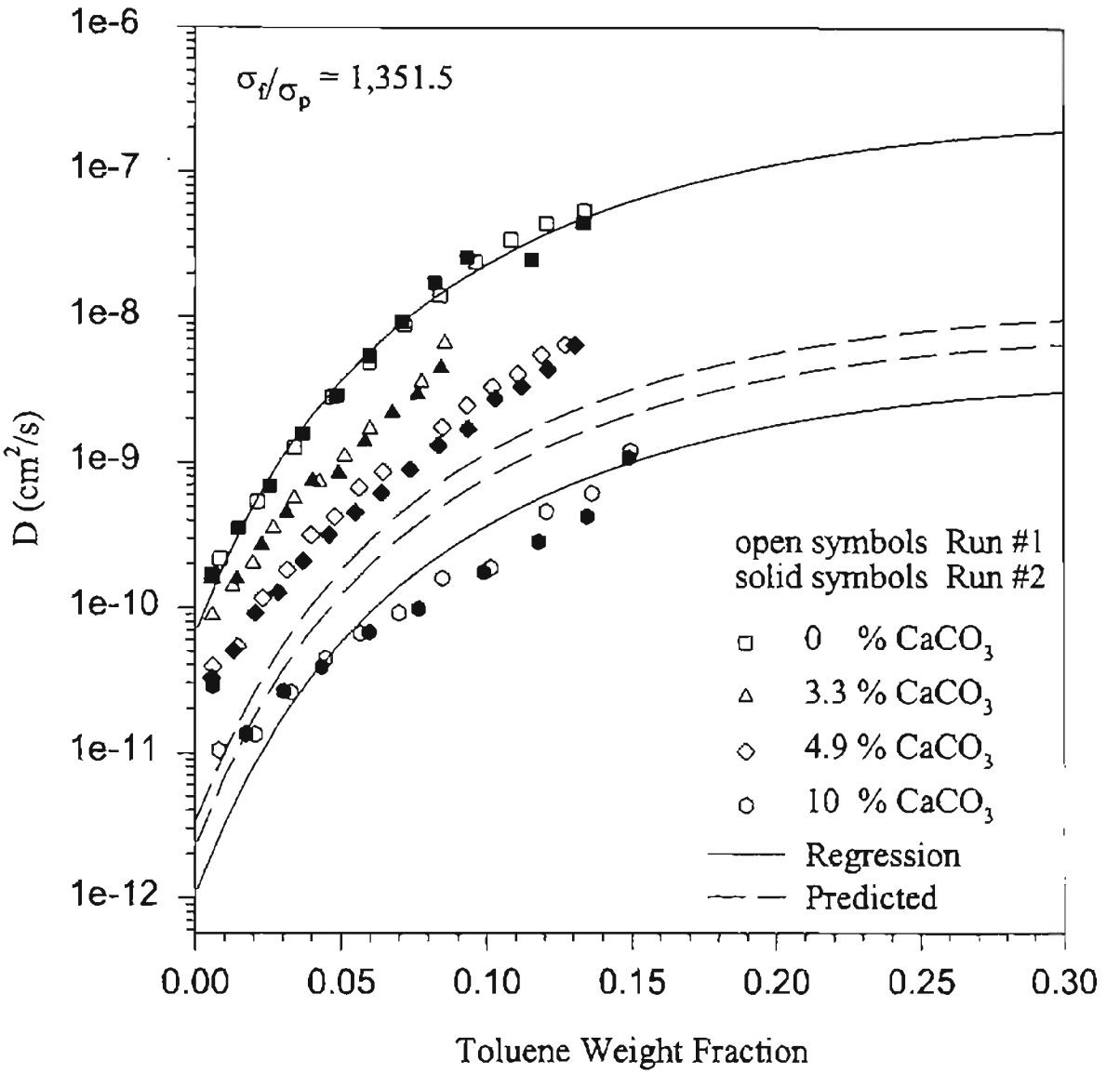

Figure 33. Comparisons of Experimental Diffusion Coefficients with Barrer and Chio's Equation for $CaCO_3$ Filled PVAC at 60°C.

equation containing a structure factor for a regular dispersion of nonconducting spheres. Sorption experiments should be performed for toluene diffusing into filled PVAC, using fillers other than $CaCO_3$. Comparing $CaCO_3$ filled PVAC-toluene data with other filled PVAC-toluene data will show, relatively, the effect of adsorption of toluene for various fillers. If the filler particles are geometrically similar and have the same adsorption effects, then reductions in diffusivity should be the same. One filler chosen should be non-adsorbing, such as glass beads, as to obtain an appropriate model for the structure factor.

Regressions Using an Equation Derived from Reaction Principles

Experimental diffusion coefficient data for toluene diffusing into $CaCO_3$ filled PVAC at 60°C was also used to test the correlative capabilities of the equations derived from treatment of adsorption as a chemical reaction. The equation, as described in Chapter II, is given as

$$D_{eff} = \frac{\kappa D_p}{R+1}, \tag{92}$$

where

$$R = \frac{C_f}{C}, \tag{93}$$

and C_f is the concentration of the penetrant which is adsorbed on the filler particles, and C is the concentration of penetrant which is free to diffuse. The free-volume equation was used for the unfilled diffusion coefficient, D_p, with parameters as given previously. The parameter R was obtained by fitting equation 92 to experimental diffusion coefficient data for $CaCO_3$ filled PVAC with a weight of 3.3%, 4.9%, and 10% $CaCO_3$. Figure 34 shows the regression of these data, as well as the previously obtained regression of neat PVAC. The diffusion coefficients obtained from the regression using equation 92 compare well with the experimental diffusion coefficients of toluene in 3.3%, 4.9%, and 10% $CaCO_3$ filled PVAC, however, each of the curves at the various filler contents were obtained by a separate non-linear regression of the experimental data. Therefore, no predictions were made using this equation. The parameter R increases with volume fraction of filler since more

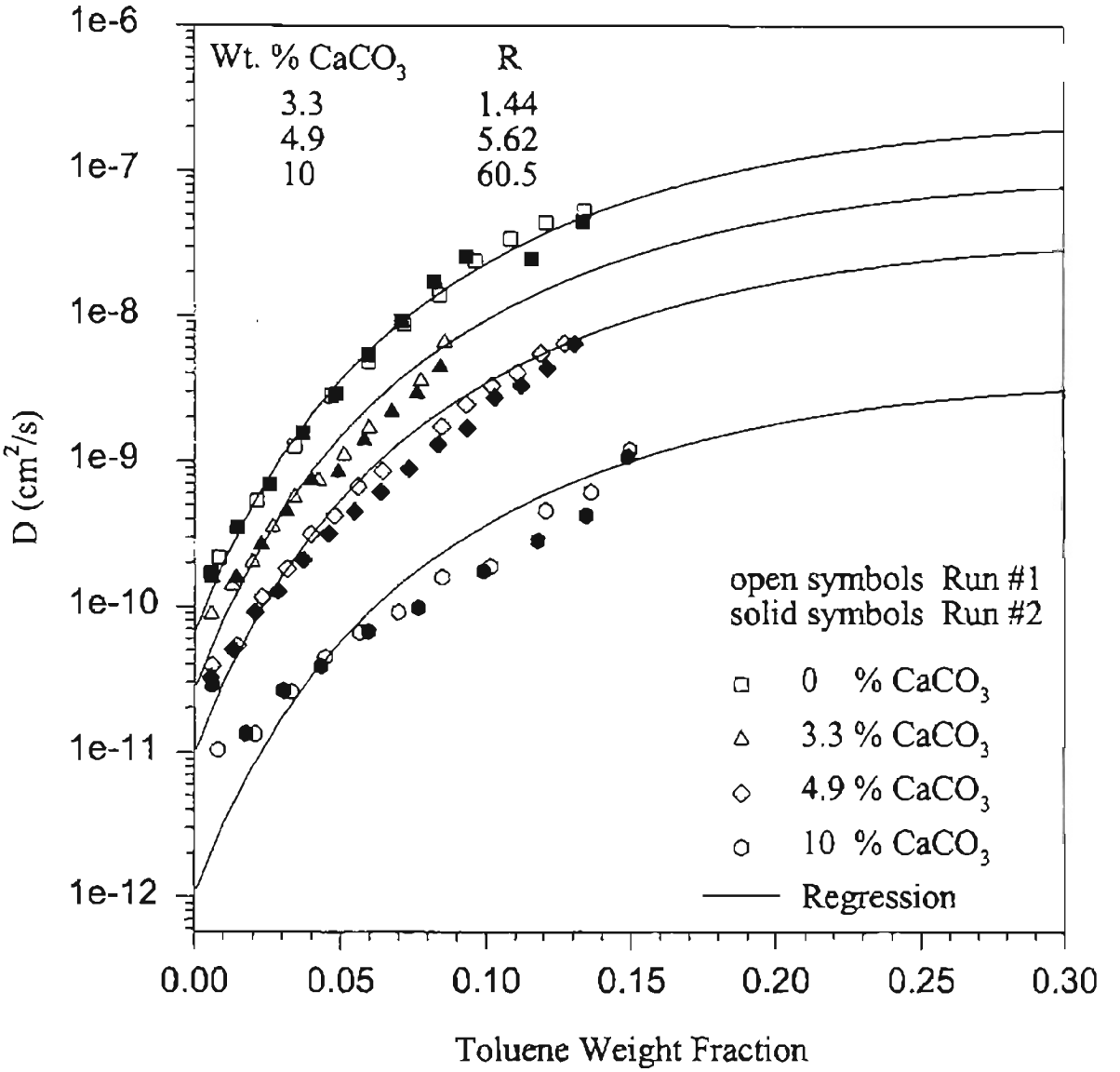

Figure 34. Comparisons of Experimental Diffusion Coefficients with an Equation Derived from Reaction Principles for $CaCO_3$ Filled PVAC at 60°C.

surface area of filler is available for adsorption of penetrant. The values of R are given in Figure 34.

Numerical Simulation and Regression of Sorption Curves

All of the methods discussed in Chapter II for obtaining the diffusion coefficient from sorption data are based on solutions of the one-dimensional diffusion equation with constant D. Therefore, to obtain diffusion coefficients over a range of penetrant concentration, a series of small step-change sorption experiments must be run. A method for obtaining the diffusion coefficient over a concentration range by analysis of only one sorption curve was studied in this work.

This method involved solving the one-dimensional diffusion equation with concentration dependent $D(C)$,

$$\frac{\partial C}{\partial t} = \frac{\partial}{\partial x}\left(D(C)\frac{\partial C}{\partial x}\right). \tag{94}$$

The initial concentration of the penetrant inside the polymer film is uniform at C_1 and at any time after $t = 0$, the surface concentration is C_0, i.e., there is a step change in surface concentration from C_1 to C_0 at $t = 0$. The boundary conditions for equation 94 are

$$C(x,0) = C_1, \tag{95}$$

$$C(0,t) = C_0, \tag{96}$$

$$\frac{\partial C}{\partial x}(L,t) = 0, \tag{97}$$

where the last boundary condition indicates that there is no loss of penetrant from the bottom of the film.

Equation 94 was solved numerically for the concentration of the penetrant in the polymer as a function of time and position in the polymer film for a given functional form of $D(C)$. The concentration profile was integrated over the whole film to obtain the mass uptake ratio as a function of time. The numerically obtained sorption curve was compared to experimental sorption data, and

the parameters of a constitutive equation for $D(C)$ were determined by non-linear regression. Once the parameters were determined, the constitutive equation for $D(C)$ was used to calculate the diffusion coefficient over a concentration range.

To simplify the numerical analysis, equation 94 was non-dimensionalized. The following is a mathematical analysis for the non-dimensionalization. The polymer film has a thickness L, and x is the distance into the film measured from the top surface. The top of the film is at $x = 0$ and the bottom of the film is at $x = L$.

A concentration dependent constitutive equation such as a free-volume equation can be used for the diffusion coefficient, $D(C)$. For illustration purposes, $D(C)$ is assumed to have the form

$$D(C) = D_0 \exp(\alpha C), \tag{98}$$

where D_0 is the diffusion coefficient at $C = 0$ and α is a constant. A non-dimensional concentration can be defined as

$$C' = \frac{C - C_1}{C_0 - C_1}. \tag{99}$$

A non-dimensional distance, X, can also be defined as

$$X = \frac{x}{L}. \tag{100}$$

Substituting equations 98, 99 and 100 into equation 94 leads to a non-dimensional time, T

$$T = \frac{t}{\tau}, \tag{101}$$

where

$$\tau = \frac{L^2}{D_0 \exp(\alpha C_1)}. \tag{102}$$

The non-dimensional diffusion equation becomes

$$\frac{\partial C'}{\partial T} = \frac{\partial}{\partial X}\left(\exp\left\{\alpha\left(C_0 - C_1\right)C'\right\}\frac{\partial C'}{\partial X}\right). \tag{103}$$

The boundary conditions for equation 103 become

$$C'(X, 0) = 0, \tag{104}$$

$$C'(0,T) = 1, \tag{105}$$

$$\frac{\partial C'}{\partial X}(1,T) = 0. \tag{106}$$

Equation 103 can be solved numerically to obtain C' as a function of X and T.

The mass of penetrant in the polymer film at any time can be given by the equation

$$M_t = \int_0^L (C - C_1) A dx, \tag{107}$$

where A is the cross-sectional area of the polymer film. At infinite time, i.e., at polymer-penetrant equilibrium, the mass of the penetrant in the polymer film is

$$M_\infty = (C_0 - C_1) AL \tag{108}$$

The fractional penetrant uptake can then be calculated by

$$\frac{M_t}{M_\infty} = \int_0^L \frac{(C - C_1)}{(C_0 - C_1)} \frac{dx}{L}. \tag{109}$$

In non-dimensional form, the fractional penetrant uptake is

$$\frac{M_T}{M_\infty} = \int_0^1 C' dX. \tag{110}$$

A sorption curve can be obtained by solving equation 110 numerically. The numerical computations were performed using FORTRAN. The programs are shown in Appendix E. Validation studies of the program are shown in Appendix D.

The free-volume equation 30 discussed in Chapter II has been used successfully to correlate diffusion coefficients in several polymer-solvent systems [Ju et al., 1981]. Therefore, this equation was chosen as the diffusion coefficient constitutive equation for equation 94. A satisfactory fit to the sorption data was not obtained, therefore predictions of the diffusion coefficient using the free-volume constitutive equation 30 were not reliable. Predictions of diffusion coefficients using this method were consistently high. More work needs to be done to determine the underlying problem of the inability to properly fit the sorption data. Results of the correlations are shown in Appendix D.

The ability to numerically obtain sorption data was also used to test the moment method of determining diffusion coefficients. The numerically obtained

sorption curve was treated as experimental data from a step-change sorption experiment and analyzed by the moment method to obtain diffusion coefficients. These results were compared to diffusion coefficients calculated by the diffusion coefficient constitutive equation used in the diffusion equation. The results compared very well and are shown in Appendix D.

CHAPTER VI

CONCLUSIONS AND RECOMMENDATIONS

This work involved the measurement of the effective diffusion coefficient for toluene diffusing into $CaCO_3$ filled PVAC films by quartz crystal microbalance sorption experiments. The experimental results from this work were compared to a free-volume theory correlation modified to account for fillers. The results were also compared to correlation equations derived by Barrer and Chio [1965], using the structure factor equations of Fricke [1931] and Runge [1925]. And, finally, results were compared to a correlation equation from Crank [1956] for simultaneous diffusion with reaction. For this work, the following conclusions and recommendations can be made.

Conclusions

1. Effective diffusion coefficients for toluene diffusing into $CaCO_3$ filled PVAC were successfully measured with a quartz crystal microbalance sorption apparatus.

2. Comparison of diffusion coefficients for toluene diffusing into PVAC with 0.0% $CaCO_3$ (neat PVAC) with diffusion coefficients from other sources validated the methods used in this work.

3. Data from the experiments show that the diffusion coefficient increases with toluene concentration, and temperature, but decreases exponentially with weight percent $CaCO_3$ filler in PVAC polymer.

4. Effective diffusion coefficient curves calculated by the modified free-volume correlation compare well with experimental data.

5. Effective diffusion coefficients calculated by equations based solely on the tortuosity of the diffusion path around filler particles show very poor comparison with experimental data.

6. Effective diffusion coefficients calculated by equations which take into account both the tortuosity of the diffusion path around filler particles and adsorption of penetrant on the surface of the filler particles do not compare well with experimental data, although they were better than curves calculated by equations based only on tortuosity.

7. Effective diffusion coefficients calculated by equations which model adsorption of penetrant on the filler particles as a reaction compare well with experimental data when fit individually to fixed filler contents. No predictive capability was found using this equation.

Recommendations

1. Methods for more uniform coating and more accurate thickness measurement of polymer films on the quartz crystal should be explored since the measurement of the thickness of the polymer film was believed to be the most significant cause of experimental error. In this work, a known weight of polymer (PVAC) was dissolved in a known volume of solvent (tetrahydrofuran). The crystals were coated from a micropipette by dropping a known volume of the polymer solution onto the crystal surface and spreading it with the tip of the micropipette. After drying, the diameter of the polymer film was measured with a ruler. The thickness of the polymer film was calculated from the diameter of the film, the volume of the solution used to coat the crystal, and the weights and densities of the polymer and solvent used to make the polymer solution. A possible error was in the measurement of the diameter of the film. The coated films were not perfectly symmetrical; therefore, several measurements of diameter were taken at different orientations and averaged to give the diameter used in the calculations. Another possible error was in the volume measurements with the micropipette. Some of the liquid could adhere to the inner surface of the micropipette tube. Since such a small volume of solution was used, significant error could result. Error also existed due to non-uniformity in the thickness of the polymer films. Visual inspection of the coated films showed that the outer edges of the films were usually thicker than the center portion.

2. Effective diffusion coefficients for toluene diffusing into filled PVAC should be determined using different fillers. Diffusion of toluene in $CaCO_3$ filled PVAC was possibly too complex to model with a diffusion equation containing a structure factor for a regular dispersion of nonconducting spheres. If sorption experiments were performed for toluene diffusing into filled PVAC using various geometrically similar fillers, these results could be compared to the results of $CaCO_3$ filled PVAC to determine the relative effect of adsorption

of toluene for various fillers. If the filler particles have the same adsorption effects, then reductions in diffusivity should be the same. One filler chosen should be non-adsorbing, such as glass beads, as to obtain an appropriate model for the structure factor.

3. A graphical instrumentation program such as LabVIEW should be set up on the data acquisition computer. This program could be used to imitate the appearance and operation of actual instruments, such as pressure and temperature monitors. All of the measured properties, pressure, temperature, and frequency, could be monitored at one location, the computer. Such a program can also produce live graphs of data during an experimental run. All calculations involved in determining the diffusion coefficient could be performed by the graphical instrumentation program.

4. The quartz crystal microbalance should be placed in an insulated oven to better control the temperature of the ambient air and the chamber.

BIBLIOGRAPHY

Atkinson, A.; "Elementary Numerical Analysis," Wiley, New York (1985).

Balik, C. M.; "On the Extraction of Diffusion Coefficients from Gravimetric Data for Sorption of Small Molecules by Polymer Thin Films," *Macromolecules* **29**, 3025-3029 (1996).

Barrer, R. M.; *in* "Diffusion in Polymers," (J. Crank and G. S. Park, eds.), 165, Academic Press, New York (1968).

Barrer, R. M., Barrie, J. A., and Raman, N. K.; "Solution and Diffusion in Silicone Rubber I-A Comparison with Natural Rubber," *Polymer* **3**, 595-603 (1962).

Barrer, R. M., Barrie, J. A., and Raman, N. K.; "Solution and Diffusion in Silicone Rubber II-Influence of Fillers," *Polymer* **3**, 605 (1962); *Rubb. Chem. Technol.* **36**, 651-659 (1963).

Barrer, R. M., Barrie, J. A., and Rogers, M. G.; "Heterogeneous Membranes: Diffusion in Filled Rubber," *J. Polym. Sci.: Part A* **1**, 2565-2586 (1963).

Barrer, R. M. and Chio, H. T.; "Solution and Diffusion of Gases and Vapors in Silicone Rubber Membranes," *J. Polym. Sci.: Part C* **10**, 111-138 (1965).

Bird, R. B., Stewart, W. E., and Lightfoot, E. N.; "Transport Phenomena," Wiley, New York (1960).

Boas, M. L.; "Mathematical Methods in the Physical Sciences," Wiley, New York (1983).

Carpenter, A. S. and Twiss, D. F.; "Measuring the Permeability of Rubber to Various Gases," *Rubb. Chem. Technol.* **13**, 326-347 (1940).

Crank, J.; "The Mathematics of Diffusion," Oxford University Press (Clarendon), London (1956).

Crank, J. and Park, G. S., eds.; "Diffusion in Polymers," Academic Press, New York (1968).

Deshpande, S.; "Development of a Piezoelectric Quartz Crystal Microbalance for the Measurment of Penetrant Sorption into Polymers," M.S. Thesis, Oklahoma State University (1993).

Duda, J. L.; *in* "Devolatilization of Polymers," (J. A. Biesenberger, ed.), 88-142, Hanser Publishers, Munich, (1983).

Duda, J. L., Ni, Y. C., and Vrentas, J. S.; "An Equation Relating Self-Diffusion and Mutual Diffusion Coefficients in Polymer-Solvent Systems," *Macromolecules* **12**, 459-462 (1979).

Duda, J. L., Vrentas, J. S., Ju, S. T., and Liu, H. T.; "Prediction of Diffusion Coefficients for Polymer-Solvent Systems," *AICHE J.* **28**, 279-285 (1982).

EerNisse, E. P.; *in* "Methods and Phenomena 7, Applications of Piezoelectric Quartz Crystal Microbalances," (C. Lu and A. W. Czanderna, eds.), 125, Elsevier, Amsterdam (1984).

Felder, R. M.; "Estimation of Gas Transport Coefficients from Differential Permeation, Integral Permeation, and Sorption Rate Data," *J. Membrane Sci.* **3**, 15-27 (1978).

Felder, R. M. and Huvard, G. S.; *in* "Methods of Experimental Physics," (R. A. Fava, ed.), **16C**, 315, Academic Press, New York (1980).

Fricke, H.; "The Electric Conductivity and Capacity of Disperse Systems," *Physics* **1**, 106-115 (1931).

Fujita, H.; *in* "Diffusion in Polymers," (J. Crank and G. S. Park, eds.), 75, Academic Press, New York (1968).

Hanspach, J. and Pinno, F.; "Concentration Dependent Diffusion of Water in Polyamide 6," *Acta. Polym.* **43**, 210-213 (1992).

Hedenqvist, M. and Gedde, U. W.; "Diffusion of Small-Molecule Penetrants in Semicrystalline Polymers," *Prog. Polym. Sci.* **21**, 299-333 (1996).

Horas, J. A. and Rizzotto, M. G.; "On the Diffusion of Gases in Partially Crystalline Polymers," *J. Polym. Sci., Polym. Phys. Ed.* **27**, 175-187 (1989).

Hou, A. C.; "Molecular Diffusion in Concentrated Polymer Solutions," Ph.D. Thesis, The Pennsylvania State University (1986).

Iijima, T. and Chung, D. J.; "Concentration Dependence of Diffusion Coefficient of P-Nitroaniline in Poly(Ethylene Terephthalate) and Polyamide," *J. Appl. Polym. Sci.* **17**, 663-665 (1973).

Ju, S. T., Liu, H. T., Duda, J. L., and Vrentas, J. S.; "Solvent Diffusion in Amorphous Polymers," *J. Appl. Polym. Sci.* **26**, 3735-3744 (1981).

Kulkarni, S. S. and Stern, S. A.; "Diffusion of CO_2, CH_4, and C_3H_8 in Polyethylene at Elevated Pressures," *J. Polym. Sci., Polym. Phys. Ed.* **21**, 441-465 (1983).

Kulkarni, S. S., Stern, S. A., and Frisch, H. L.; "Tests of a Left Double Quote Free-Volume Right Double Quote Model of Gas Permeation Through Polymer Membranes – 1. Pure CO_2, CH_4, C_2H_4, and C_3H_8 in Polyethylene," *J. Polym. Sci., Polym. Phys. Ed.* **21**, 467-481 (1983).

Lasoski, S. W. and Cobbs, W. H.; "Moisture Permeability of Polymers. I. Role of Crystallinity and Orientation," *J. Polym. Sci.* **36**, 21-33 (1959).

Maxwell, J. C.; "Electricity and Magnetism, Vol. 1," Dover, New York (1891).

Meredith, R. E. and Tobias, C. W.; "Resistance to Potential Flow Through a Cubical Array of Spheres," *J. Appl. Phys.* **31**, 1270-1273 (1960).

Michaels, A. S. and Bixler, H. J.; "Flow of Gases Through Polyethylene," *J. Polym. Sci.* **50**, 413-439 (1961).

Michaels, A. S., Bixler, H. J., and Fein, H. L.; "Gas Transport in Thermally Conditioned Linear Polyethylene," *J. Appl. Phys.* **35**, 3165-3178 (1964).

Michaels, A. S. and Parker, R. B. Jr.; "Sorption and Flow of Gases in Polyethylene," *J. Polym. Sci.* **41**, 53-71 (1959).

Mikkilineni, S. P. V. N.; "Thermophsical Properties of Penetrants in Polymers via a Piezoelectric Quartz Crystal Microbalance," M.S. Thesis, Oklahoma State University (1995).

Mikkilineni, S. P. V. N., Tree, D. A., and High, M. S.; "Thermophysical Properties of Penetrants in Polymers via a Piezoelectric Quartz Crystal Microbalance," *J. Chem. Eng. Data* **40**, 750-755 (1995).

Morris, V. N.; "Permeability of Rubber to Air," *Ind. Eng. Chem.* **23**, 837-843 (1931).

Palekar, V.; "Evaluation of Concentration Dependent Diffusion Coefficients for Sorption Experiments with Polymer-Solvent Systems," Comprehensive Exam, Penn State University (1995).

Park, G. S.; *in* "Diffusion in Polymers," (J. Crank and G. S. Park, eds.), 141, Academic Press, New York (1968).

Peterlin, A.; "Dependence of Diffusive Transport on Morphology of Crystalline Polymers," *J. Macromol. Sci. Phys.* **B28**, 57-87 (1975).

Peterlin, A.; "Transport Properties as an Extremely Sensitive Indicator of the Status of the Amorphous Component in the Elastically and Plastically Deformed Semicrystalline Polymer," *Mater. Sci. Monogr.* **21**, 585-604 (1984).

Rayleigh, Lord; *Phil. Mag.* **34**, 481 (1892).

Runge, I.; *Z. tech. Physik.* **6**, 61 (1925).

Smith, W. C.; "Compounding Butyl Rubber for Mineral-Filled Stocks," *India Rubber World* **129**, 55-60 (1953).

Stern, S. A., Fang, S. M., and Frisch, H. L.; "Effect of Pressure on Gas Permeability Coefficients. A New Application of "Free Volume" Theory," *J. Polym. Sci., Polym. Phys. Ed.* **10**, 201-219 (1972).

Stern, S. A., Mauze, G. R., and Frisch, H. L.; "Tests of a Free-Volume Model for the Permeation of Gas Mixtures Through Polymer Membranes. CO_2-C_2H_4, CO_2-C_3H_8, and C_2H_4-C_3H_8 Mixtures in Polyethylene," *J. Polym. Sci., Polym. Phys. Ed.* **21**, 1275-1298 (1983).

Stern, S. A., Sampat, S. R., and Kulkarni, S. S.; "Tests of a "Free Volume" Model of Gas Permeation Through Polymer Membranes. II. Pure Ar, SF_6, CF_4, and $C_2H_2F_2$ in Polyethylene," *J. Polym. Sci., Polym. Phys. Ed.* **24**, 2149-2166 (1986).

van Amerongen, G. J.; "The Permeability of Rubberlike Substances to Gases," *Rubb. Chem. Technol.* **20**, 479-493 (1947).

van Amerongen, G. J.; "The Effect of Fillers on the Permeability of Rubber to Gases," *Rubb. Chem. Technol.* **28**, 821-832 (1955).

van Amerongen, G. J.; "Diffusion in Elastomers," *Rubb. Chem. Technol.* **37**, 1065-1148 (1964).

Vrentas, J. S. and Duda, J. L.; "Diffusion of Small Molecules in Amorphous Polymers," *Macromolecules* **9**, 785-790 (1976).

Vrentas, J. S. and Duda, J. L.; "Molecular Diffusion in Polymer Solutions," *AICHE J.* **25**, 1-24 (1979).

Vrentas, J. S., Duda, J. L., and Huang, W. J.; "Regions of Fickian Diffusion in Polymer-Solvent Systems," *Macromolecules* **19**, 1718-1724 (1986).

Vrentas, J. S., Duda, J. L., and Ling, H. C.; "Free-Volume Theories for Self-Diffusion in Polymer-Solvent Systems. I. Conceptual Differences in Theories," *J. Polym. Sci., Polym. Phys. Ed.* **23**, 275-288 (1985).

Vrentas, J. S., Duda, J. L., and Ni, Y. C.; "Analysis of Step-Change Sorption Experiments," *J. Polym. Sci., Polym. Phys. Ed.* **15**, 2039-2045 (1977).

Vrentas, J. S. and Vrentas, C. M.; "Drying of Solvent-Coated Polymer Films," *J. Polym. Sci., Polym. Phys. Ed.* **32**, 187-194 (1994).

APPENDICES

APPENDIX A

Experimental Procedures

The contents of this appendix give detailed procedures for initial preparation and operation of the quartz crystal microbalance in order to obtain diffusion coefficients of penetrants diffusing into filled polymers.

Preparing a Polymer Solution

1. Measure and record the weight of a sample vial. In this work, a 20 ml sample vial was used.

2. Place a sample of polymer into the vial. Measure and record the weight of the vial again. The polymer used in this work was PVAC. Typically, 0.6 grams (or 9 balls of the PVAC available in the laboratory) was used.

3. Place a sample of filler into the vial. Measure and record the weight of the vial again. The filler used in this work was $CaCO_3$. The weights of filler used in this work range from 0 to 0.06 grams.

4. Fill the vial containing the polymer and filler with Tetrahydrofuran (THF). Other solvents can be used, but THF seems to work best for dissolving PVAC.

5. After the polymer dissolves, measure and record the weight of the vial once more.

These weights were used for determining the thickness of the polymer film which was coated on the quartz crystal, which will be described later.

Coating a Quartz Crystal with a Polymer Film

1. Remove a quartz crystal from its storage box and place on a flat surface. Be careful not to touch the crystal with bare fingers.

2. Mix the polymer solution contained in the sample vial by gently shaking or rotating the vial. Severe agitation of the mixture will cause excessive formation of bubbles in the solution.

3. Remove a known volume of polymer solution from the sample vial with a micropipette. In this work, 7 μl is usually withdrawn from the sample vial.

4. Immediately coat the quartz crystal with the solution in the micropipette by dropping the solution onto the crystal surface and spreading uniformly with the tip of the micropipette. Filler particles tend to flow to the outer edge of the coating if the solution is not spread onto the crystal in this manner.

5. Allow the polymer coating to dry thoroughly. Usually one day is sufficient.

Coating a polymer solution onto a quartz crystal is an art which takes much practice. A coating with uniform thickness is desired. Thickness uncertainties are one of the major sources of errors in experimentally measuring the diffusion coefficient of penetrants diffusing into polymers.

Evacuating the Quartz Crystal Microbalance

Evacuation of the quartz crystal microbalance is achieved by the use of two vacuum pumps. A rotary vane pump is used to obtain pressures of approximately 10^{-1} torr and a turbomolecular pump is then used to obtain pressures of approximately 10^{-7} torr. The level and condition of the oil in the rotary vane pump must be checked routinely. The oil should be changed every month. If the pump is operated with dirty oil, the required vacuum will not be created and the life of the pump will be reduced. Care should be taken not to contaminate the pump oil with solvent from the chamber, as this will prematurely break down the

oil as well as destroy the internal gaskets of the pump. Also, care should be taken not to contaminate the chamber with pump oil. A liquid nitrogen trap is in line between the rotary vane pump and the chamber to prevent these occurrences. The following steps should be followed whenever the chamber is to be evacuated. The right angle valve, gate valve, and solvent flask valves are assumed to be initially closed.

1. If the quartz crystal microbalance chamber contains penetrant, fill the liquid nitrogen trap with liquid nitrogen and proceed with the following steps, else go to step 2. The liquid nitrogen will boil rapidly and splatter, so gloves and safety glasses should be worn.

    - Turn on the rotary vane pump.
    - Open the right angle valve which connects the rotary vane pump to the chamber.
    - When the pressure decreases below 10^{-1} torr, close the right angle valve.
    - Turn off the rotary vane pump.
    - Remove the liquid nitrogen trap, recycle the liquid nitrogen, and place the liquid nitrogen trap in the vent hood until it thaws.
    - Clean and replace the liquid nitrogen trap.

2. Turn on the rotary vane pump.

3. Open the right angle valve which connects the rotary vane pump to the chamber.

4. When the pressure decreases below 10^{-1} torr, close the right angle valve.

5. Open the gate valve which connects the turbomolecular pump to the chamber.

6. Turn on the turbomolecular pump. The turbotronic display will show that the pump is in acceleration mode. After approximately 5 minutes, when the

turbomolecular pump has accelerated to its maximum speed it will switch to 'normal' mode of operation.

7. Once the turbomolecular pump has been turned on, the vacuum will be reduced to below 10^{-3} torr which is the minimum that the Pirani gauge can read and hence it will display 'OFF'.

8. Turn on the hot ionization pressure gauge, IG3, and press the 'DEGAS' switch.

9. Allow the chamber to evacuate for approximately 3-4 hours.

10. Close the gate valve.

11. Turn off the turbomolecular pump.

12. Turn off the rotary vane pump.

Operating the Quartz Crystal Microbalance Sorption Apparatus

Three steps are involved in obtaining the diffusion coefficient using the quartz crystal microbalance.

- Measurement of the frequency of the bare crystal.
- Measurement of the frequency of the solvent-free polymer coated crystal.
- Measurement of the frequency change during the experiment as the solvent is sorbed.

The following steps are an overall procedure for measuring diffusion coefficients of penetrants diffusing into polymers with the quartz crystal microbalance. It is assumed initially that the chamber is solvent free.

1. Place a bare crystal in the crystal holder and mount the holder in the chamber.

2. Set the thermal box temperature controller to the desired temperature.

3. Turn on the heated air circulating fan and the heating element with the two toggle switches which are mounted above the pressure and temperature gauges. The temperature should be allowed to stabilize for 12 hours or more.

4. Evacuate the chamber as described in the subsection Procedure for Evacuating the Quartz Crystal Microbalance.

5. Record the frequency of the bare crystal with the data acquisition computer until it reaches a steady value.

6. Prepare a polymer solution as described in the subsection Preparing a Polymer Solution.

7. Remove the crystal from the chamber.

8. Coat the crystal with the polymer solution as described in the subsection Procedure for Coating a Quartz Crystal with a Polymer Film.

9. Obtain an average diameter of the coated film with a ruler. This will allow for later calculations of film thickness.

10. Place the crystal into the holder and the holder into the chamber again.

11. Evacuate the chamber as described in the subsection Procedure for Evacuating the Quartz Crystal Microbalance.

12. Record the frequency of the coated crystal once it reaches a steady value. To check if the frequency has reached a steady value, record the frequency for about 15 minutes. The frequencies are recorded in a file by running a program 'XTC7.BAS' on the computer that is connected to the deposition monitor. On running the program the computer asks for a file name to record the data. The computer then asks for the command corresponding to the type of the data required. Enter the command for obtaining the crystal frequency as the output, 'S13'. The computer records the data as a function of time.

13. Close the right angle valve and the gate valve if not already.

14. Be sure the vacuum pumps and hot ionization gauge are off. If penetrant enters the hot cathode gauge, a malfunction will result.

15. Activate the deposition monitor by pressing the 'START' button.

16. Run the computer program 'XTC7.BAS' and enter the file name as required.

17. Type the command 'S13', do not press enter yet.

18. Fill the sample cylinder with penetrant from the solvent flask by opening the valve between the sample cylinder and solvent flask. This process will decrease the temperature of the solvent. The temperature of the solvent should be monitored, and the valve closed only when this temperature reaches the original temperature which was desired. The next two steps have to be carried out as quickly as possible.

19. Press the enter key on the computer keyboard to send the command 'S13'.

20. Vent the solvent vapors from the sample cylinder into the chamber by opening the valve between the sample cylinder and the chamber. This yields a step change in pressure (typically 0.1 to 0.2 psi). The computer records the frequency of the quartz crystal as a function of time as the penetrant is diffusing into the polymer.

21. Allow the experiment to run until the mass of the penetrant sorbed reaches a value that remains constant for about 30 minutes. Press Ctrl/Break on the computer keyboard to cease data recording.

22. Repeat steps 16-21 until the chamber pressure is close to the vapor pressure of the solvent at the chamber temperature (typically 2 psia reached in approximately 14 to 16 steps is sufficient).

23. When the experiments are finished, evacuate the chamber as described in the subsection Procedure for Evacuating the Quartz Crystal Microbalance.

Film Thickness Calculations

For calculation of the thickness of a polymer film which does not contain filler, the following weights are needed.

- Weight of Bottle = x grams
- Weight of Bottle + Polymer = y grams
- Weight of Bottle + Polymer + Solvent = z grams

Given these weights, the diameter of the film, and assuming uniform thickness and no volume changes on mixing, it can be shown that the thickness of the film, L, is

$$L = \left(\frac{1}{10}\right)\left(\frac{4V_m}{\pi d^2 \rho_p}\right)\left(\frac{y-x}{\left(\frac{y-x}{\rho_p}+\frac{z-y}{\rho_s}\right)}\right), \tag{111}$$

- L = thickness of coated polymer (cm)
- V_m = volume of coated solution (micropipette volume) (μl)
- ρ_p = density of polymer (g/cm^3)
- ρ_s = density of solvent (g/cm^3)
- d = diameter of coated polymer (mm)

For calculation of the thickness of a film which contains polymer and filler, the following weights are needed.

- Weight of Bottle = x grams
- Weight of Bottle + Polymer = y grams
- Weight of Bottle + Polymer + Filler = z grams
- Weight of Bottle + Polymer + Filler + Solvent = w grams

Given these weights, the diameter of the film, and assuming uniform thickness, it can be shown that the thickness of the film, L, is

$$L = \left(\frac{1}{10}\right)\left(\frac{4V_m}{\pi d^2}\right)\left(\frac{\left(\frac{y-x}{\rho_p} + \frac{z-y}{\rho_f}\right)}{\left(\frac{y-x}{\rho_p} + \frac{w-z}{\rho_s} + \frac{z-y}{\rho_f}\right)}\right), \tag{112}$$

where

- L = thickness of coated film (cm)
- V_m = volume of coated solution (micropipette volume) (μl)
- ρ_p = density of polymer (g/cm^3)
- ρ_f = density of filler (g/cm^3)
- ρ_s = density of solvent (g/cm^3)
- d = diameter of coated polymer (mm)

Typical densities used in this work are:

- Polymer, $\rho_{PVAC} = 1.18$ g/cm^3
- Filler, $\rho_{CaCO_3} = 2.93$ g/cm^3
- Solvent, $\rho_{THF} = 0.885$ g/cm^3

APPENDIX B

Derivation of the Moment Method Formula for Evaluating Diffusion Coefficients

The derivation of the moment method diffusivity equation [Felder, 1978; Palekar, 1995] begins with Fick's second law, just as for the derivation for the initial slope method diffusivity equation. As before, for one dimensional diffusion of penetrant in a plane polymer sheet, this equation is

$$\frac{\partial C}{\partial t} = D\frac{\partial^2 C}{\partial x^2}. \tag{113}$$

The boundary conditions are

$$C(x,0) = 0, \tag{114}$$

$$C(L,t) = C_0, \tag{115}$$

$$\frac{\partial C}{\partial x}(0,t) = 0. \tag{116}$$

Taking the Laplace transform of equations 113 through 116 and combining give the three equations,

$$\frac{d^2\bar{C}(x,s)}{dx^2} = \frac{s}{D}\bar{C}(x,s), \tag{117}$$

$$\bar{C}(L,s) = \frac{C_0}{s}, \tag{118}$$

$$\frac{\partial \bar{C}(0,s)}{\partial x} = 0. \tag{119}$$

The general solution to equation 117 is

$$\bar{C}(x,s) = c_1 \exp(qx) + c_2 \exp(-qx), \tag{120}$$

where

$$q = \left(\frac{s}{D}\right)^{1/2}. \tag{121}$$

Applying the boundary condition equations 118 and 119 to equation 120 gives

$$c_1 = c_2 = \frac{C_0}{s\{\exp(qL) + \exp(-qL)\}}. \tag{122}$$

Substituting equation 122 into equation 120 and rearranging gives the final result

$$\bar{C}(x,s) = \frac{C_0}{s}\left\{\frac{cosh(qx)}{cosh(qL)}\right\}. \tag{123}$$

The rate at which penetrant is absorbed into the polymer film, R, at the surface is

$$R = AD\left(\frac{dC}{dx}\right)_L, \tag{124}$$

where A is the surface area of the film. Taking the Laplace transform of equation 124 gives

$$\bar{R}(s) = AD\left(\frac{d\bar{C}}{dx}\right)_L. \tag{125}$$

The cumulative penetrant uptake by the polymer film is

$$M_t = \int_0^t R(t)dt. \tag{126}$$

The equilibrium uptake of penetrant by the polymer film is

$$M_\infty = ALC_0. \tag{127}$$

Combining equations 126 and 127 give the fractional solvent uptake by the polymer film

$$M_t = \frac{1}{ALC_0}\int_0^t R(t)dt. \tag{128}$$

Taking the Laplace transform of equation 128 and substituting for $\bar{R}(s)$ from equation 125 gives the fractional solvent uptake by the polymer film in the Laplace domain

$$\frac{\bar{M}_t}{M_\infty} = \frac{\bar{R}(s)}{sALC_0} = \frac{D}{LsC_0}\left(\frac{d\bar{C}}{dx}\right)_L. \tag{129}$$

The moment of the sorption curve is

$$\tau_s = \int_0^\infty \left[1 - \frac{M_t}{M_\infty}\right] dt. \tag{130}$$

From the moment generating property of the Laplace transform,

$$\tau_s = \lim_{s\to 0}\left\{\mathcal{L}\left[1 - \frac{M_t}{M_\infty}\right]\right\} = \lim_{s\to 0}\left\{\frac{1}{s} - \frac{\bar{M}_t}{M_\infty}\right\}. \tag{131}$$

Substituting equation 129 into equation 131 gives

$$\tau_s = \lim_{s\to 0}\left\{\frac{1}{s} - \frac{D}{LsC_0}\left(\frac{d\bar{C}}{dx}\right)_L\right\}. \tag{132}$$

Substituting for $\bar{C}$ from equation 123 into equation 132 and rearranging gives

$$\tau_s = \lim_{s\to 0}\left\{\frac{1}{s} - \frac{\tanh(qL)}{Lsq}\right\}. \tag{133}$$

The function $\tanh(qL)$ is expanded in Taylor series about $qR = 0$

$$\tanh(qL) = qL - \frac{(qL)^3}{3} + \ldots, \tag{134}$$

and using the first two terms of the expansion, equation 134 is substituted into equation 133 to give after simplification

$$\tau_s = \lim_{s\to 0}\left\{\frac{(qL)^2}{3s}\right\}. \tag{135}$$

Substituting for q from equation 121 into equation 135 gives

$$\tau_s = \lim_{s\to 0}\left(\frac{L^2}{3D}\right) = \frac{L^2}{3D}. \tag{136}$$

Thus, for this method, the diffusion coefficient can be calculated by

$$D = \frac{L^2}{3\tau_s}, \tag{137}$$

$$\tau_s = \int_0^\infty \left[1 - \frac{M_t}{M_\infty}\right] dt, \tag{138}$$

where τ_s is the first moment of the M_t/M_∞ versus time curve.

APPENDIX C

Error Analysis

Diffusion Coefficient

To estimate the uncertainty in the calculated diffusion coefficient, D, an equation must be derived for the relative error in the diffusion coefficient in terms of the experimental quantities used to calculate D and the uncertainty in the experimental quantities must be estimated. The relative error in D means the actual error in calculating D divided by the calculated diffusion coefficient.

The experimental quantities used to calculate D were the thickness of the polymer film and the measured frequencies of the quartz crystal. Time was measured with a computer clock, so the uncertainty in time is assumed to be zero. The estimated uncertainties of these quantities are as follows,

$L = \pm 5\%$

$f_1 = \pm 10$ Hz

$f_t = \pm 0.05$ Hz

$f_\infty = \pm 10$ Hz

where L is the thickness of the polymer film, f_1 is the frequency of the polymer coated crystal before the step change in pressure, f_t is the frequency of the crystal at time t while penetrant is diffusing into the polymer, and f_∞ is the frequency of the crystal when penetrant has come into equilibrium with the polymer. The uncertainty in f_t has been given by the manufacturer. The uncertainty in f_1 and f_∞ are based on experimental runs.

The equation used to calculate D was

$$D = \frac{L^2}{3\tau_s}, \tag{139}$$

where τ_s is the first moment of the mass uptake ratio, M_t/M_∞, vs. time curve,

$$\tau_s = \int_0^\infty \left(1 - \frac{M_t}{M_\infty}\right) dt. \tag{140}$$

The relative error in D, $\Delta D/D$ is approximated by using differentials and can be found by differentiating $\ln D$. From $D = L^2/3\tau_s$

$$\ln D = 2\ln L - \ln 3 - \ln \tau_s. \tag{141}$$

Then

$$\frac{dD}{D} = 2\frac{dL}{L} - \frac{d\tau_s}{\tau_s}. \tag{142}$$

The quantity τ_s is the area under the $1 - M_t/M_\infty$ vs. time curve and was calculated with the trapezoidal numerical integration rule. For simplification let

$$\tilde{M} = 1 - \frac{M_t}{M_\infty}. \tag{143}$$

The formula used to calculate τ_s was

$$\tau_s = \sum_{n=1}^{N} \left\{ (t_n - t_{n-1}) \left(\frac{\tilde{M}(t_{n-1}) + \tilde{M}(t_n)}{2} \right) \right\}, \tag{144}$$

where N is the number of subintervals used in the numerical integration and the times $t_0, t_1 \ldots, t_N$ are the numerical integration node points. The relative error in τ_s is then

$$\frac{d\tau_s}{\tau_s} = \frac{\sum_{n=1}^{N} \left\{ \frac{(t_n - t_{n-1})}{2} \left(d\tilde{M}(t_{n-1}) + d\tilde{M}(t_n) \right) \right\}}{\tau_s}. \tag{145}$$

The mass uptake ratio it calculated from

$$\frac{M_t}{M_\infty} = \frac{f_t - f_1}{f_\infty - f_1}. \tag{146}$$

Combining this equation with equation 143 gives

$$\tilde{M} = \frac{f_\infty - f_t}{f_\infty - f_1}. \tag{147}$$

The differential $d\tilde{M}$ is

$$d\tilde{M} = \frac{\partial \tilde{M}}{\partial f_\infty} df_\infty + \frac{\partial \tilde{M}}{\partial f_1} df_1 + \frac{\partial \tilde{M}}{\partial f_t} df_t. \tag{148}$$

Performing the differentiation gives

$$d\tilde{M} = \frac{f_t - f_1}{(f_\infty - f_1)^2} df_\infty + \frac{f_\infty - f_t}{(f_\infty - f_1)^2} df_1 - \frac{1}{f_\infty - f_1} df_t. \tag{149}$$

In the worst case, the signs of the errors in the experimental quantities above would be as such that all the terms in the preceding equations add. The largest value of $|dD/D|$ can be calculated with the following equations,

$$\text{Largest} \left| d\tilde{M} \right| = \left| \frac{f_t - f_1}{(f_\infty - f_1)^2} df_\infty \right| + \left| \frac{f_\infty - f_t}{(f_\infty - f_1)^2} df_1 \right| + \left| \frac{1}{f_\infty - f_1} df_t \right|, \tag{150}$$

$$\text{Largest} \left| \frac{d\tau_s}{\tau_s} \right| = \frac{\sum_{n=1}^{N} \left\{ \frac{(t_n - t_{n-1})}{2} \left(\left| d\tilde{M}(t_{n-1}) \right| + \left| d\tilde{M}(t_n) \right| \right) \right\}}{\tau_s}, \tag{151}$$

and

$$\text{Largest} \left| \frac{dD}{D} \right| = 2 \left| \frac{dL}{L} \right| + \left| \frac{d\tau_s}{\tau_s} \right|. \tag{152}$$

Penetrant Weight Fraction

The uncertainty in the calculated penetrant weight fraction, w_1, is determined by performing a similar derivation for the relative error in the penetrant weight fraction. The experimental quantities used to calculate w_1 were the frequencies of the quartz crystal as shown below with estimated errors.

$f_0 = \pm 5$ Hz

$f_1 = \pm 10$ Hz

$f_t = \pm 0.05$ Hz

$f_\infty = \pm 10$ Hz

where f_0 is the frequency of the bare crystal before coating, f_1 is the frequency of the solvent-free polymer coated crystal, f_t is the frequency of the crystal at time

t while penetrant is diffusing into the polymer, and f_∞ is the frequency of the crystal when penetrant has come into equilibrium with the polymer.

The equation used to calculate the penetrant weight fraction was

$$w_1 = \frac{f_\infty - f_1}{f_\infty - f_0}. \tag{153}$$

The differential dw_1 is

$$dw_1 = \frac{\partial w_1}{\partial f_\infty} df_\infty + \frac{\partial w_1}{\partial f_1} df_1 + \frac{\partial w_1}{\partial f_0} df_0. \tag{154}$$

Performing the differentiation and dividing by w_1 gives the relative error in w_1,

$$\frac{dw_1}{w_1} = \frac{f_1 - f_0}{(f_\infty - f_0)(f_\infty - f_1)} df_\infty - \frac{1}{f_\infty - f_1} df_1 + \frac{1}{f_\infty - f_0} df_0. \tag{155}$$

The largest value possible of $|dw_1/w_1|$ is

$$\text{Largest} \left| \frac{dw_1}{w_1} \right| = \left| \frac{f_1 - f_0}{(f_\infty - f_0)(f_\infty - f_1)} df_\infty \right| + \left| \frac{1}{f_\infty - f_1} df_1 \right| + \left| \frac{1}{f_\infty - f_0} df_0 \right|. \tag{156}$$

Sample Calculation

With the errors in polymer film thickness and crystal frequencies as given above, the relative error in D and w_1 was calculated for the unfilled PVAC-toluene system at 60 °C, given the following data.

$D = 2.18 \times 10^{-10}$ cm^2/s

$w_1 = 0.008459$

$f_0 = 5978029.3$ Hz

$f_1 = 5967230.3$ Hz

$f_\infty = 5967098.2$ Hz

$\tau_s = 114.34$ s

The error due to experimental uncertainty was calculated to be 65% for D and 15% for w_1.

APPENDIX D

Results of Numerical Simulations and Correlations

The numerical computations of the procedures described in Chapter V were performed using the FORTRAN programming language with the software Microsoft Fortran PowerStation. The program examples in the software library were modified for the specific problems. The MOLCH program was used to solve a non-dimensional diffusion equation. The QDAG program was used to perform the integration. The RNLIN program was used to perform the regression. These three programs were modified and combined to perform the steps required. The programs are shown in Appendix E.

The MOLCH program was modified to solve a differential diffusion equation such as equation 103 for a penetrant diffusing into a polymer film. This program is shown in Appendix E as Progam 3. The program was validated by using a constant diffusion coefficient to confirm that the program was working properly. The differential diffusion equation becomes

$$\frac{\partial C}{\partial t} = D\frac{\partial^2 C}{\partial x^2}, \tag{157}$$

for constant D. In non-dimensional form, equation 157 is

$$\frac{\partial C'}{\partial T} = \frac{\partial^2 C'}{\partial X^2}, \tag{158}$$

$$C' = \frac{C - C_1}{C_0 - C_1}; \quad X = \frac{x}{L}; \quad T = \frac{Dt}{L^2}. \tag{159}$$

Equation 157 was solved by Crank [1956], and the solution in non-dimensional form is

$$C' = 1 - \frac{4}{\pi}\sum_{n=0}^{\infty}\frac{(-1)^n}{2n+1}e^{-(2n+1)^2\pi^2 T/4}\cos\frac{(2n+1)\pi X}{2}. \tag{160}$$

The numerical solution of equation 158 was compared to the analytical solution by using equation 160. A program, Program 1 in Appendix E, was written to perform the calculation of equation 160. Equation 160 converges quickly. The summation was carried to $n = 100$, which was more than sufficient. Table XIII shows the analytical solution and Table XIV shows the numerical solution of equation 158. Figure 35 is a plot of these solutions. The numerical solution is essentially identical to the analytical solution, confirming the accuracy of the diffusion equation program.

The MOLCH program was combined with the QDAG program and modified to give Program 4 in Appendix E. This program performed a simultaneous solution of equations such as equation 103 and 110. This program allowed for a numerical simulation of the sorption curves. A validation of Program 4 was made using a constant diffusion coefficient. A mesh size that includes 100 values of X was found to be sufficient. With fewer values, the error in the fractional mass uptake was greater, but more values led to longer program run times without much decrease in error. In order to obtain a continuous sorption curve, 100 values of T were used. Crank [1956] gives the following solution for the fractional mass uptake with constant D,

$$\frac{M_t}{M_\infty} = 1 - \sum_{n=0}^{\infty} \frac{8}{(2n+1)^2\pi^2} e^{-D(2n+1)^2\pi^2 t/4L^2}. \tag{161}$$

The numerical solution for M_t/M_∞ was compared to the analytical solution of equation 161. Program 2 in Appendix E performed the calculation of equation 161. Equation 161 also converges quickly. The summation was carried to $n = 100$, which was more than sufficient. Figure 36 shows a plot of the the numerical solution as compared to the analytical solution. As with the concentration validation, the numerical solution is almost identical to the analytical solution, confirming the accuracy of the fractional mass uptake program.

Program 4 was used to test the accuracy of the moment method. The program gave values of M_t/M_∞ vs. t. A concentration dependent constitutive equation was used in the program to obtain a sorption curve, then from the sorption

TABLE XIII

ANALYTICAL SOLUTION OF DIFFUSION EQUATION WITH CONSTANT D

$X = 0$	$X = .14$	$X = .29$	$X = .43$	$X = .57$	$X = .71$	$X = .86$	$X = 1$
			Solution at T=0.01				
1.0000	.3124	.0434	.0024	.0001	.0000	.0000	.0000
			Solution at T=0.04				
1.0000	.6135	.3124	.1297	.0434	.0116	.0025	.0008
			Solution at T=0.09				
1.0000	.7363	.5007	.3126	.1788	.0947	.0504	.0368
			Solution at T=0.16				
1.0000	.8015	.6159	.4541	.3240	.2297	.1731	.1542
			Solution at T=0.25				
1.0000	.8461	.7003	.5701	.4621	.3813	.3314	.3146
			Solution at T=0.36				
1.0000	.8834	.7726	.6733	.5904	.5281	.4895	.4764
			Solution at T=0.49				
1.0000	.9154	.8351	.7630	.7029	.6576	.6295	.6200
			Solution at T=0.64				
1.0000	.9416	.8861	.8363	.7948	.7635	.7441	.7375
			Solution at T=0.81				
1.0000	.9616	.9251	.8924	.8651	.8445	.8318	.8274
			Solution at T=1.00				
1.0000	.9760	.9532	.9327	.9156	.9027	.8947	.8920

TABLE XIV

NUMERICAL SOLUTION OF DIFFUSION EQUATION WITH CONSTANT D

$X = 0$	$X = .14$	$X = .29$	$X = .43$	$X = .57$	$X = .71$	$X = .86$	$X = 1$
			Solution at T=0.01				
1.0006	.3124	.0430	.0026	.0001	.0000	.0000	.0000
			Solution at T=0.04				
1.0006	.6139	.3126	.1297	.0434	.0116	.0025	.0008
			Solution at T=0.09				
1.0006	.7368	.5010	.3128	.1788	.0947	.0504	.0369
			Solution at T=0.16				
1.0006	.8020	.6163	.4544	.3242	.2298	.1731	.1543
			Solution at T=0.25				
1.0006	.8466	.7007	.5705	.4624	.3815	.3316	.3147
			Solution at T=0.36				
1.0006	.8839	.7731	.6737	.5908	.5284	.4897	.4766
			Solution at T=0.49				
1.0006	.9160	.8356	.7635	.7033	.6580	.6298	.6203
			Solution at T=0.64				
1.0006	.9422	.8866	.8368	.7953	.7640	.7445	.7380
			Solution at T=0.81				
1.0006	.9622	.9257	.8930	.8656	.8451	.8323	.8280
			Solution at T=1.00				
1.0006	.9766	.9537	.9333	.9162	.9033	.8953	.8926

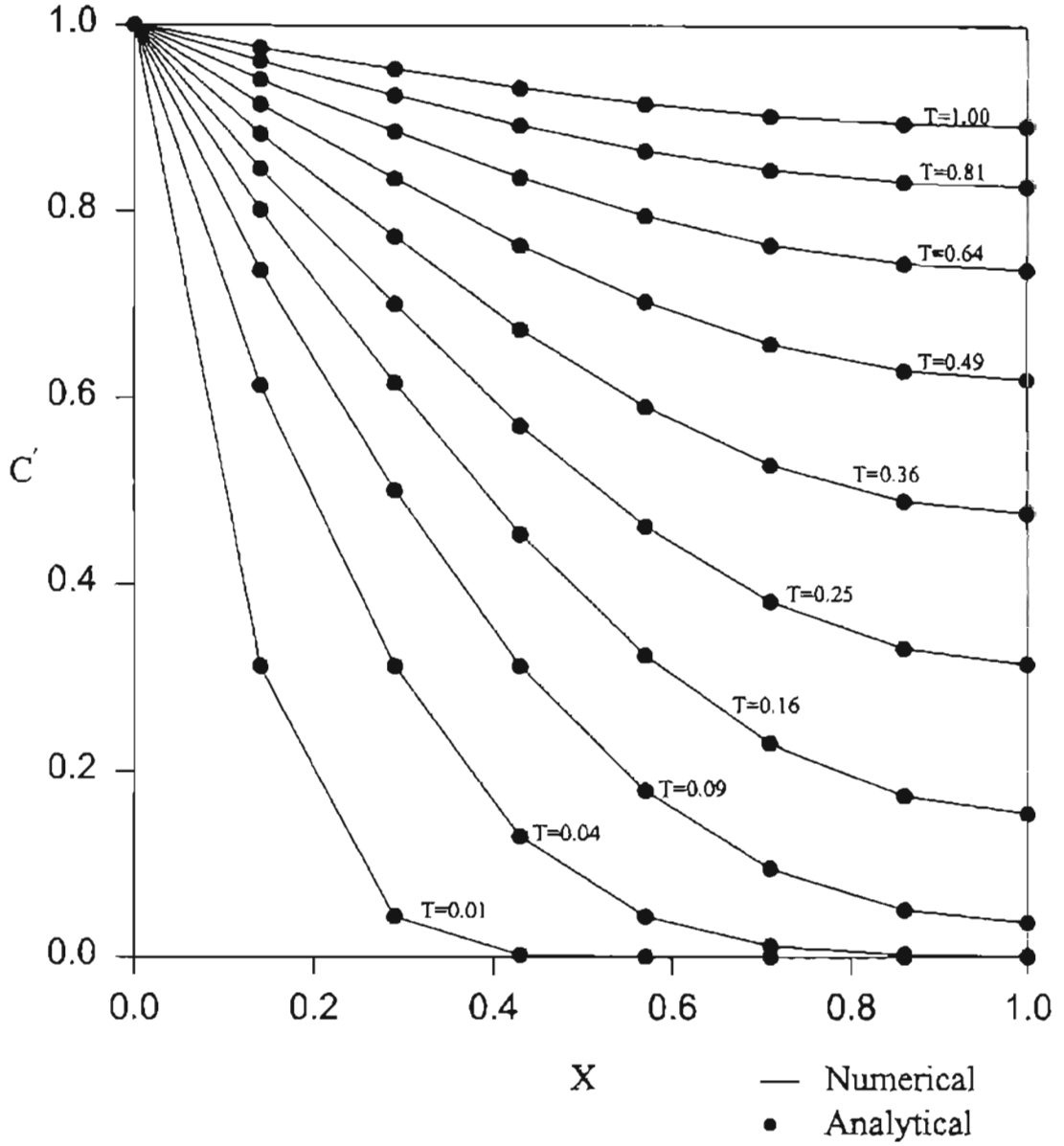

Figure 35. Comparison of Numerical and Analytical Solutions of a Diffusion Equation with Constant Diffusion Coefficient.

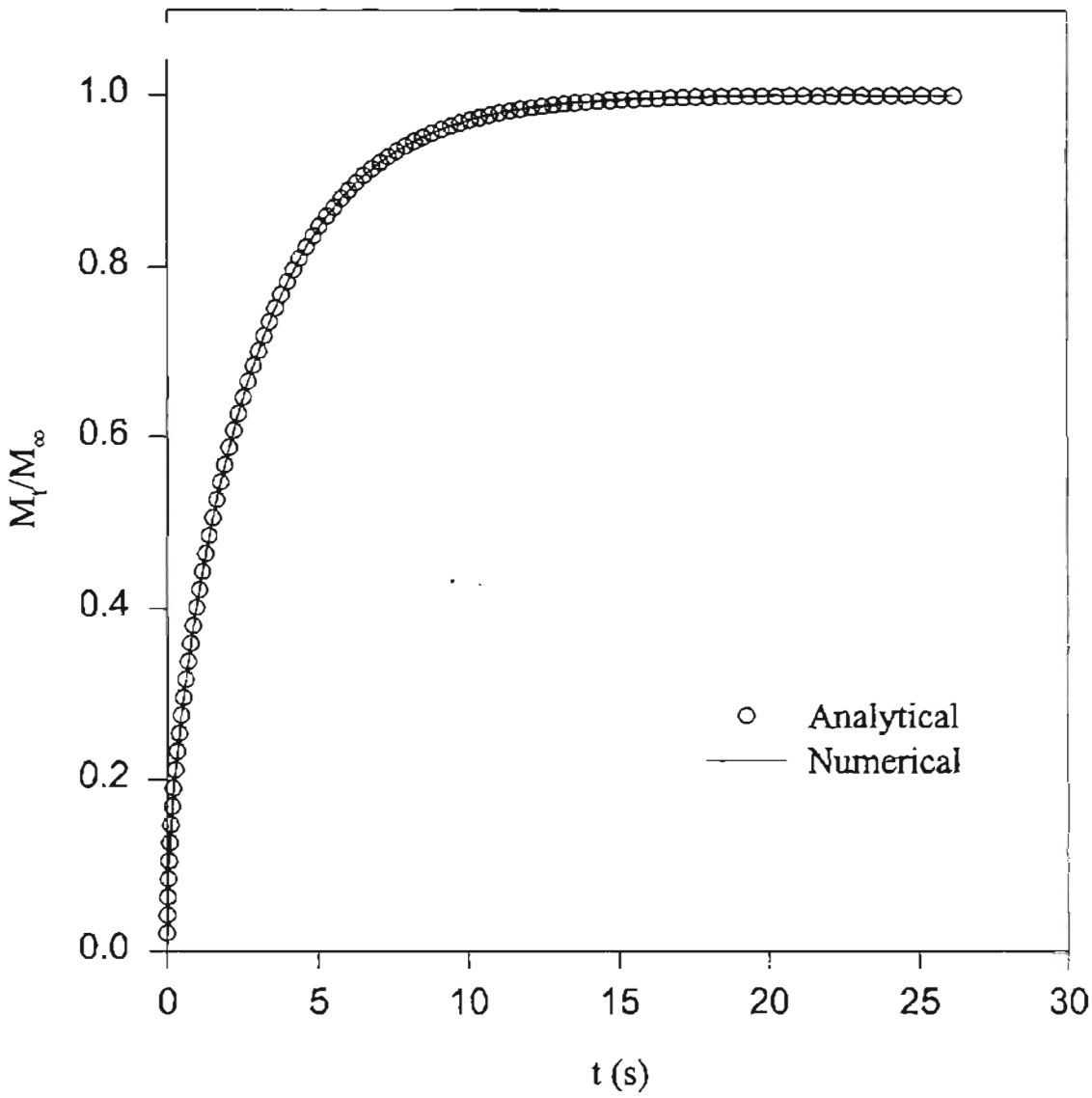

Figure 36. Comparison of Numerical and Analytical Solutions for the Fractional Mass Uptake with Constant Diffusion Coefficient.

curve, values of $1 - M_t/M_\infty$ vs. t were obtained. The numerically obtained sorption curve was treated as data obtained from a step-change sorption experiment and analyzed with the moment method in order to obtain diffusion coefficients (see Chapter II for details on diffusivity calculations using the moment method). A simple concentration dependence, $D(C)$, was chosen

$$D(C) = D_0 e^{\alpha C}, \tag{162}$$

where α is a constant chosen to be $\alpha = 100$, and D_0, the diffusivity at zero penetrant concentration was given a value $D_0 = 5.0 \times 10^{-11}$. The non-dimensional diffusion equation solved was

$$\frac{\partial C'}{\partial T} = \frac{\partial}{\partial X}\left\{\exp[\alpha(C_0 - C_1)C']\frac{\partial C'}{\partial X}\right\}, \tag{163}$$

$$C' = \frac{C - C_1}{C_0 - C_1}, \tag{164}$$

$$X = \frac{x}{L}, \tag{165}$$

$$T = \frac{t}{\tau}, \tag{166}$$

$$\tau = \frac{L^2}{D_0 \exp(\alpha C_1)}. \tag{167}$$

A constant step-change in concentration was chosen, $C_0 - C_1 = 0.01$. The moment method gives an average value of diffusivity, so a corresponding average concentration was used

$$\bar{C} = C_1 + 0.7(C_0 - C_1). \tag{168}$$

Figure 37 compares the diffusivities calculated from a moment method evaluation of numerical sorption curves, $\bar{D}$ vs. $\bar{C}$, with the diffusivities calculated straight from the constitutive equation 162, D vs. C. The moment method value of D agrees very well with the actual D, validating the accuracy of the moment method for calculating diffusion coefficients.

A validation was then performed on the combined MOLCH, QDAG and RNLIN program, Program 5 in Appendix E. This program was used to regress the mass uptake ratio data. As before, a constant diffusivity was used to initially

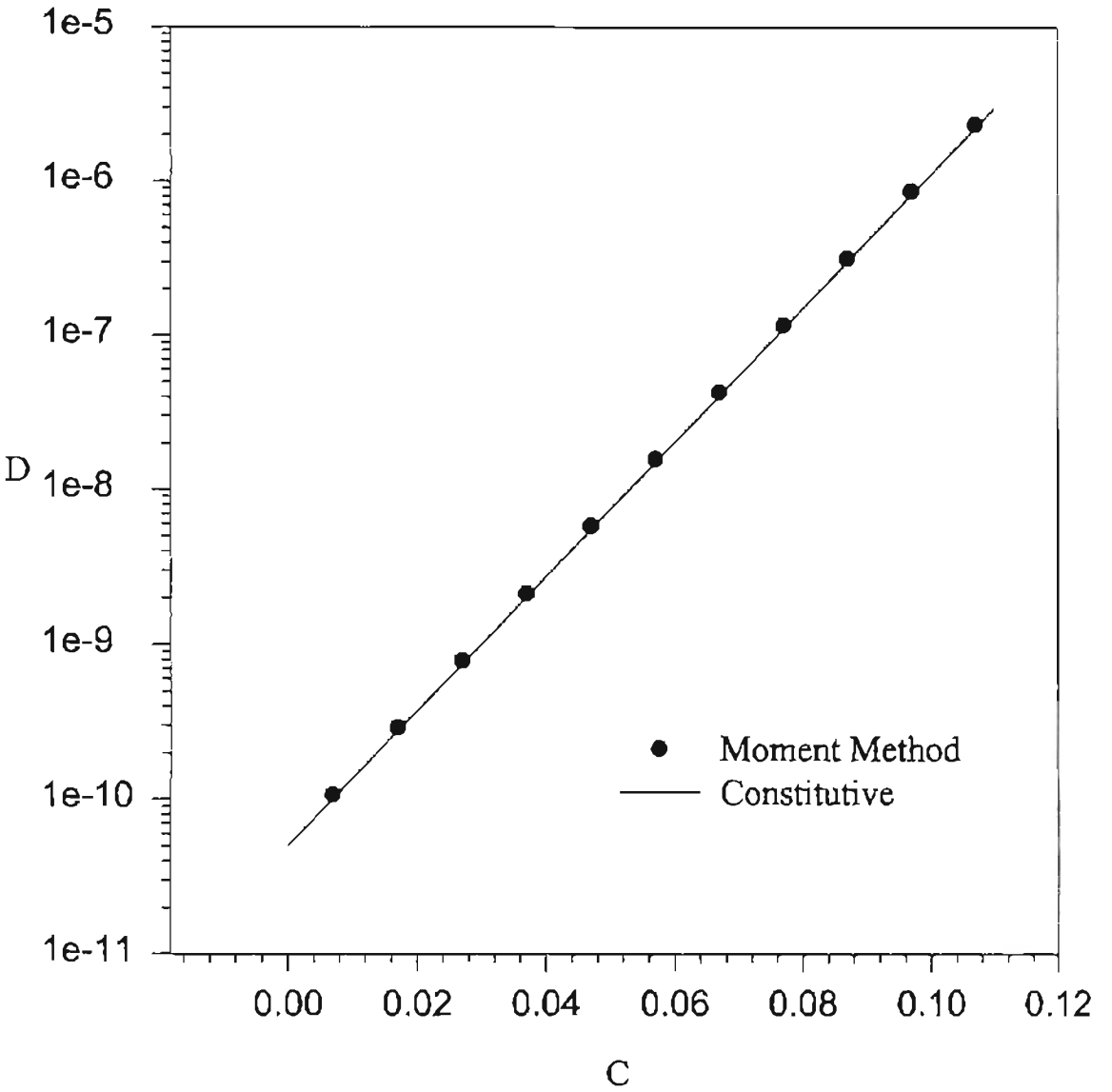

Figure 37. Comparison of Diffusion Coefficients Calculated from a Moment Method Evaluation of Sorption Data with Diffusion Coefficients Calculated from a Constitutive Equation.

validate the program since this was the simplest case. The data which was regressed was numerically simulated by Program 4, given a value for diffusivity of $D = 1 \times 10^{-8}$. In the regression program, Program 5, an initial guess of $D = 5 \times 10^{-8}$ was chosen. Program 5 fit the numerical data perfectly and returned the original value of the diffusivity, $D = 1 \times 10^{-8}$. Figure 38 shows the simulated data with $D = 1 \times 10^{-8}$ along with the mass uptake ratios with the diffusivity adjusted to $D = 5 \times 10^{-8}$. Figure 39 shows the correlation to the simulated data. This test shows that the correlation program returns the exact parameter for the constant diffusivity case.

Since the Program 5 worked well for constant diffusivity, it was then tested for the case when diffusivity varies with penetrant concentration. A simple form for the diffusivity was chosen

$$D = a + bC, \tag{169}$$

where a and b are constants. As with the constant diffusivity case above, the data which were regressed were numerically simulated. The parameters chosen to obtain these simulated data were $a = 1 \times 10^{-9}$ and $b = 1.3 \times 10^{-7}$. The change in penetrant concentration, C, was from 0 to 0.1. In Program 5, an initial guess of $a = 3 \times 10^{-9}$ and $b = 2.6 \times 10^{-7}$ was chosen. Program 5 returned a reasonable fit to the numerical data, but did not return the original values of the parameters a and b. Program 5 returned $a = 3.5 \times 10^{-9}$ and $b = 9.0 \times 10^{-8}$. Figure 40 shows the simulated data along with the mass uptake ratios with the the parameters a and b as initially guessed, as well as the regression to the simulated data.

Program 5 was then used to regress experimentally obtained sorption data. The data used was for toluene diffusing into neat PVAC at 60 °C. For the regression of the experimental sorption data, the free-volume constitutive equation for diffusivity was used. Vrentas and Dudas' free-volume equation was chosen since they have many studies in this area,

$$D = D_1(1 - \phi_1)^2(1 - 2\chi\phi_1), \tag{170}$$

$$D_1 = D_{01} \exp\left(-\frac{\gamma(w_1\widehat{V}_1^* + w_2\xi\widehat{V}_2^*)}{\widehat{V}_{FH}}\right), \tag{171}$$

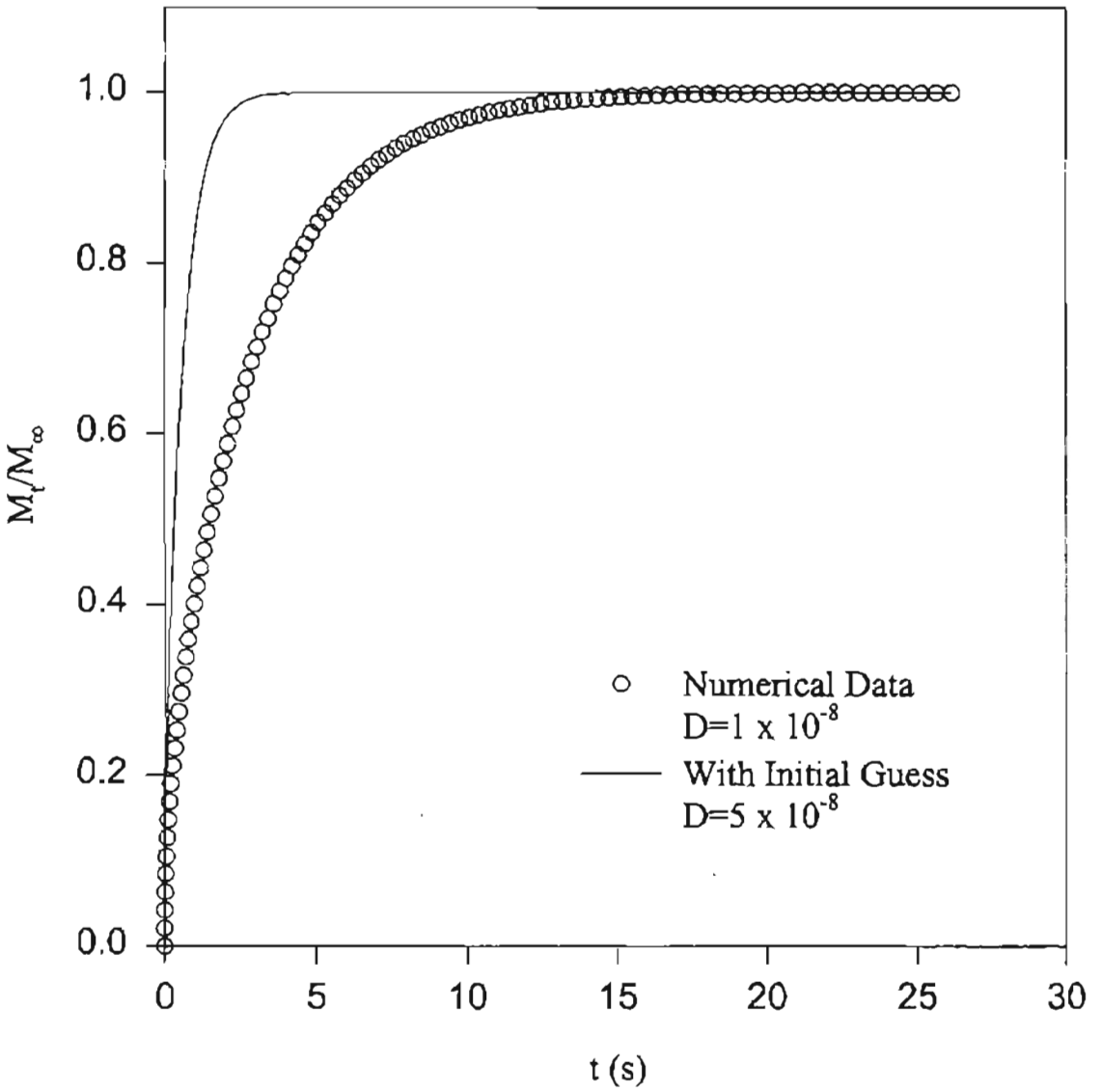

Figure 38. Comparison of Simulated Sorption Data with Constant Diffusivity, $D = 1 \times 10^{-8}$, to Mass Uptake Ratios with the Diffusivity Changed to $D = 5 \times 10^{-8}$.

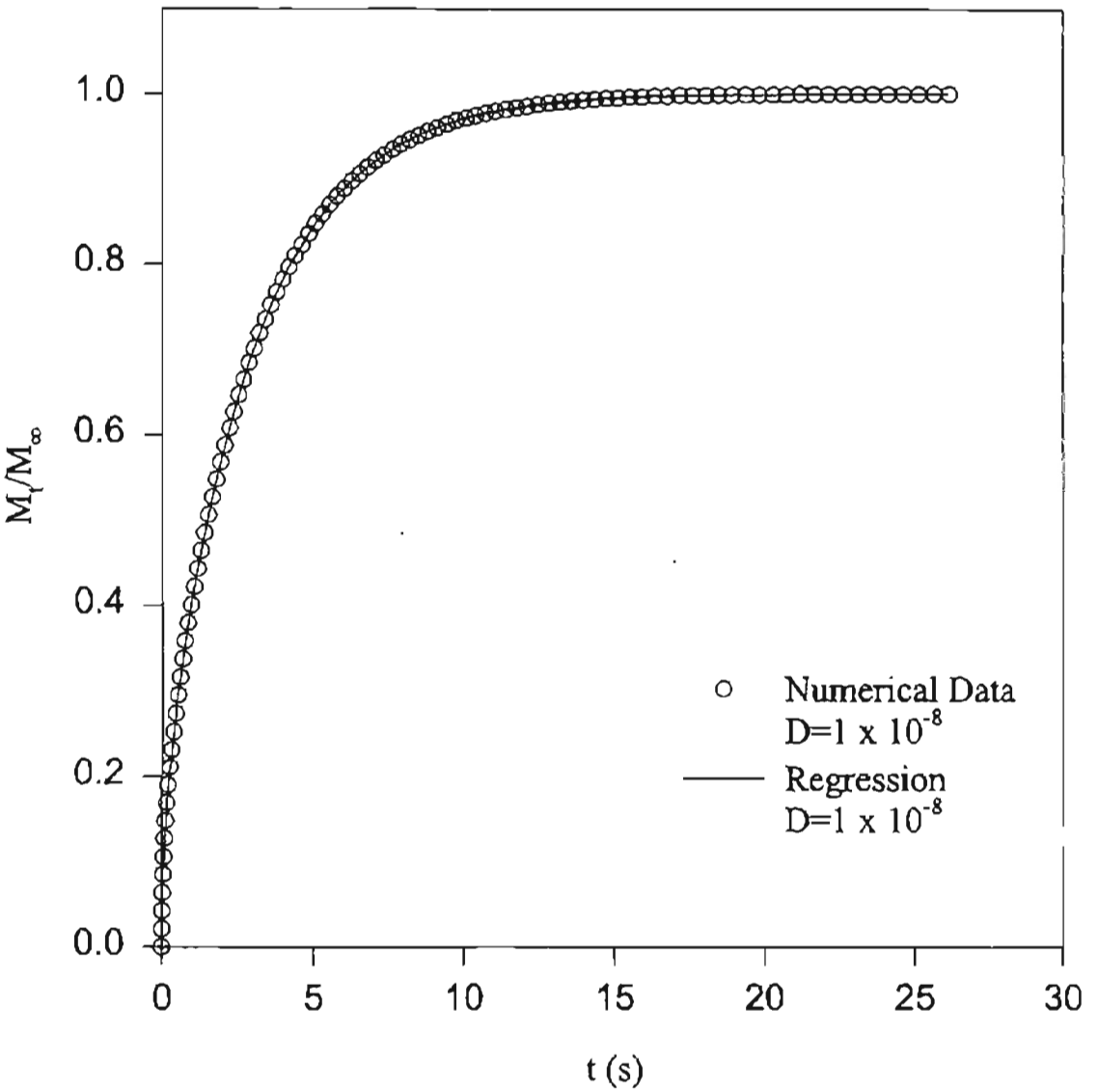

Figure 39. Regression of Simulated Sorption Data with Constant Diffusivity, $D = 1 \times 10^{-8}$.

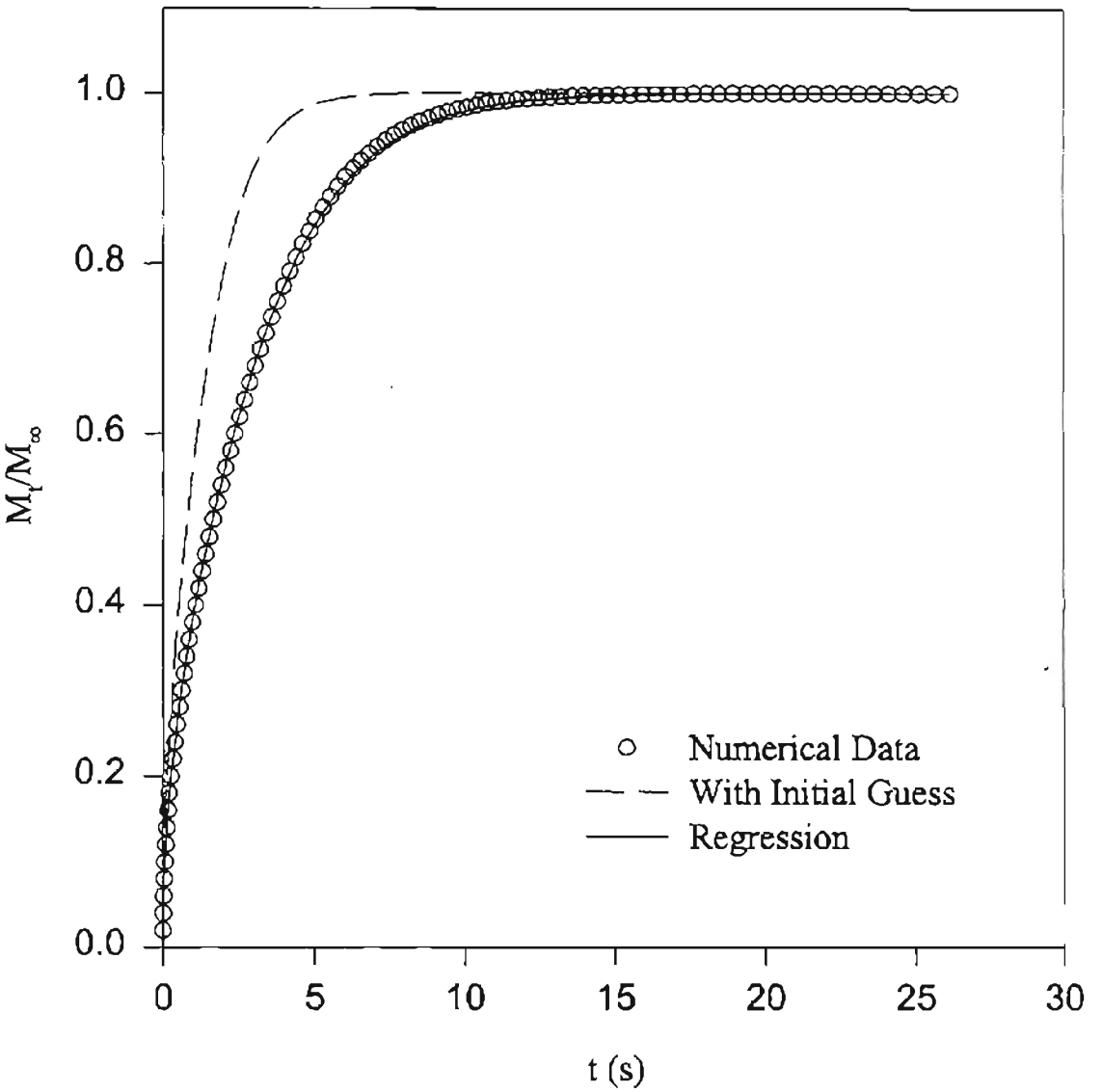

Figure 40. Regression of Simulated Sorption Data with a Simple Concentration Dependent Diffusivity, $D = a + bC$.

$$\frac{\widehat{V}_{FH}}{\gamma} = w_1 \frac{K_{11}}{\gamma}(K_{21} + T - T_{g1}) + w_2 \frac{K_{12}}{\gamma}(K_{22} + T - T_{g2}). \qquad (172)$$

The free volume parameters K_{11}/γ, $K_{21} - T_{g1}$, K_{12}/γ, $K_{22} - T_{g2}$, $\widehat{V}_1^*$, $\widehat{V}_2^*$, and χ were as given in Chapter V. Program 5 fit the experimental sorption data by adjusting the parameters D_{01} and ξ in the free-volume equation 170. Figure 41 shows the resulting fit to the experimental sorption data. The numerical sorption curve does not compare well with the experimentally obtained sorption data. A possible explanation is that the free-volume equation does not sufficiently describe penetrant diffusion in polymers.

Comparisons were made of the diffusivities obtained with equation 170 using free-volume parameters correlated with Program 5, as given in Table XV, and plotted in Figure 41 with diffusivities obtained by a moment method analysis on the experimentally obtained sorption curves. Figure 42 shows this comparison. The experimentally obtained diffusion coefficients do not compare well with those calculated by equation 170. The calculated values are consistently higher than the experimental data.

Free-volume parameters obtained by fitting equation 170 to the experimental diffusion coefficient data were used in the Program 5 to obtain a numerical sorption curve. Comparisons were made of the numerically obtained sorption curve with experimentally obtained sorption data. Figure 43 shows this comparison. The experimentally obtained sorption data do not compare well with the numerical sorption curve. Table XV shows the free-volume parameters for neat PVAC-toluene at 60 °C obtained from both a regression of sorption data and a regression of diffusivity data.

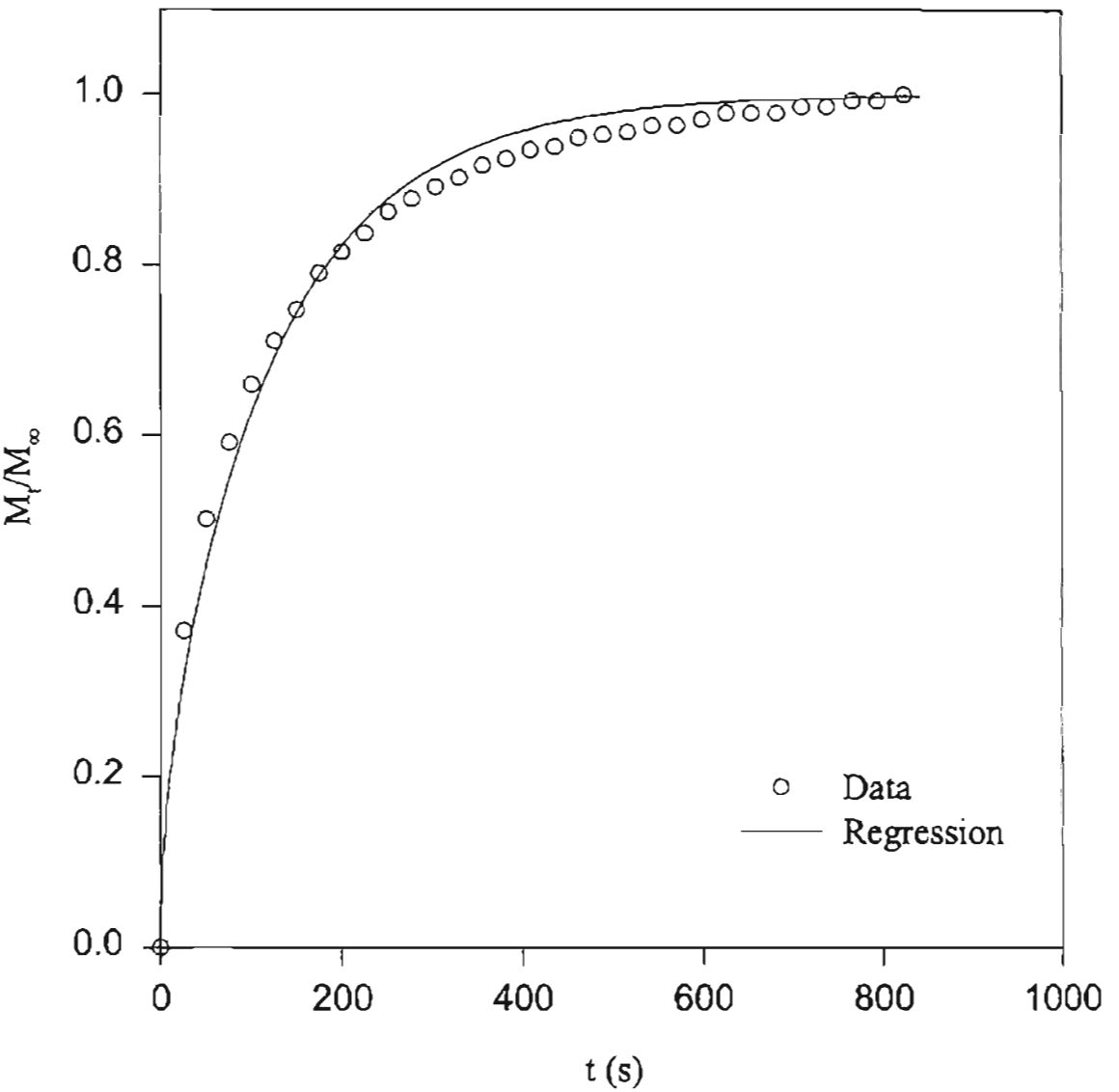

Figure 41. Regression of Experimental Sorption Data for Neat PVAC-Toluene at 60 °C Using a Free-Volume Theory Constitutive Equation.

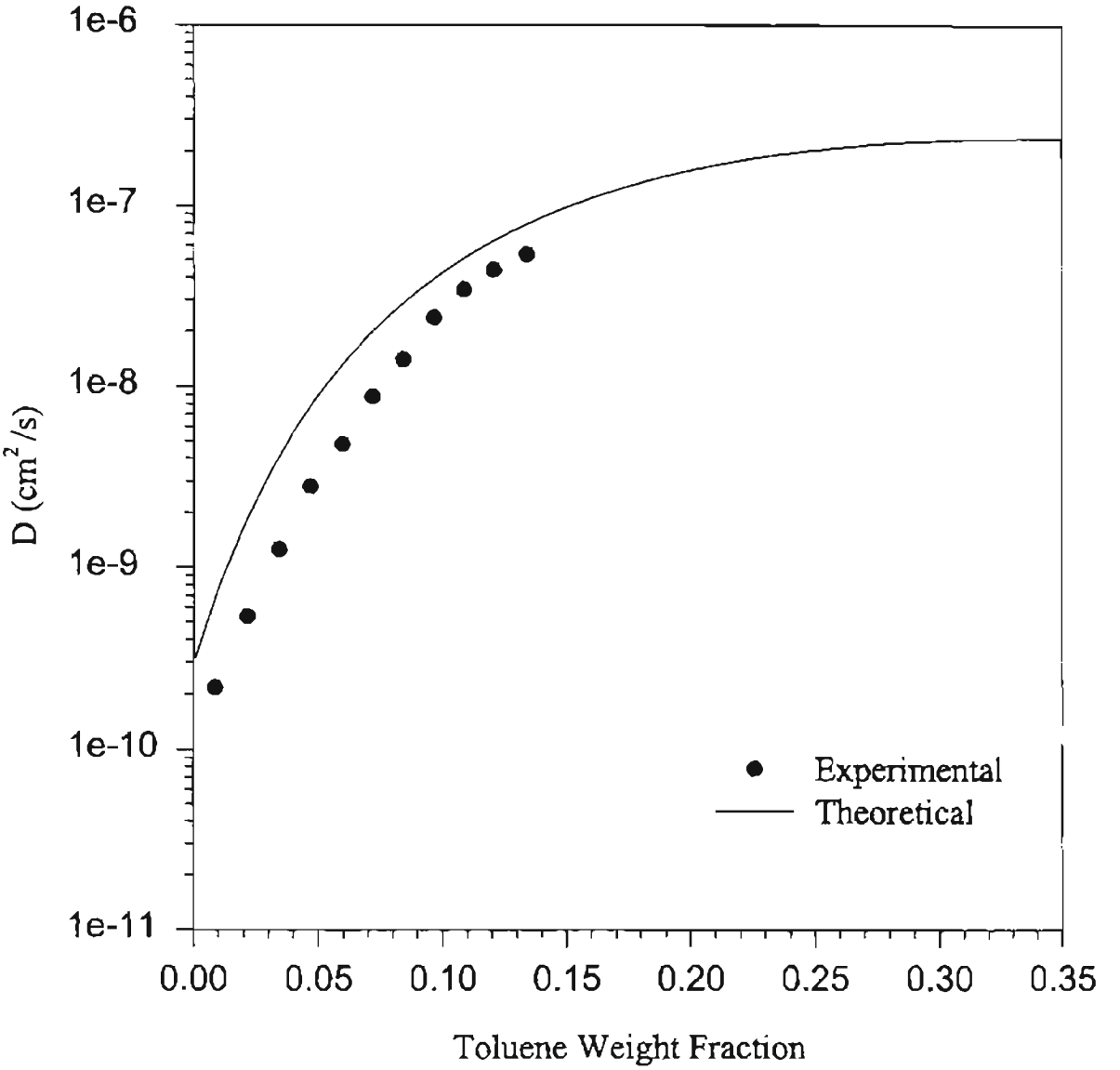

Figure 42. Comparison of Experimental Diffusion Coefficients with a Diffusion Coefficient Curve Calculated from the Free-Volume Equation for Neat PVAC at 60 °C.

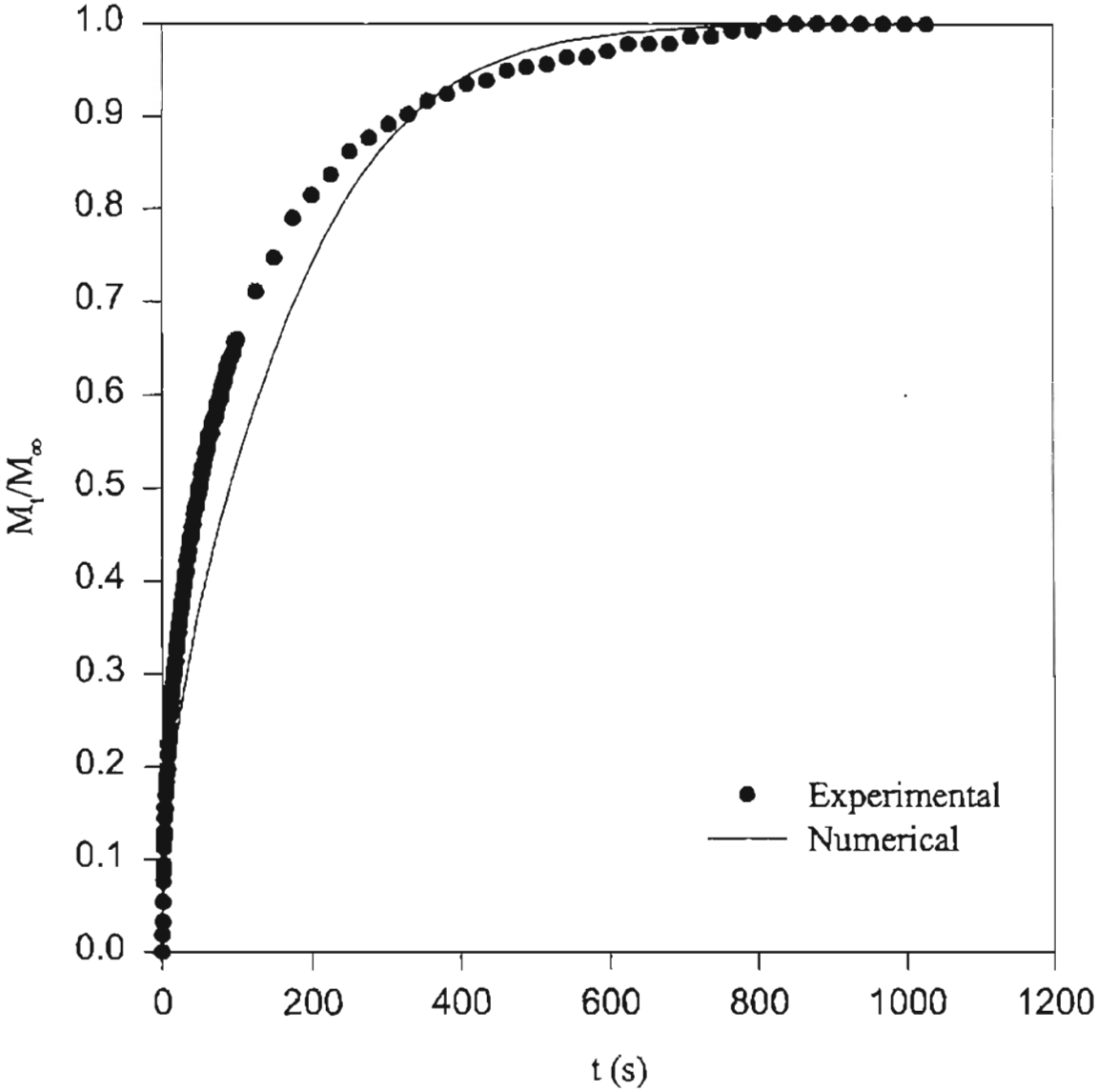

Figure 43. Comparison of Experimental Sorption Curve with a Simulated Sorption Curve Using the Free-Volume Constitutive Equation for Neat PVAC at 60 °C.

TABLE XV

FREE-VOLUME EQUATION PARAMETERS
FOR PVAC-TOLUENE AT 60 °C

Parameter	From Sorption Data Regressions	From Diffusivity Regressions
K_{11}/γ	1.57×10^{-3} cm^3/g K	1.57×10^{-3} cm^3/g K
K_{12}/γ	4.33×10^{-4} cm^3/g K	4.33×10^{-4} cm^3/g K
$K_{21} - T_{g1}$	-90.5 K	-90.5 K
$K_{22} - T_{g2}$	-256 K	-256 K
$\hat{V}_1^*$	0.917 cm^3/g	0.917 cm^3/g
$\hat{V}_2^*$	0.728 cm^3/g	0.728 cm^3/g
χ	0.42	0.42
D_{01}	5.00×10^{-5} cm^2/s	5.48×10^{-5} cm^2/s
ξ	0.55	0.63

APPENDIX E

Computer Programs

The computer programs that were written to simulate and regress sorption data are presented in this Appendix.

Program 1

The first program shown below was written to test the results of another program, Program 3. This program calculates the analytical solution of a diffusion equation with constant *D*, and gives concentration as a function of time and distance into the polymer film. The equation used in the program is taken from Crank [1956].

```
C       THIS PROGRAM CALCULATES THE ANALYTICAL SOLUTION OF A
C       DIFFUSION EQUATION WITH CONSTANT D.  EQUATION TAKEN
C       FROM CRANK, 1ST EDITION.  EQ. 4.17
C
        INTEGER     I,K,J,NX
        REAL*8      L,D,PI,SUM,T,X,VAL,Y(8),M,N,R,NXR
        NX=8
        L=1.
        D=1.
        PI=3.141592654
        DO 10 J=1,10
              M=J
              T=(M/10)**2
        DO 20 K=1,NX
              SUM=0.
              R=K
              NXR=NX
              X=1.-(R-1.)/(NXR-1.)
        PRINT*, X
        DO 30 I=0,100
              N=I
              VAL=((-1)**N/(2.*N+1.))*DEXP(-D*(2.*N+1.)**2
```

```
     &              *PI**2*T/(4.*L**2.))
     &              *COS((2.*N+1.)*PI*X/(2.*L))
                SUM=SUM+VAL
      30    CONTINUE
                Y(K)=1-(4./PI)*SUM
      20    CONTINUE
C                   Print results
      OPEN(1, FILE='CRANK.DAT',
STATUS='OLD',ACCESS='SEQUENTIAL')
      WRITE (1,'(/A,F4.2)') '              Solution at T =', T
      WRITE (1,100)(Y(I),I=1,NX)
100   FORMAT(1X,8F10.4)
10    CONTINUE
      END
```

Program 2

This program was used to test the results of Program 4. This program solves for the mass uptake ratio M_t/M_∞ as a function of time using an analytical solution for a finite slab and constant *D*. The equation used in this program was taken from Crank [1956].

```
C     THIS PROGRAM SOLVES FOR M/M(inf) AS A FUNCTION OF TIME
C     USING AN ANALYTICAL SOLUTION FOR A FINITE SLAB.
C     SOLUTION TAKEN FROM CRANK, 1ST EDITION.
C
      INTEGER    I, J, NSTEP, NANAL
      REAL       PI, L, D, S, TEND, TIME, SUM, VAL, RESULT
      INTRINSIC  FLOAT
      REAL       FLOAT
C
      OPEN(9, FILE='ANAL.DAT')
C
      WRITE (9,*) '     TIME          M/M(INF)       VAL'
      PI = 3.141592654
      L=0.000273466
      D=0.00000001
      S=3.5
C
      NANAL = 500
C
      NSTEP = 100
      J = 0
20    CONTINUE
      J = J + 1
      TEND = FLOAT(J)/FLOAT(NSTEP)
C
      TEND = TEND**2
C
      TIME = (S*L*L*TEND)/D
C
      SUM = 0.0
      DO 10 I = 0, NANAL
            VAL = (8/(((2*I+1)**2)*PI**2))*
     &      EXP((-D*((2*I+1)**2)*(PI**2)*TIME)/(4*(L**2)))
            SUM = SUM + VAL
10    CONTINUE
C
```

```
      RESULT = 1 - SUM
C
      IF (J .LE. NSTEP) THEN
C
            WRITE (9,*) TIME, RESULT, VAL
            GO TO 20
      END IF
      CLOSE (9)
      END
```

Program 3

This program solves a one dimensional diffusion equation for non-dimensional concentration of solvent in a polymer film as a function of non-dimensional distance, X, through the polymer film, and non-dimensional time, T. The PDE solver, MOLCH, was taken from Microsoft Fortran Powerstation MSIMSL Library, and modified for the case of solvent diffusing into a polymer film. The program uses the method of lines to solve a system of partial differential equations of the form $u_t = f(x, t, u, u_x, u_{xx})$. XBREAK is an array of length NX containing the break points and should be set in the parameter statement.

```
C     THIS PROGRAM SOLVES A ONE DIMENSIONAL DIFFUSION
C     EQUATION FOR NON-DIMENSIONAL CONCENTRATION AS A
C     FUNCTION OF X AND T FOR SOLVENT DIFFUSING INTO
C     POLYMER.  XBREAK IS AN ARRAY OF LENGTH NX CONTAINING
C     THE BREAK POINTS FOR SOLVING THE PDE.  NX IS THE NUMBER
C     OF MESH POINTS AND SHOULD BE SET IN THE PARAMETER
C     STATEMENT.    THE PDE SOLVER IS TAKEN FROM THE
C     MICROSOFT FORTRAN POWERSTATION MSIMSL LIBRARY
C     (MOLCH)
C
C                    SPECIFICATIONS FOR LOCAL VARIABLES
C
      USE            MSIMSL
      INTEGER        LDY, NPDES, NX
      PARAMETER (NPDES=1, NX=8, LDY=NPDES)
C
C                    SPECIFICATIONS FOR LOCAL VARIABLES
C
      INTEGER        I, IDO, J, NOUT, NSTEP
      REAL           HINIT, T, TEND, TOL, XBREAK(NX), Y(LDY,NX)
      CHARACTER  TITLE*19
C
C                    SPECIFICATIONS FOR INTRINSICS
C
      INTRINSIC  FLOAT
      REAL     FLOAT
C
C                    SPECIFICATIONS FOR SUBROUTINES
C
C     EXTERNAL   MOLCH, UMACH, WRRRN
```

```
C
C                   SPECIFICATIONS FOR FUNCTIONS
C
      EXTERNAL  FCNBC, FCNUT
      REAL      FCNBC, FCNUT
C
C                   Set breakpoints and initial
C                   conditions
C
      U0 = 0.0
      DO 10  I=1, NX
            XBREAK(I) = FLOAT(I-1)/(NX-1)
            Y(1,I)    = U0
10    CONTINUE
C
C                   Set parameters for MOLCH
C
      TOL  = SQRT(AMACH(4))
      HINIT = 0.01*TOL
      T    = 0.0
      IDO  = 1
      NSTEP = 10
      CALL UMACH (2, NOUT)
      J = 0
20    CONTINUE
      J   = J + 1
      TEND = FLOAT(J)/FLOAT(NSTEP)
C
C                   This puts more output for small
C                   t values where action is fastest.
C
      TEND = TEND**2
C
C                   Solve the problem
C
      CALL MOLCH (IDO, FCNUT, FCNBC, NPDES, T, TEND, NX, XBREAK,
     &         TOL, HINIT, Y, LDY)
      IF (J .LE. NSTEP) THEN
C
C                   Print results
C
      OPEN(1, FILE='MOLCH.DAT',STATUS='OLD',ACCESS='SEQUENTIAL')
      WRITE (1,'(/A,F4.2)') '              Solution at T =', T
      WRITE (1,100)(Y(1,I),I=1,NX)
100   FORMAT(1X,8F10.4)
```

```
C       CALL WRRRN (TITLE, NPDES, NX, Y, LDY, 0)
C
C                       Final call to release workspace
C
        IF (J .EQ. NSTEP) IDO = 3
        GO TO 20
        END IF
        END
C
        SUBROUTINE FCNUT (NPDES, X, T, U, UX, UXX, UT)
C
C                       SPECIFICATIONS FOR ARGUMENTS
C
        INTEGER   NPDES
        REAL      X, T, U(*), UX(*), UXX(*), UT(*)
C
C                       Define the PDE
C
        B=1
        UT(1) = EXP(B*U(1))*UXX(1)+B*EXP(B*U(1))*UX(1)*UX(1)
        RETURN
        END
C
        SUBROUTINE FCNBC (NPDES, X, T, ALPHA, BETA, GAMP)
C
C                       SPECIFICATIONS FOR ARGUMENTS
C
        INTEGER   NPDES
        REAL      X, T, ALPHA(*), BETA(*), GAMP(*)
C
C                       SPECIFICATIONS FOR PARAMETERS
C
        REAL      TDELTA, U0, U1
        PARAMETER  (TDELTA=0.00001, U0=0.0, U1=1.0)
C
C                       SPECIFICATIONS FOR LOCAL VARIABLES
C
        INTEGER   IWK(2), NDATA
        REAL      DFDATA(2), FDATA(2), XDATA(2)
C
C                       SPECIFICATIONS FOR SAVE VARIABLES
C
        REAL      BREAK(2), CSCOEF(4,2)
        LOGICAL   FIRST
        SAVE      BREAK, CSCOEF, FIRST
```

```
C
C                   SPECIFICATIONS FOR SUBROUTINES
C
      EXTERNAL  C2HER, WRRRN
C
C                   SPECIFICATIONS FOR FUNCTIONS
C
      EXTERNAL  CSDER
      REAL      CSDER
C
      DATA FIRST/.TRUE./
C
      IF (FIRST) GO TO 20
10    CONTINUE
C
C                   Define the boundary conditions
C
      IF (X .EQ. 0.0) THEN
C                   These are for x=0.
      ALPHA(1) = 1.0
      BETA(1)  = 0.0
      GAMP(1)  = 0.0
C                   If in the boundary layer,
C                   compute nonzero gamma prime.
      IF (T .LE. TDELTA) GAMP(1) = CSDER(1,T,1,BREAK,CSCOEF)
      ELSE
C                   These are for x=1.
      ALPHA(1) = 0.0
      BETA(1)  = 1.0
      GAMP(1)  = 0.0
      END IF
      RETURN
20    CONTINUE
C
C                   Compute the boundary layer data.
C
      NDATA    = 2
      XDATA(1) = 0.0
      XDATA(2) = TDELTA
      FDATA(1) = U0
      FDATA(2) = U1
      DFDATA(1) = 0.0
      DFDATA(2) = 0.0
C                   Do Hermite cubic interpolation.
      CALL C2HER (NDATA, XDATA, FDATA, DFDATA, BREAK, CSCOEF,
```

```
&IWK)
  FIRST = .FALSE.
  GO TO 10
  END
```

Program 4

This program solves a one dimensional diffusion equation for non-dimensional concentration as a function of X and T for solvent diffusing into a polymer film, then for each time step, M_T/M_∞ is solved by integrating over X from 0 to 1. The integration program, QDAG, was taken from the Microsoft Fortran Powerstation MSIMSL Library, and combined with Program 3 to solve for M_T/M_∞. The integration program, QDAG, integrates a function using a globally adaptive scheme based on Gauss-Kronrod rules. XBREAK is an array of length NX containing the break points for solving the PDE. NX is the number of mesh points and should be set in the parameter statements of both the main program and the subroutine FVALUES.

```
C     THIS PROGRAM SOLVES A ONE DIMENSIONAL DIFFUSION
C     EQUATION FOR NON-DIMENSIONAL CONCENTRATION AS A
C     FUNCTION OF X AND T FOR SOLVENT DIFFUSING INTO POLYMER.
C     THEN FOR EACH TIME STEP, M(T)/M(inf) IS SOLVED FOR BY
C     INTEGRATING OVER X FROM 0 TO 1.  XBREAK IS AN ARRAY OF
C     LENGTH NX CONTAINING THE BREAK POINTS FOR SOLVING THE
C     PDE.  NX IS THE NUMBER OF MESH POINTS AND SHOULD BE SET C
      IN THE PARAMETER STATEMENTS OF BOTH THE MAIN PROGRAM
C     AND THE SUBROUTINE FVALUES. THE PDE SOLVER IS TAKEN
C     FROM MSIMSL (MOLCH), AS WELL AS THE INTEGRATION
C     ROUTINE (QDAG)
C
C                  SPECIFICATIONS FOR LOCAL VARIABLES
C
      USE     MSIMSL
      INTEGER     LDY, NPDES, NX
      PARAMETER  (NPDES=1, NX=101, LDY=NPDES)
C
C                  SPECIFICATIONS FOR LOCAL VARIABLES
C
      INTEGER     I, IDO, J, NOUT, NSTEP
      REAL        HINIT, T, TEND, TOL, XBREAK(NX), Y(LDY,NX)
      REAL        RESULT, ERREST, SC, L, TIME
C
C                  SPECIFICATIONS FOR INTRINSICS
C
      INTRINSIC   FLOAT
```

```
      REAL         FLOAT
C
C                  SPECIFICATIONS FOR FUNCTIONS
C
      EXTERNAL  FCNBC, FCNUT
      REAL         FCNBC, FCNUT
C
C                  COMMON VARIABLES AND PARAMETERS
C
      COMMON    XBREAK, Y
C
      COMMON /SC/ SC
      OPEN(2, FILE='DIFFPROG.DAT')
      OPEN(1, FILE='QDAG.DAT')
      OPEN(9, FILE='THEORY2.DAT')
C
C                  Set breakpoints and initial
C                  conditions
C
      U0 = 0.0
      DO 10  I=1, NX
      XBREAK(I) = FLOAT(I-1)/(NX-1)
      Y(1,I)   = U0
10    CONTINUE
C
C                  Set parameters for MOLCH
C
      TOL   = SQRT(AMACH(4))
      HINIT = 0.01*TOL
      T  = 0.0
      IDO   = 1
      NSTEP = 100
      CALL UMACH (2, NOUT)
      J = 0
20    CONTINUE
      J    = J + 1
      TEND = FLOAT(J)/FLOAT(NSTEP)
C
C                  This puts more output for small
C                  t values where action is fastest.
C
      TEND = TEND**2
C
C                  Solve the problem
C
```

```
      .CALL MOLCH (IDO, FCNUT, FCNBC, NPDES, T, TEND, NX, XBREAK,
     &TOL, HINIT, Y, LDY)
      IF (J .LE. NSTEP) THEN
C
C                     Write results
C
C   COMMENT WRITE STATEMENTS FOR WRITING SOLUTION OF THE
C   DIFFERENTIAL EQ.IF THE MATRIX IS TOO BIG!!
C
C
C                     WRITING SOLUTION OF DIFFERENTIAL EQUATION
C                     FOR ONE TIME AT A TIME!!
C
C       WRITE (2,'(/A,F4.2/)') '              Solution at T =', T
C       WRITE (2,200)(Y(1,I),I=1,NX)
C 200   FORMAT(1X,8F10.4,/)
C
C                     CALL INTEGRATION SUBROUTINE TO INTEGRATE
C                     OVER X FOR A SINGLE TIME!!
C
      CALL INTPROG (RESULT, ERREST)
C
C                     WRITING SOLUTION TO INTEGRATION
C
      WRITE (1,100) TEND, RESULT, ERREST
100   FORMAT (' T =', F8.6, 13X, ' M(T)/M(inf) =', F14.9,
     &              '          Error estimate =', 1PE10.3)
C
C                       CALCULATE TIME
C
      L=0.000273466
      D0=5.4819e-5
      TIME=(SC*L*L*TEND)/D0
C
C               WRITING TIME AND M(t)/M(inf) TO THEORY.DAT
C
      WRITE(9,*) TIME, RESULT

C                     Final call to release workspace
C
      IF (J .EQ. NSTEP) IDO = 3
      GO TO 20
      END IF
      CLOSE (2)
      CLOSE (1)
```

```
      END
C
C*********************************************************************
C
      SUBROUTINE FCNUT (NPDES, X, T, U, UX, UXX, UT)
C
C                  SPECIFICATIONS FOR ARGUMENTS
C
      INTEGER    NPDES
      REAL       X, T, U(*), UX(*), UXX(*), UT(*)
      REAL       TEMP, WNOT, WONE, ZI, KI, KONEGAMMA
      REAL       KTWOGAMMA, KTONE, KTTWO, VONESTAR
      REAL       VTWOSTAR
      REAL       VONENOT, VTWONOT, BC, CC, DC, EC, FP, GP
      REAL       HC, IC, JP, KP, LP, MP, NP, SC
      COMMON /SC/ SC
C
C                  Define the PDE
C   FREE VOLUME PARAMETERS FOR PVAC-TOLUENE AT 60C
C
      SC=1000000.
      TEMP=333.15
      WNOT=0.012084786
      WONE=0.0
      ZI=0.6253
      KI=0.4249
      KONEGAMMA=0.00157
      KTWOGAMMA=0.000433
      KTONE=-90.5
      KTTWO=-256.
      VONESTAR=0.917
      VTWOSTAR=0.728
      VONENOT=1.205
      VTWONOT=0.847
      BC=VONESTAR
      CC=ZI*VTWOSTAR
      DC=KONEGAMMA*(KTONE+TEMP)
      EC=KTWOGAMMA*(KTTWO+TEMP)
      HC=VONENOT
      IC=VTWONOT
      JP=((WNOT-WONE)*U(1)+WONE)
      PHI=HC*JP/(HC*JP+IC*(1-JP))
      FP=(1-PHI)*(1-PHI)
      GP=1-2*KI*PHI
```

```
      KP=EXP(-(BC*JP+CC*(1-JP))/(DC*JP+EC*(1-JP)))
      LP=IC*HC*(WNOT-WONE)/((HC*JP+IC*(1-JP))*(HC*JP+IC*(1-JP)))
      MP=(1-((HC*JP)/(HC*JP+IC*(1-JP))))
      NP=(BC*EC-CC*DC)*(WNOT-WONE)/((DC*JP+EC*(1-
     &JP))*(DC*JP+EC*(1-JP)))
      UT(1) = SC*KP*FP*GP*UXX(1)-SC*(2*KP*FP*KI*LP+
     &2*KP*GP*MP*LP+FP*GP*KP*NP)*UX(1)*UX(1)
      RETURN
      END
C
C*********************************************************************
C
      SUBROUTINE FCNBC (NPDES, X, T, ALPHA, BETA, GAMP)
C
C                  SPECIFICATIONS FOR ARGUMENTS
C
      INTEGER   NPDES
      REAL      X, T, ALPHA(*), BETA(*), GAMP(*)
C
C                  SPECIFICATIONS FOR PARAMETERS
C
      REAL          TDELTA, U0, U1
      PARAMETER  (TDELTA=0.00001, U0=0.0, U1=1.0)
C
C                  SPECIFICATIONS FOR LOCAL VARIABLES
C
      INTEGER     IWK(2), NDATA
      REAL        DFDATA(2), FDATA(2), XDATA(2)
C
C                  SPECIFICATIONS FOR SAVE VARIABLES
C
      REAL        BREAK(2), CSCOEF(4,2)
      LOGICAL     FIRST
      SAVE        BREAK, CSCOEF, FIRST
C
C                  SPECIFICATIONS FOR SUBROUTINES
C
      EXTERNAL  C2HER, WRRRN
C
C                  SPECIFICATIONS FOR FUNCTIONS
C
      EXTERNAL  CSDER
      REAL        CSDER
C
      DATA FIRST/.TRUE./
```

```
C
      IF (FIRST) GO TO 30
40    CONTINUE
C
C                  Define the boundary conditions
C
      IF (X .EQ. 0.0) THEN
C
C                  These are for x=0.
C
      ALPHA(1) = 1.0
      BETA(1)  = 0.0
      GAMP(1)  = 0.0
C
C                  If in the boundary layer,
C                  compute nonzero gamma prime.
C
      IF (T .LE. TDELTA) GAMP(1) = CSDER(1,T,1,BREAK,CSCOEF)
      ELSE
C
C                  These are for x=1.
C
      ALPHA(1) = 0.0
      BETA(1)  = 1.0
      GAMP(1)  = 0.0
      END IF
      RETURN
30    CONTINUE
C
C                  Compute the boundary layer data.
C
      NDATA    = 2
      XDATA(1) = 0.0
      XDATA(2) = TDELTA
      FDATA(1) = U0
      FDATA(2) = U1
      DFDATA(1) = 0.0
      DFDATA(2) = 0.0
C
C                  Do Hermite cubic interpolation.
C
      CALL C2HER (NDATA, XDATA, FDATA, DFDATA, BREAK, CSCOEF,
     &IWK)
      FIRST = .FALSE.
      GO TO 40
```

```
      END
C
C*************************************************************************
C
      SUBROUTINE INTPROG (RESULT, ERREST)
      USE          MSIMSL
      INTEGER      IRULE
      REAL         A, B, ERRABS, ERREST, ERRREL
     &             F, RESULT
      EXTERNAL     F
C
C                  Get output unit number
C
      CALL UMACH (2, NOUT)
C
C                  Set limits of integration
      A = 0.0
      B = 1.0
C
C                  Set error tolerances
C
      ERRABS = 0.0
      ERRREL = 0.001
C
C                  Parameter for non-oscillatory
C                  function
C
      IRULE = 2
      CALL QDAG (F, A, B, ERRABS, ERRREL, IRULE, RESULT, ERREST)
      RETURN
      END
C
C*************************************************************************
C
      REAL FUNCTION F (X)
      REAL     X
      CALL FVALUES (F, X)
      RETURN
      END
C
C*************************************************************************
C
      SUBROUTINE FVALUES (CP,XP)
      INTEGER   NX, LDY
      PARAMETER  (NPDES=1, NX=101, LDY=NPDES)
```

```
      REAL     XBREAK(NX), Y(LDY,NX), CP, XP
      COMMON   XBREAK, Y
C
C                  DO LINEAR INTERPOLATION ON ARRAY XBREAK
C                  TO FIND FUNCTION.
C
      DO 50 K=1, NX
            IF (XP .EQ. XBREAK(K)) THEN
                  CP = Y(LDY,K)
            ELSEIF (XP .GT. XBREAK(K)) THEN
                  IF (XP .LT. XBREAK(K+1)) THEN
                        CP = ((XP-XBREAK(K))/(XBREAK(K+1)-
     &XBREAK(K)))*(Y(LDY,K+1)-Y(LDY,K))+Y(LDY,K)
                  ENDIF
            ENDIF
50    CONTINUE
      RETURN
      END
```

Program 5

This program solves a one dimensional diffusion equation for non-dimensional concentration as a function of X ant T for solvent diffusing into a polymer film. For each time step, M_T/M_∞ is solved for by integrating over X from 0 to 1, then dimensionalized to give M_t/M_∞ vs. t. Parameters in a constitutive equation for *D* in the PDE are determined by a non-linear regression of experimental sorption data. The non-linear regression program, RNLIN, was taken from Microsoft Fortran Powerstation MSIMSL Library, and combined with Program 4. The experimental data is read from a file. XBREAK is an array of length NX containing the break points and should be set in the parameter statements of the subroutine DIFFPROG and the subroutine FVALUES. NPARM is the number of parameters and should be set in the parameter statements of the main program. The number of points in the theoretical sorption curve can be set by setting the number of time steps (NSTEP) in the parameter statement of the subroutine DIFFPROG. Initial guesses of the parameters are to be input by the user in the main program.

```
C     THIS PROGRAM SOLVES A ONE DIMENSIONAL DIFFUSION
C     EQUATION FOR NON-DIMENSIONAL CONCENTRATION AS A
C     FUNCTION OF X AND T FOR SOLVENT DIFFUSING INTO POLYMER.
C     THE CONSTITUTIVE EQUATION USED IN THE DIFFUSION PDE IS
C     THE FREE VOLUME EQUATION.  FOR EACH TIME STEP, M(T)/M(inf)
C     IS SOLVED FOR BY INTEGRATING OVER X FROM 0 TO 1.  XBREAK
C     IS AN ARRAY OF LENGTH NX CONTAINING THE BREAK POINTS
C     FOR SOLVING THE PDE.  NX IS THE NUMBER OF MESH POINTS
C     AND SHOULD BE SET IN THE PARAMETER STATEMENTS OF THE
C     SUBROUTINE DIFFPROG AND THE SUBROUTINE FVALUES.  A
C     SORPTION CURVE OF M(t)/M(inf) VS t IS OBTAINED AND THE FREE
C     VOLUME PARAMETERS D0 AND ZI ARE REGRESSED BY
C     COMPARING THE THEORETICAL SORPTION CURVE TO ACTUAL
C     DATA.  NPARM IS THE NUMBER OF PARAMETERS AND SHOULD
C     BE SET IN THE PARAMETER STATEMENTS OF THE MAIN
C     PROGRAM.  THE NUMBER OF POINTS IN THE THEORETICAL
C     SORPTION CURVE CAN BE SET BY SETTING THE NUMBER OF
C     TIME STEPS (NSTEP) IN THE PARAMETER STATEMENT OF THE
C     SUBROUTINE DIFFPROG.  INITIAL GUESSES OF THE FREE VOLUME
C     PARAMETERS ARE TO BE INPUT BY THE USER IN THE MAIN
```

```
C     PROGRAM.  THE PDE SOLVER IS TAKEN FROM MSIMSL (MOLCH),
C     AS WELL AS THE INTEGRATION ROUTINE (QDAG) AND THE
C     REGRESSION ROUTINE (RNLIN).
      USE         MSIMSL
      INTEGER     LDR, NOBS, NPARM, WKPARM
      PARAMETER  (NPARM=4, LDR=NPARM, WKPARM=11*NPARM+4)
C
      INTEGER     IDERIV, IRANK, IPARAM(6), IWK(NPARM)
      REAL        DFE, R(LDR,NPARM), SSE, THETA(NPARM)
      REAL        RPARAM(7), SCALE(NPARM), WK(WKPARM)
      REAL        TIM, RES
      LOGICAL     WRTH
      EXTERNAL    EXAMPL
C
      COMMON /INTA/ NOBS
C
      WRTH = .FALSE.
C
C     FREE VOLUME UNKNOWN PARAMETERS; D0,ZI,KONEGAMMA,KI
      THETA(1)=4.306623e-5
      THETA(2)=0.5951618
      THETA(3)=1.57e-3
      THETA(4)=0.4249
C
      OPEN (1, FILE='QDAG.DAT')
      OPEN (2, FILE='DIFFPROG.DAT')
      OPEN (8, FILE='RLINTEST.DAT')
      OPEN (9, FILE='THEORY.DAT')
      OPEN (11,FILE='SCRATCH.DAT')
      OPEN (12,FILE='DATA.DAT')
C
C     FIND OUT HOW MANY OBSERVABLES (NOBS) ARE IN THE
C     DATA.DAT FILE
      REWIND (12)
      NOBS=0
14    READ(12,*,END=16)
      NOBS=NOBS+1
      GOTO 14
16    CONTINUE
      REWIND (12)
C
      IDERIV = 0
      CALL R8LIN (IPARAM, RPARAM)
      IPARAM(5) = 10000
      RPARAM(1) = 0.0
```

```
      RPARAM(2) = 1.0E-10
      RPARAM(3) = 0.0
      RPARAM(4) = 0.0
      IPARAM(6) = 0
      RPARAM(5) = 0.0
      SCALE(1) = 1.0/ABS(THETA(1))
      SCALE(2) = 1.0/ABS(THETA(2))
      SCALE(3) = 1.0/ABS(THETA(3))
      SCALE(4) = 1.0/ABS(THETA(4))
      CALL R2LIN (EXAMPL, NPARM, IDERIV, THETA, R, LDR, IRANK,
     &DFE, SSE, IPARAM, RPARAM, SCALE, IWK, WK)
      WRITE (8,*) 'THETA = ', THETA
      WRITE (8,*) 'IRANK = ', IRANK, '  DFE = ', DFE
      WRITE (8,*) '  SSE = ',           SSE
C
      DO 500 J=1,NPARM
            WRITE (8,*)
            WRITE (8,*) R(J,1),R(J,2),R(J,3),R(J,4)
500   CONTINUE
      WRITE (8,*) 'INIT = ', IPARAM(1), '   NDIGIT = ', IPARAM(2),
     &      '   ITER = ', IPARAM(3)
      WRITE (8,*) 'NFCN = ', IPARAM(4), '   NJAC = ', IPARAM(5),
     &      '   MODE = ', IPARAM(6)
      WRITE (8,*) 'FJACTL = ', RPARAM(1), '   STEPTL = ', RPARAM(2),
     &      '   RFTOL = ', RPARAM(3), '   AFTOL = ', RPARAM(4)
      WRITE (8,*) 'FALSTL = ', RPARAM(5), '   STEPMX = ', RPARAM(6),
     &      '   DELTA = ', RPARAM(7)
      DO 550 M=1,NPARM
            WRITE (8,*)
            WRITE (8,*) 'SCALE(',M,') =', SCALE(M)
550   CONTINUE
      DO 600 I=1,NPARM
            WRITE (8,*)
            WRITE (8,*) 'IWK(',I,') =', IWK(I)
600   CONTINUE
      DO 700 K=1,WKPARM
            WRITE (8,*)
            WRITE (8,*) 'WK(',K,') = ', WK(K)
700   CONTINUE
C
      REWIND(9)
      TIM = 0.0
      RES = 0.0
      WRITE (9,*) TIM, RES
      WRTH = .TRUE.
```

```
C
      REWIND (12)
17    READ(12,*,END=18) XDATA, YDATA
      GOTO 17
18    CONTINUE
      REWIND (12)
C
      CALL DIFFPROG (NPARM, THETA, XDATA, YTHEORY, WRTH)
C
      CLOSE (1)
      CLOSE (2)
      CLOSE (8)
      CLOSE (9)
      CLOSE (12)
C
      END
C
C     ****************************************************************
C
      SUBROUTINE EXAMPL (NPARM, THETA, IOPT, IOBS, FRQ, WT, E,
     &DE, IEND)
      INTEGER     NPARM, IOPT, IOBS, IEND, NOBS, JIOBS
      REAL        THETA(NPARM), FRQ, WT, E, DE(1)
C
      REAL        XDATA, YDATA, YTHEORY
      LOGICAL     WRTH
C
      COMMON /INTA/ NOBS
C
      WRTH = .FALSE.
C
      IF (IOBS .NE. JIOBS) THEN
            BACKSPACE (12)
      ENDIF
      IF (IOBS .LE. NOBS) THEN
            READ (12,*) XDATA, YDATA
            PRINT*, 'RUN IN PROGRESS:  ','DATA#:',IOBS,
     &      '  TOTAL DATA:',NOBS
            JIOBS=IOBS+1
            WT   = 1.0E0
            FRQ  = 1.0E0
            IEND = 0
C
            IF (XDATA .NE. 0.) THEN
                  CALL DIFFPROG (NPARM, THETA, XDATA, YTHEORY,
```

```
     &                                    WRTH)
            ELSE
                  YTHEORY = 0.0
            ENDIF
            E   = YDATA - YTHEORY
      ELSE
            IEND = 1
            REWIND (12)
      END IF
      RETURN
      END
C
C  ***********************************************************************
C
C                  SPECIFICATIONS FOR LOCAL VARIABLES
C
      SUBROUTINE DIFFPROG (NPARM, THETA, XDATA, RESULT, WRTH)
      INTEGER     LDY, NPDES, NX, NPARM
      PARAMETER  (NPDES=1, NX=101, LDY=NPDES)
C
C                  SPECIFICATIONS FOR LOCAL VARIABLES
C
      INTEGER     I, IDO, J, NOUT, NSTEP
      REAL        HINIT, T, TEND, TOL, XBREAK(NX), Y(LDY,NX)
      REAL        RESULT, ERREST, THETA(NPARM), L, D0, ZI, TIME, SC
      REAL        XDATA, KONEGAMMA, KI
      LOGICAL     WRTH
C
C                  SPECIFICATIONS FOR INTRINSICS
C
      INTRINSIC   FLOAT
      REAL        FLOAT
C
C                  SPECIFICATIONS FOR FUNCTIONS
C
      EXTERNAL    FCNBC, FCNUT
      REAL        FCNBC, FCNUT
C
C                  COMMON VARIABLES AND PARAMETERS
C
      COMMON /ARRA/ XBREAK, Y
      COMMON /VARA/ L, SC, ZI, KONEGAMMA, KI
C
C     FREE VOLUME UNKNOWN PARAMETERS
      D0=THETA(1)
```

```
      ZI=THETA(2)
      KONEGAMMA=THETA(3)
      KI=THETA(4)
      SC=500000.0000
      L=0.000273466
      IF (WRTH) THEN
            SC = (D0*XDATA)/(L*L)
            WRITE(11,*) 'SC=  ', SC, '  XDATA=  ', XDATA
      ENDIF
C
C
C                 Set breakpoints and initial
C                 conditions
C
      U0 = 0.0
      DO 10  I=1, NX
      XBREAK(I) = FLOAT(I-1)/(NX-1)
      Y(1,I)   = U0
10    CONTINUE
C
C                 Set parameters for MOLCH
C
      TOL   = SQRT(AMACH(4))
      HINIT = 0.01*TOL
      T     = 0.0
      IDO   = 1
      CALL UMACH (2, NOUT)
      J = 0
20    CONTINUE
      J   = J + 1
C
      IF (WRTH) THEN
            NSTEP = 100
            TEND = FLOAT(J)/FLOAT(NSTEP)
C
C                 This puts more output for small
C                 t values where action is fastest.
C
            TEND = TEND**2
      ELSE
            NSTEP = 1
            TEND = (D0*XDATA)/(SC*L*L)
      ENDIF
C
C                 Solve the problem
```

```
C
      CALL MOLCH (IDO, FCNUT, FCNBC, NPDES, T, TEND, NX, XBREAK,
     &TOL, HINIT, Y, LDY)
      IF (J .LE. NSTEP) THEN
C
C                  CALL INTEGRATION SUBROUTINE TO INTEGRATE
C                  OVER X FOR A SINGLE TIME!!
C
            CALL INTPROG (RESULT, ERREST)
C
C                     CALCULATE TIME
C
            TIME=(SC*L*L*TEND)/D0
C
C       WRITING TIME AND M(t)/M(inf) TO THEORY.DAT
C
            WRITE(9,*) TIME, RESULT
C
C                  Final call to release workspace
C
      IF (J .EQ. NSTEP) IDO = 3
      GO TO 20
      END IF
      REWIND (1)
      REWIND (9)
      RETURN
      END
C
C*************************************************************************
C
      SUBROUTINE FCNUT (NPDES, X, T, U, UX, UXX, UT)
C
C                  SPECIFICATIONS FOR ARGUMENTS
C
      INTEGER     NPDES
      REAL        X, T, U(*), UX(*), UXX(*), UT(*)
      REAL        TEMP, WNOT, WONE, ZI, KI, KONEGAMMA
      REAL        KTWOGAMMA, KTONE, KTTWO
      REAL        VONESTAR, VTWOSTAR
      REAL        VONENOT, VTWONOT, BC, CC, DC, EC, FP, GP
      REAL     HC, IC, JP, KP, LP, MP, NP, SC, L
C
      COMMON /VARA/ L, SC, ZI, KONEGAMMA, KI
C
C                  Define the PDE
```

```
C       FREE VOLUME PARAMETERS FOR PVAC-TOLUENE AT 60C
C
        TEMP=333.15
        WNOT=0.012084786
        WONE=0.0
C       KI=0.4249
C       KONEGAMMA=1.5700e-3
        KTWOGAMMA=4.3300e-4
        KTONE=-90.5
        KTTWO=-256.
        VONESTAR=0.917
        VTWOSTAR=0.728
        VONENOT=1.205
        VTWONOT=0.847
        BC=VONESTAR
        CC=ZI*VTWOSTAR
        DC=KONEGAMMA*(KTONE+TEMP)
        EC=KTWOGAMMA*(KTTWO+TEMP)
        HC=VONENOT
        IC=VTWONOT
        JP=((WNOT-WONE)*U(1)+WONE)
        PHI=HC*JP/(HC*JP+IC*(1-JP))
        FP=(1-PHI)*(1-PHI)
        GP=1-2*KI*PHI
        KP=EXP(-(BC*JP+CC*(1-JP))/(DC*JP+EC*(1-JP)))
        LP=IC*HC*(WNOT-WONE)/((HC*JP+IC*(1-JP))*(HC*JP+IC*(1-JP)))
        MP=(1-((HC*JP)/(HC*JP+IC*(1-JP))))
        NP=(BC*EC-CC*DC)*(WNOT-WONE)/((DC*JP+EC*(1-
     &JP))*(DC*JP+EC*(1-JP)))
        UT(1) = SC*KP*FP*GP*UXX(1)-SC*(2*KP*FP*KI*LP+
     &2*KP*GP*MP*LP+FP*GP*KP*NP)*UX(1)*UX(1)
        RETURN
        END
C
C*****************************************************************
C
        SUBROUTINE FCNBC (NPDES, X, T, ALPHA, BETA, GAMP)
C
C                   SPECIFICATIONS FOR ARGUMENTS
C
        INTEGER     NPDES
        REAL        X, T, ALPHA(*), BETA(*), GAMP(*)
C
C                   SPECIFICATIONS FOR PARAMETERS
C
```

```
      REAL        TDELTA, U0, U1
      PARAMETER  (TDELTA=0.00001, U0=0.0, U1=1.0)
C
C                 SPECIFICATIONS FOR LOCAL VARIABLES
C
      INTEGER     IWK(2), NDATA
      REAL        DFDATA(2), FDATA(2), XDATA(2)
C
C                 SPECIFICATIONS FOR SAVE VARIABLES
C
      REAL        BREAK(2), CSCOEF(4,2)
      LOGICAL     FIRST
      SAVE        BREAK, CSCOEF, FIRST
C
C                 SPECIFICATIONS FOR SUBROUTINES
C
      EXTERNAL  C2HER, WRRRN
C
C                 SPECIFICATIONS FOR FUNCTIONS
C
      EXTERNAL  CSDER
      REAL        CSDER
C
      DATA FIRST/.TRUE./
C
      IF (FIRST) GO TO 30
40    CONTINUE
C
C
C                 Define the boundary conditions
C
      IF (X .EQ. 0.0) THEN
C
C                 These are for x=0.]
C
            ALPHA(1) = 1.0
            BETA(1)  = 0.0
            GAMP(1)  = 0.0
C
C                 If in the boundary layer,
C                 compute nonzero gamma prime.
C
      IF (T .LE. TDELTA) GAMP(1) = CSDER(1,T,1,BREAK,CSCOEF)
      ELSE
C
```

```
C                    These are for x=1.
C
      ALPHA(1) = 0.0
      BETA(1)  = 1.0
      GAMP(1)  = 0.0
      END IF
      RETURN
30    CONTINUE
C
C                    Compute the boundary layer data.
C
      NDATA    = 2
      XDATA(1) = 0.0
      XDATA(2) = TDELTA
      FDATA(1) = U0
      FDATA(2) = U1
      DFDATA(1) = 0.0
      DFDATA(2) = 0.0
C
C                    Do Hermite cubic interpolation.
C
      CALL C2HER (NDATA, XDATA, FDATA, DFDATA, BREAK, CSCOEF,
     &                    IWK)
      FIRST = .FALSE.
      GO TO 40
      END
C
C*************************************************************************
C
      SUBROUTINE INTPROG (RESULT, ERREST)
      USE          MSIMSL
      INTEGER      IRULE
      REAL         A, B, ERRABS, ERREST, ERRREL
     &             F, RESULT
      EXTERNAL     F
C
C                    Get output unit number
C
      CALL UMACH (2, NOUT)
C
C                    Set limits of integration
C
      A = 0.0
      B = 1.0
C
```

```
C                   Set error tolerances
C
      ERRABS = 0.0
      ERRREL = 0.001
C
C                   Parameter for non-oscillatory
C                   function
C
      IRULE = 2
      CALL QDAG (F, A, B, ERRABS, ERRREL, IRULE, RESULT, ERREST)
      RETURN
      END
C
C*********************************************************************
C
      REAL FUNCTION F (X)
      REAL        X
      CALL FVALUES (F, X)
      RETURN
      END
C
C*********************************************************************
C
      SUBROUTINE FVALUES (CP,XP)
      INTEGER     NX, LDY
      PARAMETER  (NPDES=1, NX=101, LDY=NPDES)
      REAL        XBREAK(NX), Y(LDY,NX), CP, XP
      COMMON /ARRA/ XBREAK, Y
C
C                   DO LINEAR INTERPOLATION ON ARRAY XBREAK
C                   TO FIND FUNCTION.
C
      DO 50 K=1, NX
            IF (XP .EQ. XBREAK(K)) THEN
                  CP = Y(LDY,K)
            ELSEIF (XP .GT. XBREAK(K)) THEN
                  IF (XP .LT. XBREAK(K+1)) THEN
                        CP = ((XP-XBREAK(K))/(XBREAK(K+1)-
     &XBREAK(K)))*(Y(LDY,K+1)-Y(LDY,K))+Y(LDY,K)
                  ENDIF
            ENDIF
50    CONTINUE
      RETURN
      END
```

VITA

STEVEN LEE WILLOUGHBY

Candidate for the Degree of

Master of Science

Thesis: EFFECTIVE DIFFUSSION COEFFICIENTS FOR TOLUENE IN CALCIUM CARBONATE FILLED POLY(VINYL ACETATE) FROM QUARTZ CRYSTAL MICROBALANCE SORPTION EXPERIMENTS

Major Field: Chemical Engineering

Biographical:

Personal Data: Born in Mangum, Oklahoma, on September 23, 1967, the son of Troy and Cindy Willoughby.

Education: Graduated from Gould High School, Gould, Oklahoma, May, 1985; received Associate of Science degree in Mathematics at Western Oklahoma State College, Altus, Oklahoma, May, 1989; received Bachelor of Science degree in Physics at Cameron University, Lawton, Oklahoma, May, 1992; received Master of Science degree in Physics at Oklahoma State University, Stillwater, Oklahoma, December, 1994; completed the requirements for the Master of Science Degree in Chemical Engineering at Oklahoma State University, Stillwater, Oklahoma, May, 1998.